Identification and Characterization of Intermediates during Folding on the ß-Barrel Assembly Machine in Escherichia coli

Identification and Characterization of Intermediates during Folding on the β-Barrel Assembly Machine in *Escherichia coli*

A dissertation presented

by

Mingyu Xue

to

The Department of Chemistry and Chemical Biology

in partial fulfillment of the requirements

for the degree of

Doctor of Philosophy

in the subject of

Chemistry

Harvard University

Cambridge, Massachusetts

May 2014

Dissertation Advisor: Daniel Kahne **Mingyu Xue**

Identification and Characterization of Intermediates during Folding on the β-Barrel Assembly Machine in *Escherichia coli*

Abstract

β-barrel membrane proteins play important structural and functional roles in Gram negative bacteria and in mitochondria and chloroplasts of eukaryotes. A conserved machine is responsible for the folding and insertion of β-barrel membrane proteins but its mechanism remains largely unknown. In *E. coli*, a five protein β-barrel assembly machine (Bam) assembles β-barrel proteins into the outer membrane (OM). Among all β-barrel membrane proteins in *E. coli*, the β-barrel component of the OM LPS translocon is one of only two essential β-barrels, the other being the central component of the Bam machinery itself. The OM LPS translocon, which consists of OM β-barrel protein LptD (lipopolysaccharide transport) and OM lipoprotein LptE, is responsible for the final export of LPS molecules into the outer leaflet of the OM, resulting in an asymmetric bilayer that blocks the entry of toxic molecules such as antibiotics. This thesis describes the characterization of the biogenesis pathway of the OM LPS translocon and its folding and insertion into the OM by the Bam machinery.

An *in vivo* S^{35}-Methionine pulse-labeling assay was developed to identify intermediates along the biogenesis of the OM LPS translocon. Seven intermediates were identified along the pathway. We show that proper assembly of the OM LPS translocon involves an oxidative disulfide

bond rearrangement from a nonfunctional intermediate containing non-native disulfides. We also found that the rate determining step of OM LPS translocon biogenesis is β-barrels folding process by the Bam machinery.

Using *in vivo* chemical crosslinking, we accumulated and trapped a mutant form of LptD on BamA, the central component of the Bam machinery. We extended the S^{35}-Methionine pulse-labeling method to allow chemical crosslinking of substrates on the Bam complex and trapped LptD while it was being folded on the Bam machine. We demonstrated that the interaction between LptD and BamA is independent of LptE, while that between LptD and BamD, the other essential component of the Bam complex beside BamA, is LptE dependent. Based on these findings, we proposed a model of Bam-assisted folding of the OM LPS translocon in which LptE templates the folding of LptD.

Table of Contents

Abstract iii

Table of Contents v

Acknowledgement x

List of Figures/Tables xii

Chapter One – Introduction 1

1.1 Introduction 2

1.1.1 Outer membrane of Gram-negative bacteria is an asymmetric bilayer 3

1.1.2 Lipopolysaccharide biogenesis 7

1.1.2.1 Lipopolysaccharide biosynthesis in the cytoplasm 7

1.1.2.2 Lipopolysaccharide translocation across the inner membrane 8

1.1.2.3 Lipopolysaccharide transport from the IM to the OM 10

1.1.2.3.1 Identification of Lpt proteins 11

1.1.2.3.2 LPS transport across the periplasm via OstA-bridge 13

1.1.2.4 LPS insertion at the OM 16

1.1.3 Biogenesis of OM lipoprotein 18

1.1.4 Outer membrane β-barrel protein assembly 20

1.1.4.1 Overview of membrane integral protein assembly 20

1.1.4.2 Identification of the β-barrel assembly machine at the OM 23

1.1.4.3 Structure of Bam proteins 23

1.1.4.4 Mechanistic studies of the Bam complex 26

1.2 Perspectives 28

1.3 References 30

Chapter Two – Characterization of the Biogenesis Pathway of the Outer Membrane Lipopolysaccharide Translocon

2.1 Introduction 40

2.2 Results and Discussion 41

2.2.1 A non-native disulfide-bonded intermediate (1) is observed during oxidative folding of LptD *in vivo* 41

2.2.2 Intermediate 1 is "on-pathway" to mature LptD 45

2.2.3 Folding of the β-barrel domain is slow and precedes disulfide bond rearrangement 46

2.2.4 Wild-type LptD can only assemble efficiently if folding proceeds through intermediate 1 49

2.2.5 A disulfide bond between Cys_{724} and Cys_{725} ([3-4]) is likely formed in intermediate 1 50

2.2.6 LptD intermediates containing mixed-disulfide adducts with DsbA can be detected *in vivo* allowing the complete oxidative folding pathway for LptD to be delineated 53

2.2.7 Disulfide rearrangement of intermediate 1 is triggered by LptE to activate the OM translocon for LPS export 56

2.2.8 OM LPS translocon mutants have defective triggering mechanisms 58

2.3 Conclusion and Future Work 60

2.4 Materials and Methods 62

2.4.1 Bacterial strains 62

2.4.2 Plasmid construction 63

2.4.3 Growth of AM689 for OM analysis 63

2.4.4 Isolation of OM for analysis of LptD oxidation states 64

2.4.5 Pulse-chase analysis 64

2.4.6 Maleimide-PEG (Mal-PEG12k) alkylation of [^{35}S]-pulse-labeled samples 65

2.4.7 Seminative pulse-chase analysis 66

2.4.8 Trypsin digestion following seminative pulse-chase experiment 67

2.4.9 Affinity purification 67

2.4.10 Bioinformatics 67

2.4.11 Antibodies 68

2.5 References 69

Chapter Three – Characterization of Lipopolysaccharide Translocon Folding by the Bam Complex 72

3.1 Introduction 73

3.2 Results and Discussion 74

3.2.1 LptD and LptE can be chemically crosslinked to BamA *in vivo* 74

3.2.2 The chemically trapped LptD on BamA is a characterized intermediate along the LptD biogenesis pathway 76

3.2.3 LptD can be trapped by chemical crosslinking during folding on BamA as on-pathway folding intermediates 78

3.2.4 Loading of LptD to BamA is independent of LptE 79

3.2.5 LptE mediates the interaction between LptD and BamD 81

3.2.6 LptE and BamA form a stable complex *in vitro* 82

3.2.7 LptE modulates the activity of BamA *in vitro* 84

3.2.8 A model for LptD folding on Bam complex 85

3.3 Conclusion and Future Work 87

3.4 Materials and Methods 88

3.4.1 Bacterial strains and growth conditions 88

3.4.2 Plasmid construction 88

3.4.3 *In vivo* DSP crosslinking 89

3.4.4 *In vivo* DSP crosslinking of [^{35}S]-pulse-labeled cells 90

3.4.5 *In vivo* EGS crosslinking 92

3.4.6 Isolation of OM for analysis of LptD oxidation states 93

3.4.7 Growth of MC4100 *ara*$^{+}$ *lptE*$^{-}$ λ_{att}(*P*$_{BAD}$-*lptE)* for OM analysis and DSP crosslinking 93

3.4.8 Expression and Isolation of Denatured BamA or FLAG-BamA 94

3.4.9 Expression and Purification of LptE-His 94

3.4.10 Expression and Purification of BamCDE-His 95

3.4.11 Folding and Purification of BamA 96

3.4.12 Folded FLAG-BamA Affinity Purifications 96

3.4.13 Size-Exclusion Chromatography with BamA and LptE-His 97

3.4.14 Preparation of Proteliposomes Containing BamA or BamA/LptE-His 97

3.4.15 Folding of FLAG-BamA into Proteoliposomes 98

3.4.16 Pulse-chase analysis 98

3.4.17 Antibodies 99

3.5 References 100

Acknowledgements

The past six years as a PhD student is one of the best times I have ever had in my life so far. It would not be possible without the help, advice and support from many people whom I am eternally indebted to. My advisor, Dan Kahne, is truly an incredible mentor from whom I learn how to be a scientist. He taught me how to approach an important scientific problem with imagination, creativity and yet at the same time, the highest level of rigor and criticism. The way he manages scientific projects has greatly influenced how I think about research. Our conversations have always been a great source of stimulation and inspiration to me. I cherish our friendship and hope it will continue and grow for many years to come.

I would like to thank my committee members, Prof. Jonathan Beckwith, Prof. Tom Rapoport and Prof. Christopher Walsh for their support and advice over the years. I learned enormous amount from our collaboration with Prof. Jonathan Beckwith. Prof. Tom Rapoport and Prof. Christopher Walsh gave me lots of helpful advices at various stages of my PhD and I truly appreciate their interest in my project and help.

The Kahne lab is a pleasant, friendly and highly motivated environment to work in. My thesis would not be what it is without contributions from many members of the Kahne lab. Dr. Shu Sin Chng is a wonderful mentor and a role model of my graduate career who taught me how to work with bacteria and do protein biochemistry. We worked very closely on characterizing the biogenesis pathway of an essential membrane protein, which is described in Chapter Two of this thesis. Dr. Luisa Gronenberg also was a great help to me when I started my PhD by letting me start with a project that she had been working on. Aaron Garner, Dr. Joseph Wzorek and James Lee are wonderful collaborators within the lab. Prof. Natividad Ruiz (Ohio State University) has been a great collaborator who offered enormous support in bacteria genetics. Dr. Hiroshi Kadokura

(Nara Institute of Science and Technology) offered invaluable help in development of a key radio-labelling assay. Dr. Dana Boyd (Harvard Medical School) provided bioinformatics support.

There are many other people I would like to thank in the Kahne lab. They helped me in all possible ways and made my graduate school experience memorable. I really appreciate the friendship and support from Dr. Suguru Okuda, Dr. Elizaveta Freinkman, Dr. Christine Hagan, Dr. Tania Lupoli, Dr. Goran Malojcic, Dr. Megan Bolla, Dr. Tohru Taniguchi, David Sherman, Alex Geroge, David Westwood, Vadim Baidin, Janine May, Matt Lebar, Fred Rubino, Katie Schaefer and John Janetzko. In addition, I must thank our group administrators, Helen Corriero and Mike Quinn, whose dedication to the lab keeps the lab running.

I am extremely fortunate to have a caring and supportive family. They give me all the best things in life and support their only child to pursue a career in a foreign country on the other side of the planet.

Last but not least, I would like to thank the Savory Food Truck on Oxford St where I got most of my lunch and dinner for the past six years. My PhD life will be very different without them.

List of Figures/Tables

Figure 1.1. Structure of the gram-negative cell envelope.

Figure 1.2. Electron micrograph (EM) of *Veillonella* illustrating the ultrastructure of the Gram-negative cell envelope.

Figure 1.3. Structure of Escherichia coli LPS.

Figure 1.4. Biosynthesis of Kdo_2-lipid A.

Figure 1.5. Three conformations of homodimeric MsbA.

Figure 1.6. The structure of LptC and LptA.

Figure 1.7. Model of LPS transport across the periplasm.

Figure 1.8. Ordered assembly of the Lpt machinery.

Figure 1.9. A model of OM lipoprotein trafficking.

Figure 1.10. Cell envelope protein biogenesis.

Figure 1.11. Structure of BamA from *N. gonorrhoeae* and *H. ducreyi*.

Figure 2.1. The Lpt machinery forms a trans-envelope bridge that exports LPS to the cell surface.

Figure 2.2. A previously-reported LptE-limiting strain makes different levels of LptE protein (lower than the wild-type strain) at various stages of growth even under non-depletion conditions.

Figure 2.3. An LptD species containing non-functional disulfide bond is accumulated when LptE is limiting.

Figure 2.4. The $LptD_{CCSS}$ double cysteine-less mutant protein migrates slightly faster than reduced LptD during non-reducing SDS-PAGE.

Figure 2.5. LptD containing the non-native Cys_{31}-Cys_{173} ([1-2]) and Cys_{724}-Cys_{725} ([3-4]) disulfide bonds (intermediate **1**) is an intermediate along the LptD assembly pathway *in vivo*.

Figure 2.6. LptD containing the non-consecutive Cys_{173}-Cys_{725} (**[2-4]**) disulfide bond accumulates in the absence of DsbA.

Figure 2.7. Folding of the LptD β-barrel domain is slow and precedes disulfide bond rearrangement.

Figure 2.8. DsbA is required for efficient assembly of mature LptD through intermediate **1**.

Figure 2.9. A disulfide bond between Cys_{724} and Cys_{725} may be formed in intermediate **1**.

Figure 2.10. LptD intermediates containing mixed-disulfide adducts with DsbA can be detected *in vivo*.

Figure 2.11. The $dsbA_{P151T}$ mutation results in the accumulation of mixed-disulfide adducts between DsbA and Cys_{31} of LptD.

Figure 2.12. Cys_{173} and Cys_{725} are very highly conserved among LptD homologs.

Figure 2.13. Formation of the mature functional OM LPS translocon proceeds via pre-assembly of a non-functional LptD/E intermediate that is activated via disulfide bond rearrangement.

Figure 2.14. The **[1-2][3-4]**-LptD$_{\Delta 330\text{-}352}$ mutant protein can assemble with LptE, but is defective in disulfide bond rearrangement to form mature LptD.

Figure 3.1. LptD and LptE can accumulates on BamA in an LptD mutant.

Figure 3.2. The mutant that accumulates on BamA is a characterized intermediate on the assembly pathway of LptD.

Figure 3.3. LptD can be trapped by chemical crosslinking during folding on BamA.

Figuue 3.4. Loading of LptD to BamA is independent of LptE.

Figure 3.5. LptE mediates the interaction between LptD and BamD.

Figure 3.6. BamA co-purifies with LptE *in vitro*.

Figure 3.7. BamA-LptE forms a stable complex *in vitro*.

Figure 3.8. LptE-BamA forms an active complex in vitro.

Figure 3.9. A model for LptD folding by Bam complex.

Figure 3.10. SurA is required to fold LptD.

Chapter One

Introduction

1.1. Introduction

Gram-negative bacteria have a unique structure. They are comprised of two aqueous compartments enclosed by two different kinds of lipid bilayer membranes. The cytoplasm, where all protein synthesis takes place, is engulfed by the inner membrane (IM). The periplasm, where the peptidoglycan layer, known commonly as cell wall, is located, is sandwiched between the IM and the outer membrane (OM) which directly contacts extracellular environment (Fig. 1.1). This unique double-membrane structure offers Gram-negative bacteria more protection from their surroundings than those Gram-positives which have only a single membrane. Between the two membranes of Gram-negative bacteria, the OM is of special interest, as it contains unique structural features that contribute largely to the impermeability against toxic compounds such as antibiotics and bile salts (*1*). This special feature is the presence of a lipopolosaccharide (LPS) layer that composes the outer leaflet of the OM, which makes the OM an asymmetric bilayer with the outer leaflet being LPS and inner leaflet being phospholipids (PL) (Fig. 1.1) (*1*).

This thesis presents biochemical studies on the folding and assembly pathway of the key component in LPS transport, the LPS translocon at the OM of the model Gram-negative organism, *Escherichia coli*. This work is focused on two main questions that we are trying to answer: 1. What is the biogenesis pathway of the LPS OM translocon? 2. How is the LPS OM translocon folded into the OM?

This chapter provides an introduction to OM biogenesis. Firstly, we take a general look at the composition of OM in terms of its lipids and proteins. Secondly, we will discuss LPS biogenesis, with a focus on LPS transport and assembly to its final destination. Thirdly, we are going to provide an overview of how proteins at the OM are assembled, with an emphasis on β-barrel protein biogenesis.

1.1.1. Outer membrane of Gram-negative bacteria is an asymmetric bilayer

Biological membranes not only define cellular compartments but also determine the permeability of those compartments. They control the traffic in and out of the compartments to obtain optimal cell growth and regulation. In Gram-negative bacteria, the OM mainly serves as a selective permeability barrier that limits entry to the cell to a small and very well defined group of molecules (*1*).

Typical phospholipid bilayer membranes, such as the IM of Gram-negative bacteria, form a tight barrier to hydrophilic molecules, but due to their largely hydrophobic nature, they are not very effective in blocking the entry of hydrophobic molecules from entering the cell. What is unique about the OM of Gram-negative bacteria is that it is very effective in preventing both hydrophobic and hydrophilic molecules from cell entry yet at the same time allowing the uptake of necessary compounds such as nutrients (*1*). The OM of Gram-negative bacteria must have some very special structural features to achieve this highly sophisticated functional goal (Fig. 1.1 and 1.2).

The OM of Gram-negative bacteria is special both on a protein level and a lipid level. On a protein level, which we will discuss in detail later, it contains two different kinds of proteins (Fig. 1.1): membrane β-barrel proteins (*2*) and membrane lipoproteins (*3*). Outer membrane β-barrel proteins (OMPs) are integral membrane proteins that adopt a barrel-like structure in which β-sheets are wrapped around to form a cylinder shape with hydrogen bond (H-bond) interaction between each single β-strand including the first and last one (*2, 4*). OMPs have very stable secondary structures that are not easily perturbed since there are no unsatisfied H-bond interaction between β-strands, (*2, 4*). Moreover, as OMPs form a cylindrical shape at the OM, they provide hydrophilic channels that connect the periplasm with extracellular environment. Such channels provide

passage to small hydrophilic molecules (< 600 Da), allowing them to passively-diffuse into the cell (*1*). OMPs are also involved in many other important cellular functions, such as active transport of specific nutrients (*5*), export of toxic small molecules (*6*), protein secretion (*7*), and the assembly of the OM(*8*). Membrane lipoproteins at the OM tether to the inner leaftlet of the OM via a lipid anchor (*9*). A large fraction of the total lipoprotein population attach to the cell wall either by covalent bond (*10*) or non-covalent interaction (*11*), presumably providing support for the cell envelope.

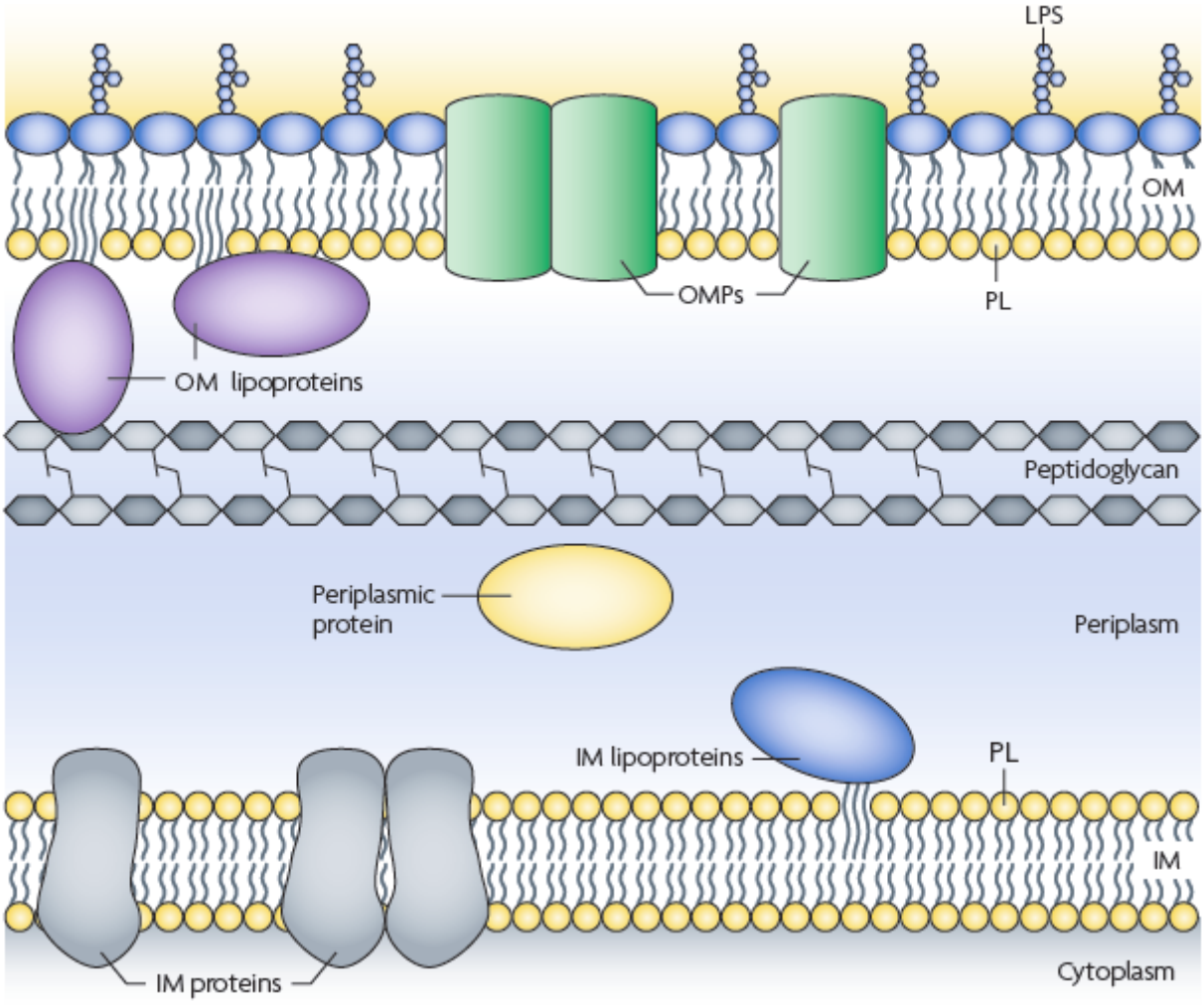

Figure 1.1. (Taken directly from ref. 12 with caption). Structure of the gram-negative cell envelope. In Gram-negative bacteria, the cytoplasm is surrounded by the inner membrane (IM),

that is, a phospholipid (PL) bilayer that also contains proteins. There are two types of proteins in the IM: integral IM proteins, which span the membrane through α-helical transmembrane domains, and IM lipoproteins, which are anchored to the outer leaflet through a lipid moiety. The periplasm is the aqueous compartment bounded by the IM and the outer membrane (OM); it contains soluble proteins and the peptidoglycan layer. The OM is anchored to the rest of the cell via proteins that are covalently attached to the peptidoglycan. The OM is asymmetric, as it contains phospholipids in the inner leaflet and lipopolysaccharide (LPS) in the outer leaflet. In addition, the OM contains two types of proteins, integral OM proteins (OMPs) and lipoproteins.

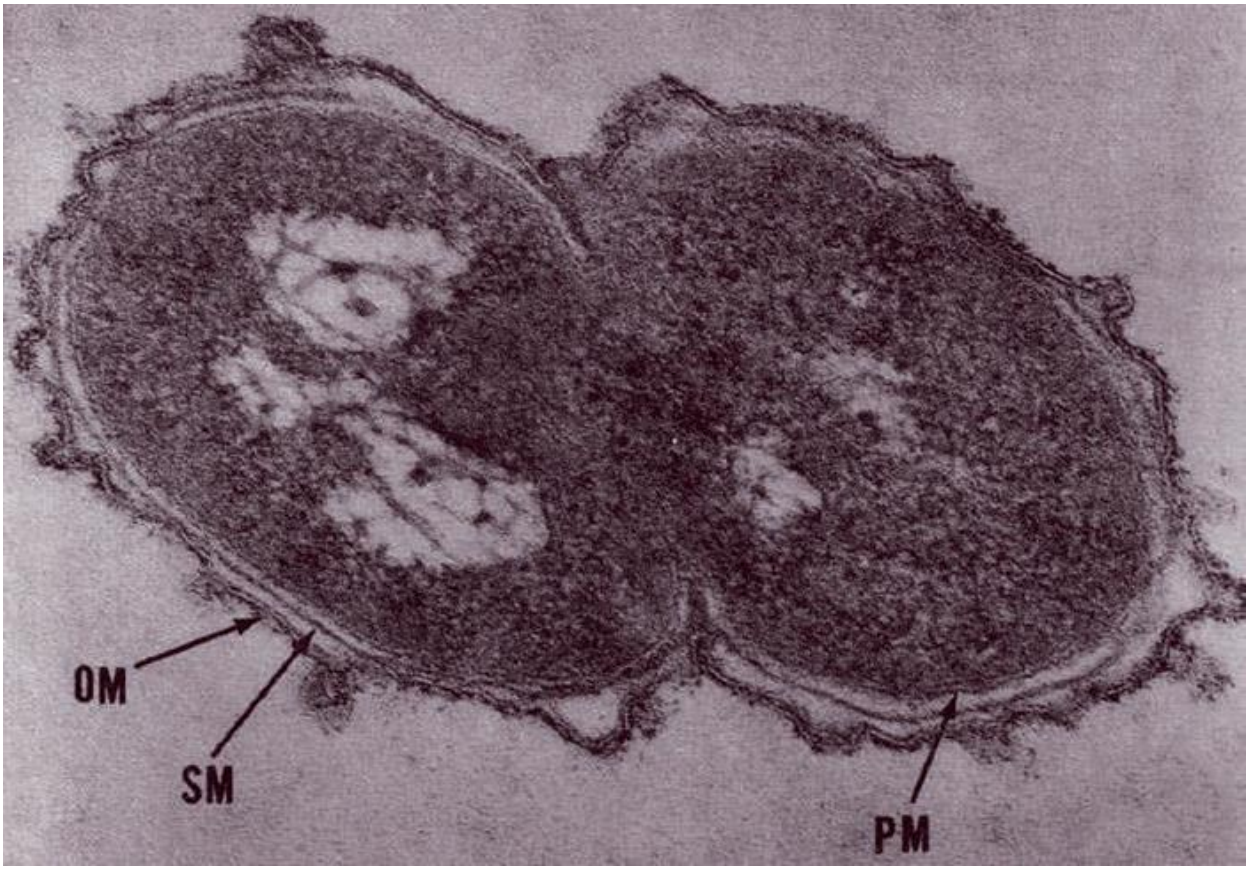

Figure 1.2. (Taken directly from ref. 12 with caption). Electron micrograph (EM) of *Veillonella* illustrating the ultrastructure of the Gram-negative cell envelope. Bladen and Mergenhagen published this micrograph in 1964 (ref. 13) and they labelled the different structures as the outer membrane (OM), the solid membrane (SM), which is known nowadays as the peptidoglycan, and the plasma membrane (PM), which we refer to as the inner or cytoplasmic membrane. Figure is reproduced, with permission, from ref. 13 © (1964) American society for Microbiology.

On a lipid level, the OM of Gram-negative bacteria is a lipid bilayer with asymmetric lipid composition, the inner leaflet being phospholipids and the outer leaflet LPS, a large amphiphilic molecule that is essential for viability in most Gram-negative bacteria (Fig. 1.3) (*1*, *12-17*). This remarkable discovery was made decades ago through a series of EM and biochemical labeling experiments which taken together conclude that LPS is only found on the outer leaflet of the OM (*15-17*).

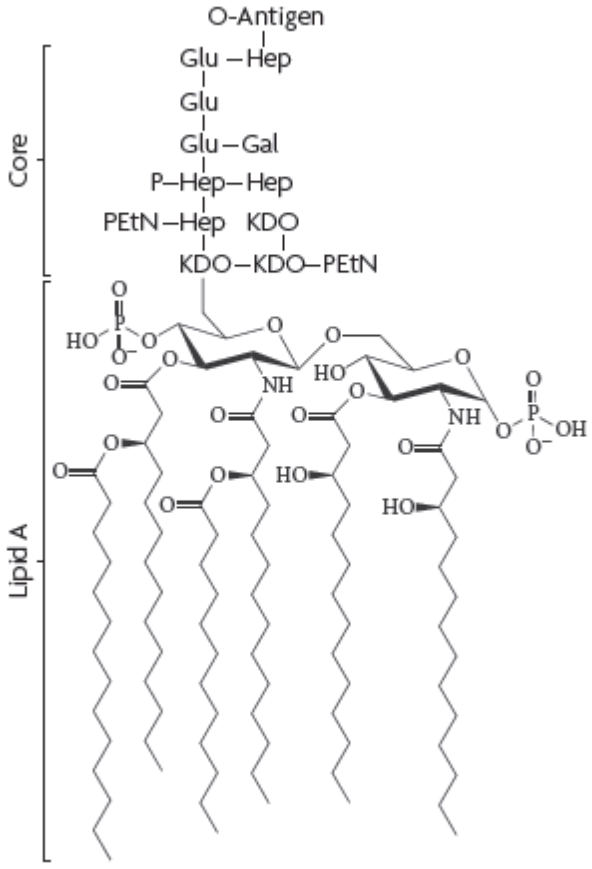

Figure 1.3. (Taken directly from ref. 12 with caption). Structure of Escherichia coli LPS. The structure of E. coli LPS with a K-12 core region is shown. The structure of LPS among different species is very diverse (*18*) and bacteria can further modify the typical LPS structure in response to environmental signals and defects in envelope conditions (*19-22*). EtN, ethanolamine; Gal, d-galactose; Glu, d-glucose; Hep, l-glycerod- manno-heptose; KDO, 3-deoxy-d-manno-oct-2-ulosonic acid; P phosphate.

LPS molecules are polyanionic due to the phosphate groups on the polar heads. At the OM, those anionic moieties form ionic interactions with divalent cations such as Mg^{2+}, resulting in a tight mesh with very limited lateral diffusion efficiency (*1*). Such structural features of the LPS layer give rise to the impermeability of the OM, protecting Gram-negative bacteria from harsh growth conditions (*1*).

1.1.2. Lipopolysaccharide biogenesis

1.1.2.1. Lipopolysaccharide biosynthesis in the cytoplasm

The biosynthesis pathway of LPS has been extensively studied in the past, partly because of its role in triggering strong immune response (*14*). The hydrophobic core of LPS, called Lipid A (Fig. 1.3), can activate Toll-like receptor 4 (TLR4), which leads to an over-production of inflammation-related proteins cascades and triggers septic shock (*23*). Studies on the biosynthetic pathway of LPS provides opportunities to use small molecules that inhibit the function of key enzymes which eventually could shut down the production of LPS (*24*, *25*). Some of the inhibitors are already in clinical trials.

In *E. coli*, LPS is composed of two parts: a hydrophobic hexa-acylated glucosamine disaccharide anchor and a hydrophilic core oligosaccharide group plus O-antigen polysaccharides (Figure 1.3) (*14*). LPS synthesis starts in the cytoplasm with the assembly of Kdo_2-lipid A, which has been extensively characterized and reconstituted by Raetz and co-workers (*14*). This pathway consists of nine steps that converts starting material UDP-*N*-acetylglucosamine (UDP-GlcNAc) to Kdo_2-lipid A (Fig. 1.4), which is then decorated by subsequent addition of the inner and outer core sugars (*14*).

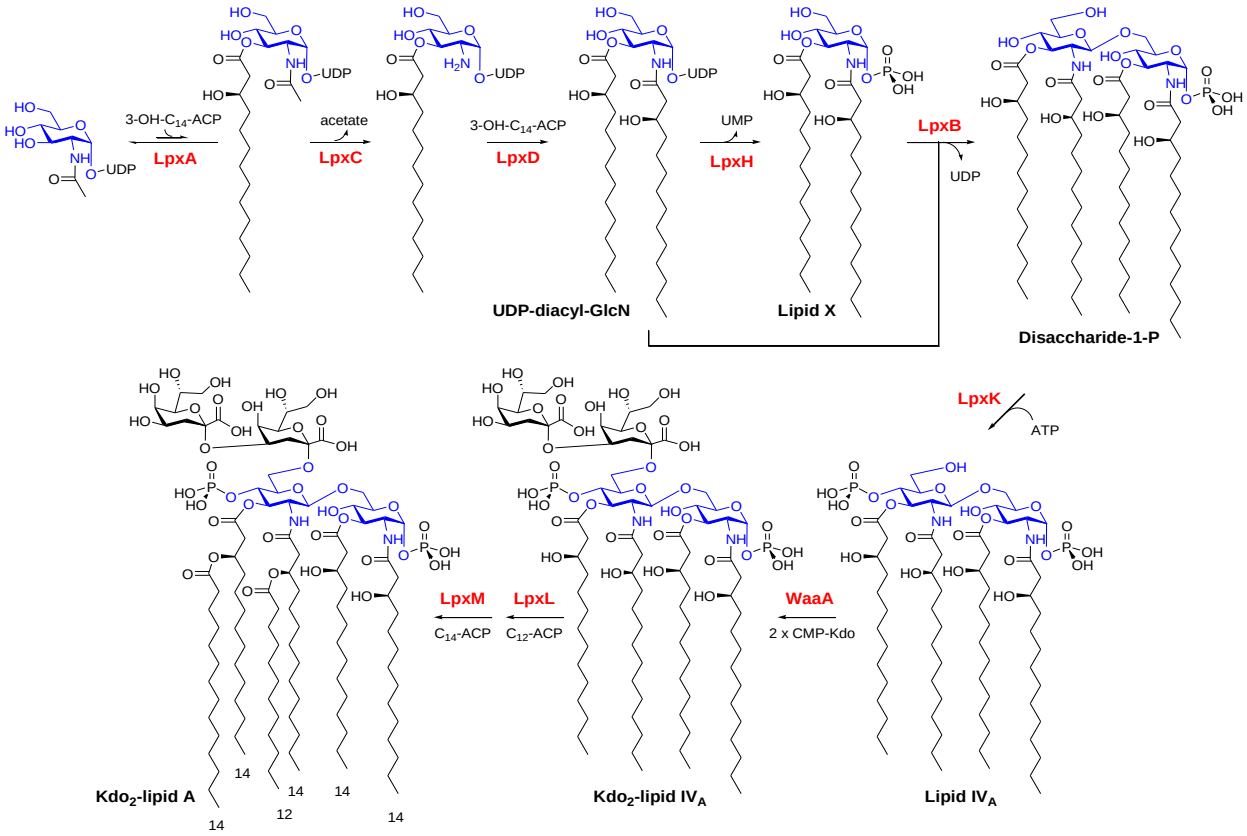

Figure 1.4. Biosynthesis of Kdo_2-lipid A (taken directly from Dr. Shu Sin Chng's dissertation).

1.1.2.2. Lipopolysaccharide translocation across the inner membrane

LPS precursor molecules need to be flipped from the inner leaflet of the IM to the outer leaflet of the IM before sugar modifications and subsequent transport to the OM can take place (*1*). This flipping process requires energy as the barrier for a polar "head group" to pass the non-polar lipidic membrane is high. The polar head groups will undergo a de-solvation and re-solvation process during the flip, in which the water molecules that surround the polar head groups need to first dissociate before those head groups can pass the membrane and subsequently re-solvate in the periplasm with water molecules there.

The protein that powers the translocation of LPS across the IM is MsbA, which is an essential IM integral protein that forms an ABC transporter that utilizes ATP as the energy source (*26-28*). MsbA was initially identified as a suppressor for a mutant that produced defective LPS (*26*). It was later shown that wild-type LPS stimulates ATP hydrolysis by MsbA better than the defective LPS, suggesting that MsbA may be directly involved in LPS transport (*27*). Finally, Doerrler and coworkers used location specific LPS modification enzymes to show that MsbA is in fact an LPS flippase that moves LPS from the inner leaflet of IM to the outer leaflet of IM (*28*). In their experiment, they found that the modification of newly synthesized LPS by two enzymes that only tailor LPS molecules at the outer leaflet of the IM is MsbA dependent, however, modification of newly synthesized LPS by a different enzyme that functions at the inner leaflet of the IM is not (*28*).

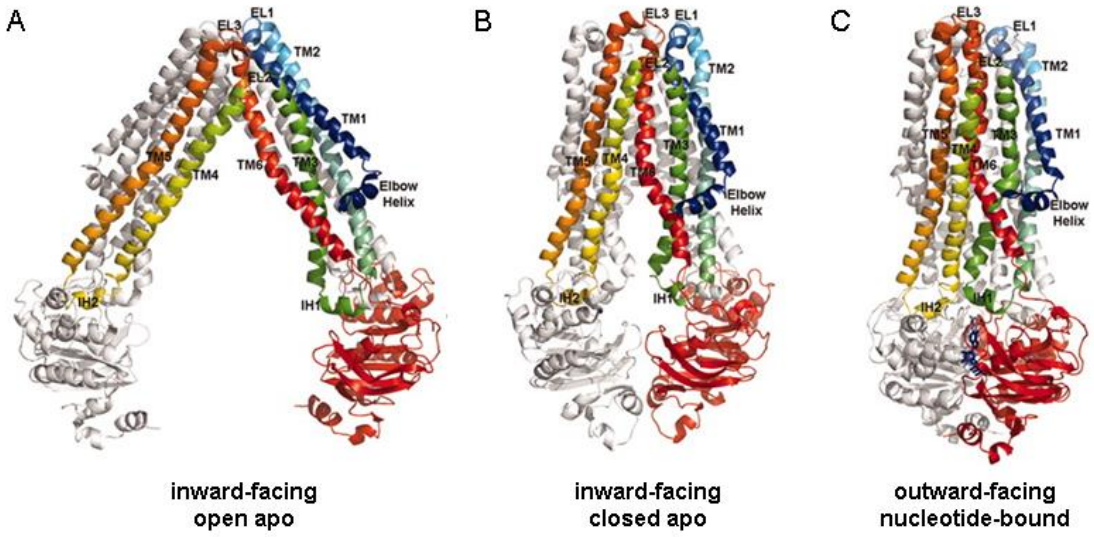

Figure 1.5. Three conformations of homodimeric MsbA (taken directly from ref. 90). One monomer in each model is colored with a rainbow gradient (N-terminus is blue, C terminus is red), and the other is white. AMP-PNP molecules are displayed as blue sticks in the nucleotide-bound structure.

MsbA orthologs have been crystalized in different conformations, and a model of how MsbA flips LPS molecules was proposed based on those structures (*29*). Three different conformations (Fig. 1.5) of MsbA from three closely related bacteria were shown: an inward opening conformation of apo-MsbA from *E. coli*; an inward closed conformation of apo-MsbA from *Vibrio cholerae*; and finally a conformation of MsbA from *S. typhimurium* that is outward-facing and bound to a nucleotide analog, ATP-PNP (*29*). These different conformations imply that MsbA may undergo a substantial conformational change when catalyzing the LPS translocation reaction powered by ATP-hydrolysis. LPS is likely to bind to the inward opening conformation, which may trigger a conformational change that transits the protein to an inward closed conformation (*29*). Translocation of LPS could then take place when MsbA shifts to the outward-facing conformation, possibly induced by ATP binding. Subsequently, ATP hydrolysis completes the catalytic cycle and resets MsbA to the original inward opening conformation.

1.1.2.3. Lipopolysaccharide transport from the IM to the OM

How LPS molecules are transported from the IM to their final destination at the outer leaflet of the OM is less well known. It is a challenging problem for the cell to pull out such large, amphiphilic molecules from the IM, transport them through the aqueous periplasm and finally release them across the OM. Seven essential proteins that form a trans-envelop Lpt (lipopolysaccharide transport) machinery have been identified in recent years, which is proposed to transport LPS from IM to its final destination (*12*, *30*). Four of these Lpt proteins, LptBCFG, form a complex that partly consists of an ABC transporter that utilizes ATP hydrolysis energy to initiate LPS movement from the IM (*31-38*). This complex has been purified and performs ATPase activity (*34*). Two OM proteins, LptD and LptE, which are OM integral β-barrel protein and OM

lipoprotein, respectively, form a tight plug-and-barrel complex that mediates the final insertion of LPS into the outer leaflet of the OM (*39-44*). A periplasmic protein LptA mediates the interaction between the IM and OM Lpt proteins, allowing the formation of a protein-based bridge that serves as the passage of LPS molecules across the periplasm (*45-49*).

1.1.2.3.1. Identification of Lpt proteins

LptD was originally implicated to relate to OM permeability about twenty five years ago (*50*). It was first found in a mutant allele, *imp4213* (now referred to as *lptD4213*), that suppresses the lethal *lamB*$^{-}$ deletion when maltodextrins is the only nutrient available. This mutation presumably makes cells more permeable so maltodextrins could diffuse into the cell in the absence of importer LamB (*50*). The *lptD4213* mutant rescues the lethality of *lamB*- allele when growing in medium in which maltodextrins is the only carbon source (*50*). However, since *lptD4213* has a much more permeable OM, it is very susceptible to small molecules such as antibiotics and detergents that wild type cells are normally resistant to (*50*). LptD is a highly conserved (*39*) essential integral β-barrel protein, with a small N-terminal periplasmic domain and a large C-terminal β-barrel domain (*42*). LptD contains four cysteine residues, two of which reside in the N-terminal periplasmic domain and the other two in the C-terminal β-barrel domain; three out of the four cysteine residues are well conserved across species (*39, 43*). Mobility of LptD on SDS-PAGE is different when samples are pre-treated with or without *β*-mercaptoethanol (*β*-ME), a thiol reducing agent, suggesting that the cysteine residues in LptD form intramolecular disulfide bonds (*1, 39, 43*). Depletion of LptD in *E. coli* produces abnormal OM; when LptD is depleted newly synthesized LPS molecules accumulate in the IM, which implies that LptD may be involved in LPS transport (*39, 41*).

In most Gram-negative bacteria, LPS is essential for cell viability. Thus it is not possible to delete LptD and observe phenotypes related to LptD deletion if LptD is in fact related to LPS biogenesis. However, in *Neisseria meningitidis*, LPS is not essential (*51, 52*), which makes it possible to delete the *lptD* gene. In a mutant where the *lptD* gene is disrupted, LPS molecules produced could not be modified by tailoring enzymes at the OM or in the extracellular environment, suggesting that LPS transport is impaired in this mutant (*51*). These results implicated that LptD is involved in the transport of LPS. In *E. coli*, LptD was later shown to co-purify with an essential OM lipoprotein LptE (*41*). Similar to LptD, depleting LptE also results in mislocalization of newly-synthesized LPS, as they would accumulate in the IM instead (*41*). LptD and LptE could be purified as a stable complex *in vitro*, in which the lipoprotein is protected from protease degradation, suggesting that a large part of LptE sits in the lumen of the β-barrel of LptD (*42*). Further evidence to support this plug-and-barrel structure was obtained by introducing photo-activatable amino acids into randomly chosen positions of LptE and detecting positions that physically contact LptD (*44*). Five positions around LptE were found that interact with LptD, among which one of the positions interacts with a putative extracellular loop of LptD, suggesting that LptE sits inside of LptD (*44*).

Random transposon mutagenesis in *E. coli* leads to the discovery of another three essential genes involved in LPS biogenesis. When transposon-insertion disrupted *lptA*, *lptB* and *lptC* , cells become dead (*53, 54*). Furthermore, similar to that of LptD and LptE, depletion of LptA, LptB or LptC prevents newly-synthesized LPS from translocating to the OM, suggesting that all three proteins are involved in LPS biogenesis (*31, 32*). Additionally, WaaL, an LPS modifying enzyme that attaches the O-antigen to LPS molecules at the outer leaftlet of the IM, has been shown to modify the accumulated LPS molecules at the IM (*32, 55*).

lptF and *lptG*, two IM transmembrane proteins that are part of an ABC transporter system with LptB, were identified by bioinformatics (*33*). This approach took advantage of the fact that LPS is one of the defining character of Gram-negative bacteria, thus genes involved in LPS biogenesis should be found in all Gram-negative bacteria, including those endosymbionts that have extremely small genomes. By comparing the genome of the bacterial endosymbiont *Blochmannia floridanus* with that of *E. coli*, two more essential genes with previously unassigned function were found. These two genes were *lptF* and *lptG*. Depletion studies on these two genes produced similar results to that of other Lpt protein depletions. Furthermore, depletion of LptF and LptG prevents PagP modification of newly-synthesized LPS, suggesting that both proteins are required for LPS translocation to the OM (*33*).

1.1.2.3.2. LPS transport across the periplasm via OstA-bridge

Historically, there were two different models proposed on how LPS molecules travel across the aqueous periplasmic space (*8, 12, 30*). One model proposes that, similar to the Lol system that transport OM lipoproteins (discussed below in Section. 1.1.3.), LPS molecules are transported by a periplasmic LPS chaperone, likely LptA, that receives LPS from the inner membrane LptBCFG complex and delivers to the outer membrane LptDE complex. In a different model, the Lpt complex forms a seven-protein trans-envelop machinery that spans two membranes, in which LPS molecules travels in a continuous fashion from the IM to the OM. There were reports back in the late 1960s that suggested the existence of junctions that connect the two membranes from EM snapshots (*56, 57*). Those proposed junctions, commonly known as "Bayer junctions", were suggested as passages for protein and lipid trafficking between the two membranes. Although the existence of "Bayer junctions" and their relation to protein and lipid transport are very much

controversial, it has been reported that newly synthesized LPS molecules were observed near those putative "Bayer junctions" (*58*). Furthermore, LPS accumulates, although transiently, in an OM fraction that is lighter than regular OM (*59*). This fraction, OM_L, in which all seven Lpt proteins can be found, contains IM, cell wall, and OM (*49, 59*). Additionally, LPS transport to the OM still takes place in spheroplasts, where presumably everything that does not attach to the IM is no longer present (*60*). In those spheroplasts, PagP is still capable of modifying freshly made LPS molecules, suggesting that the LPS transport machinery must remain functional (together with some part of the OM) even if the vast majority of periplasm and OM are gone. These results all favor the bridge model of LPS transport.

Some recent evidence suggested that LPS molecules do take advantage of a protein-based bridge that is formed by Lpt proteins to move across the periplasm (*38, 48-49, 61-62*). LptD/E, the OM components of the Lpt proteins and LptA, the periplasmic Lpt protein, all co-purify with his-tagged LptB, LptC or LptF in an affinity pull down, suggesting that they form a physically attached complex (*49*). The X-ray crystal structures of LptA and the periplasmic domain of LptC look very similar to each other; they both adopt β-jellyroll structure, in which hydrophobic amino acids sitting inside the jellyroll create a lipid-friendly patch, suggesting a possible passage of LPS molecules (Fig. 1.6, *49, 61*). Furthermore, in the structure of LptA, multiple β-jellyrolls connect head-to-tail, creating an extended hydrophobic groove along the structure (Fig. 1.6, *49*). Intriguingly, the periplasmic domain of LptC, LptA and the N-terminal periplasmic domain of LptD all belong to the same OstA superfamily, suggesting that similarly structured OstA domains could form a protein bridge where LPS molecules can travel along the hydrophobic groove (*49, 61-62*).

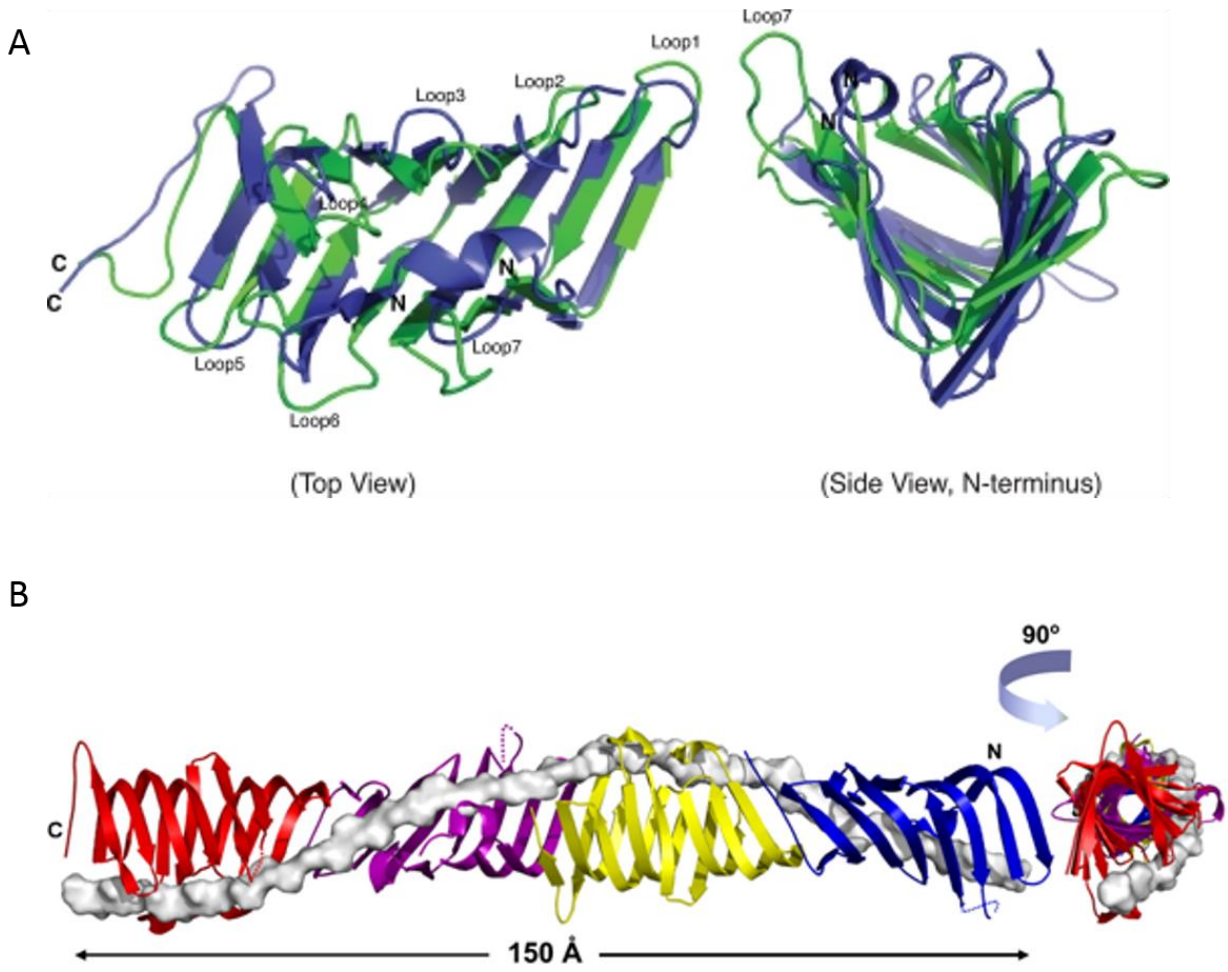

Figure 1.6. (Taken directly from ref. 49 and 61). The structure of LptC and LptA. (A) The structure of LptC. (B) The structure of LptA. Multipule copies of LptA attach to each other in a head-to-tail fashion, creating this fibril structure in which a hydrophobic groove (shown in the figure in a space-filling model) can be found.

In vivo biochemical experiments further support this bridge model (*38*, *48*). LptC, LptA and LptD with photo-activatable amino acids incorporated show site-specific interaction between LptC-LptA, LptA-LptA and LptA-LptD (*48*). These interactions take place at the edge of the β-jellyrolls, suggesting that similar to what the crystal structure indicated, the β-jellyrolls indeed interact in a head-to-tail fashion in the cell. LptA-LptA interaction indicates that the bridge may contain more than one LptA molecule. Interestingly, specific positions that engage in LptA-LptA

interaction were also found to interact with LptD, suggesting that components of the OstA bridge connect in a very similar fashion (*48*). Furthermore, using the same photo-activatable amino acid incorporation technique, LPS has been successfully accumulated on LptC and subsequently released to LptA, providing a molecular picture of LPS movement from LptC to LptA (*38*). This movement is dependent on the presence of the ABC transporter LptBFG and ATP as an energy source, indicating that the LPS movement from the IM to the OM is powered by ATP hydrolysis (Fig. 1.7, *38*).

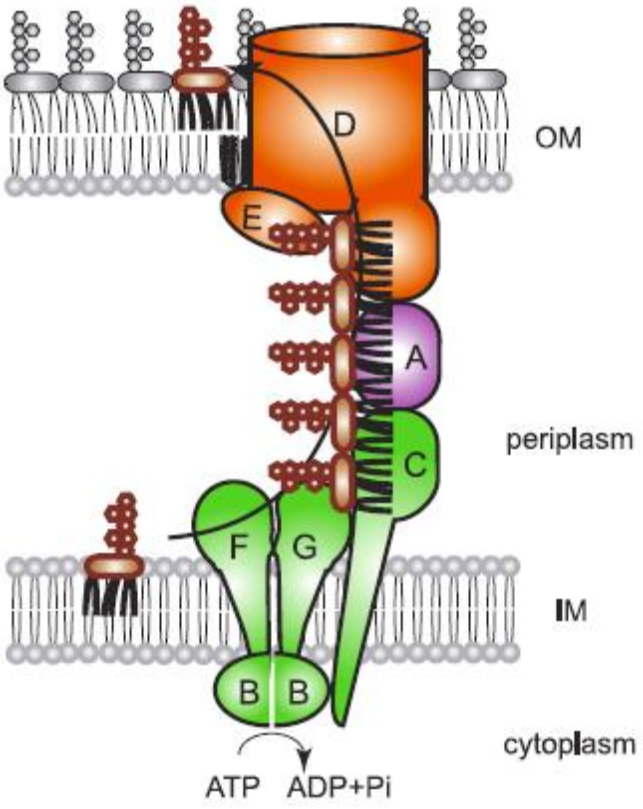

Figure 1.7. (Taken directly from ref. 38) Model of LPS transport across the periplasm. The ABC transporter LptBFG complex utilizes ATP hydrolysis energy to release LPS molecules from the IM, deliver it them to LptC, where they would be continuously pushed to LptA and LptD.

1.1.2.4. LPS insertion at the OM

LptD and LptE form a tight plug-and-barrel structure at the OM that is responsible for receiving LPS molecules that have traveled across the periplasm and eventually putting them into the outer leaflet of OM (*42-44, 48*). How the LptD/E complex inserts LPS molecules into the outer leaflet of the OM is largely unknown.

Recently, it was shown that intramolecular disulfide bonds in LptD are crucial for its activity (*1, 43, 48*). Wild type LptD contains four cysteines, two of them in the N-terminal periplasmic domain (Cys_{31} and Cys_{173}) and the other two in the C-terminal β-barrel domain (Cys_{724} and Cys_{725}) (*43*). In a mature LptD, there are two non-consecutive disulfide bonds that connect the two domains, formed between Cys_{31} and Cys_{724} (**[1,3]**), and Cys_{173} and Cys_{725} (**[2,4]**), resulting in an oxidized **[1,3][2,4]-**LptD. Either one of the two disulfide bonds are sufficient for cell growth, however, disulfide bonds that connect the two domains but are not **[1,3]** or **[2,4]**, such as **[1,4]** or **[2,3]**, do not support growth, suggesting that not all inter-domain disulfide bonds result in a functional LptD (*43*).

Disulfide bond configuration in LptD also plays an important role in the formation of the seven-protein trans-envelop Lpt machinery (*48*). Among a set of LptD cysteine mutants that includes $LptD_{CCSS}$, $LptD_{SSCC}$, $LptD_{SCSC}$ and $LptD_{SCCS}$, only the functional mutant $LptD_{SCSC}$ is able to interact with the periplasmic protein LptA, as judged by photo-activatable crosslinking (*48*). This suggests that only functional LptD is allowed to form the OstA-bridge that spans the two membranes with the rest of Lpt proteins (Fig. 1.8), possibly to prevent the formation of non-functional Lpt machinery that may misplace LPS into undesired places such as the periplasm or the inner leaflet of the OM.

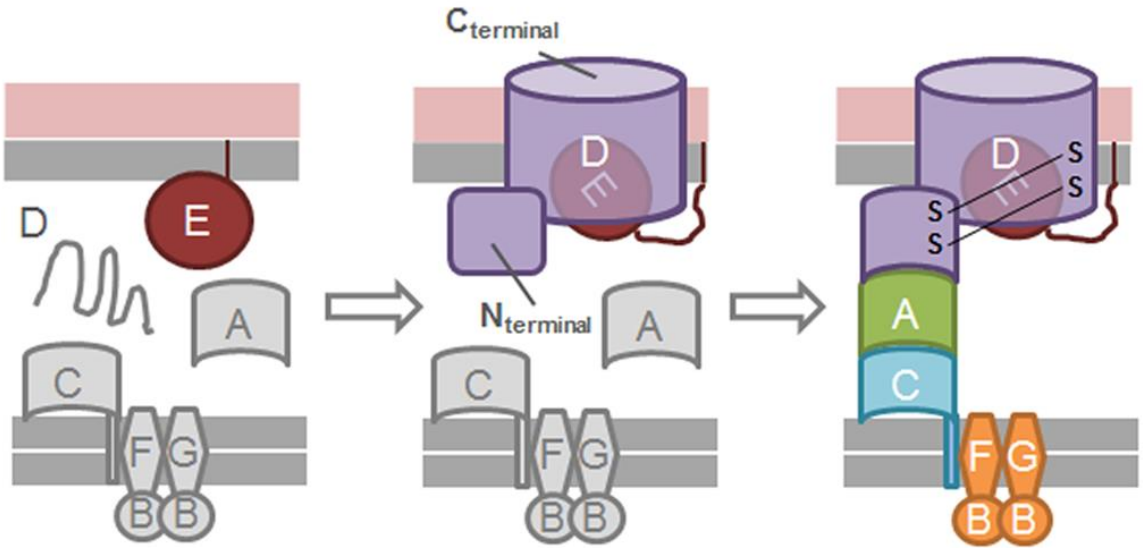

Figure 1.8. (Taken directly from ref. 48). Ordered assembly of the Lpt machinery. Formation of the seven-protein trans-envelop Lpt machine is dependent on correct disulfide bond configuration in LptD. The presence of native disulfide bonds allows the N-terminal periplasmic domain of LptD to interact with LptA.

1.1.3. Biogenesis of OM lipoprotein

Lipoprotein biogenesis in *E. coli* has been extensively studied (*63*, *64*). Like all other periplasmic and OM proteins, the synthesis of OM lipoproteins takes place in the cytoplasm as a precursor with an N-terminal signal peptide. The signal pepide acts as a sorting signal that targets these proteins to the secretion channel that consists of a protein complex SecYEG, where they are secreted across the IM (*65*). Once they cross the IM, those pre-lipoproteins undergo a series of tailoring modifications that eventually produce mature lipoproteins. Firstly, the sulfur atom from the first cysteine (after the signal sequence) receives a diacylglyceryl group from a phosphatidylglycerol (PG) followed by cleavage of the signal peptide occurs at the modifided Cysteine residue. Then the new N-terminal amino acid (the aforementioned cysteine) is acylated,

resulting in a mature lipoprotein that anchors to the membrane by three acyl chains at the very N-terminus (*66*).

Over the past two decades, Tokuda and co-workers have demonstrated that the Lol (localization of lipoprotein) machinery, which consists of five essential proteins (LolABCDE) chaperones OM lipoproteins from the IM to the OM (Fig 1.9, *63, 64*). This process takes place in three steps: the extraction of OM lipoproteins from the IM, the transport of those proteins across the aqueous periplasm and the final insertion of them into the inner leaflet of the OM. The first step is performed by an ABC transporter made of three proteins at the IM, LolCDE. It has been shown that LolCDE recognizes OM lipoproteins in the IM and extracts them from the IM by ATP hydrolysis (*67-69*). OM lipoproteins are then transferred to LolA, a periplasmic protein that chaperones OM lipoprotein across the periplasm (*70*). The sorting of the lipoproteins is achieved by LolCDE as those lipoproteins that are bound to stay in the IM would not be released by the ABC transporter due to a characteristic aspartate residue right after the first cysteine (*71*).

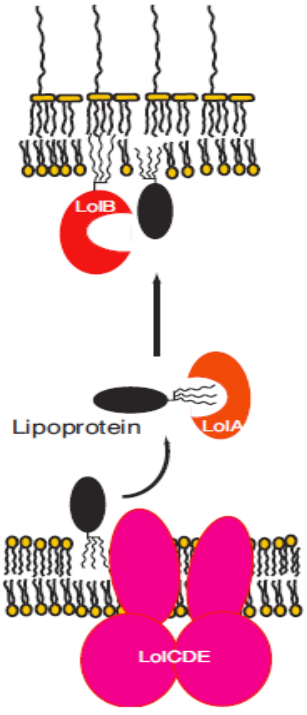

Figure 1.9. (Taken directly from ref. 63). A model of OM lipoprotein trafficking. OM destined lipoproteins are released from the IM by LolCDE complex, chaperoned to the OM by LolA, received and subsequently inserted into the OM by LolB.

Periplasmic chaperone LolA interacts with the lipid anchor of OM lipoproteins and keeps them from aggregation in the aqueous compartment. LolA then delivers its lipoprotein cargo to LolB, an OM lipoprotein itself (Fig. 1.9, *70*). It is still not clear how LolB releases the OM lipoprotein into the inner leaflet of the OM. Structurally, LolB is highly homologous to LolA, both having a large hydrophobic pocket that is thought to host the lipoprotein cargo by interacting with the lipid anchor (*72*). Cargo transfer between LolA and LolB is believed to occur in a "mouth-to-mouth" fashion in which the two hydrophobic cavities align towards each other and the lipid anchor "slides through" from LolA to LolB, as suggested by surveying the LolA-LolB interaction surface via incorporation of photo-activatable amino acids (*73*). LolB has stronger affinity to OM lipoproteins than LolA, which thermodynamically drives the lipoproteins to the OM (*74*).

1.1.4. Outer membrane β-barrel protein assembly

1.1.4.1. Overview of membrane integral protein assembly

There are two different kinds of integral membrane proteins in living organisms, α-helical and β-barrel, which describe the structure of their characteristic membrane spanning domain (*4*). α-helical membrane proteins have helical bundles that leave hydrophobic amino acids on the outside of the bundles, engaging in hydrophobic interaction with membrane lipids. β-barrel membrane protein, on the contrary, spans the membrane by wrapping an extended β-sheet into a barrel shape. These β-barrels have hydrophobic amino acids facing outward to the lipids and

hydrophilic amino acids facing inward, forming a channel that allows the passage of small hydrophilic molecules to passively diffuse across the membrane.

Membrane insertion of α-helical integral membrane proteins has been extensively studied (Fig. 1. 10, *75, 76*). The Sec machinery folds and inserts each α-helical segment into the membrane by releasing the newly formed α-helix via a lateral gate in the machine (*77, 78*). This mechanism ensures that those individual helices are inserted into the membrane without exposing their hydrophobic residues to an aqueous environment.

Folding and assembly of membrane β-barrel proteins are less well understood. These proteins are found in the OM of Gram-negative bacteria and the outer membrane of mitochondria and chloroplasts. Machineries that responsible for their folding and assembly are conserved from bacteria to man, therefore, we focus on the assembly pathway in *E. coli* as a model of β-barrel protein assembly. Similar to OM lipoproteins, OM β-barrel proteins also cross the IM via the Sec channel, followed by the cleavage of signal peptide by signal peptidase. In the periplasm, they will interact with chaperones like SurA, Skp and DegP, which prevent OM β-barrel proteins from aggregation and keep them in a folding-competent state (*4, 79-84*). These chaperones are believed to deliver the unfolded OMPs to the β-barrel assembly machine at the OM where they are folded and inserted into the membrane (Fig. 1. 10).

Folding and assembly of OM β-barrel proteins face many challenges that are not seen at the assembly of IM α-helical proteins. Unlike α-helical proteins, in which each individual α-helix segments are relatively stable in a lipid membrane thus can be inserted into the membrane one-by-one, individual β-sheets are highly unstable in a hydrophobic environment as they would have unsatisfied H-bonds at the edges of the β-sheets. These H-bonds are only satisfied once the entire β-barrel structure is formed, thus the folding and membrane insertion of β-barrel proteins must be

a coupled step at the membrane. Additionally, unlike the assembly of IM integral proteins, which can utilize energy source like ATP, OMP assembly takes place at the OM where no apparent energy source is readily available.

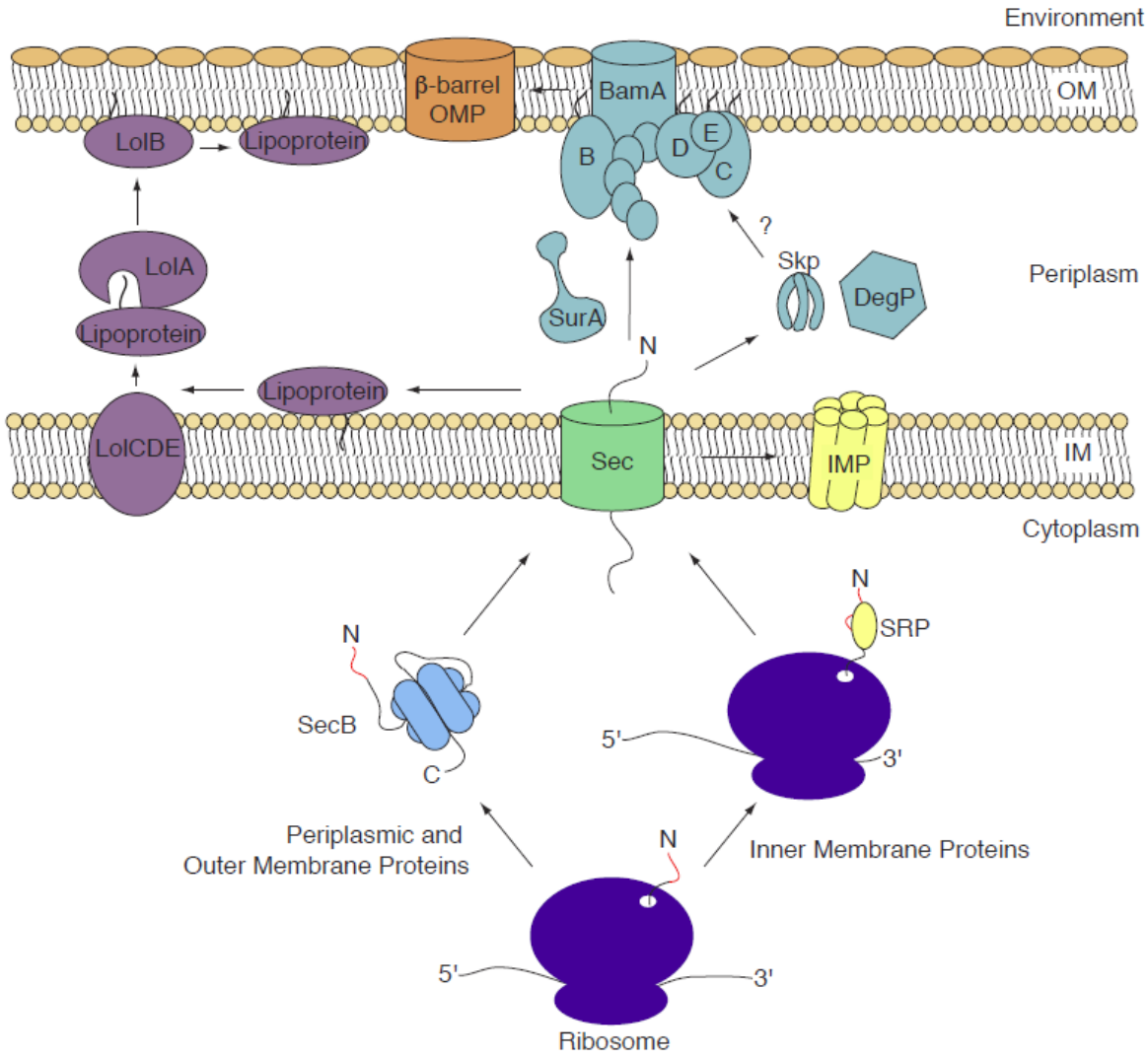

Figure 1. 10. (Taken directly from ref. 4 with caption) Cell envelope protein biogenesis. All proteins destined for the periplasm and two membranes are ribosomally synthesized in the cytoplasm. Inner membrane (IM) proteins (IMPs) are cotranslationally directed to Sec and inserted into the membrane, whereas periplasmic and outer membrane proteins (OMPs) are posttranslationally translocated. Soluble periplasmic proteins then fold in this second aqueous compartment. Outer membrane (OM) lipoproteins are lipidated at the outer leaflet of the IM and then transported to the OM by the Lol pathway. β-barrel OMPs transit the periplasm in unfolded

states with the help of chaperones and are then folded and inserted into the OM by the five-protein Bam complex.

1.1.4.2. Identification of the β-barrel assembly machine at the OM

Components of the machinery that assembles β-barrel proteins were identified through a series of discoveries. BamA, the central component of the Bam complex, was first identified by comparing sequence homology of *Neisseria meningitidis* and chloroplasts and found to be involved in OMP assembly (*85, 86*).

Other Bam proteins are not that conserved among species so they could not be identified by similar methods. BamB was identified by looking at specific suppressors that rescue OM permeability defects caused by a mutation in LptD (*lptD4213*) (*87, 88*). A *bamB* null mutation suppressed some OM defects in *lptD4213* by not allowing certain antibiotics from getting into the periplasm. Affinity purification using a his-tagged BamB revealed that BamB is in a complex with BamA and three other OM lipoproteins, BamC, D and E (*87, 90*). Bam proteins form a stable complex both *in vivo* and *in vitro*. The entire Bam complex can be pull down by any of the individual components. Stable sub-complexes with different Bam protein compositions can be over-expressed and purified (*91*).

1.1.4.3. Structure of Bam proteins

X-ray crystal structures of individual Bam components have been obtained very recently, although little is known with regard to how they interact with each other. The only complex that has been solved is BamCD.

BamA, the central component and the most well conserved protein of the Bam complex, has two domains: a soluble periplasmic domain and a membrane integrating β-barrel domain. In *E. coli*, the soluble periplasmic domain is consist of five POTRA (polypeptide transport associated) domains which are believed to interact with substrates and chaperones. The first piece of X-ray crystallographic structural information of the Bam components was on the POTRA domains of BamA from *E. coli* (*92*). Each POTRA domain consists of two α-helices and three β-strands. The five POTRA domains are the docking sites of Bam lipoproteins, as deleting the POTRA domains would result in dissociation of Bam lipoproteins (*92*). Deleting POTRA 5 (P5) disrupts the interaction between BamA and BamCDE, while deleting any of the P2-5 would cause BamB to dissociate. Based on the crystal structure, it is proposed that POTRA domains may engage OMP substrates via "β-strand augmentation", in which the edges of the unfolded OMP's β-strands interact with POTRA domains by forming H-bonds with the β-strands in those domains (*92*).

Very recently, X-ray crystallographic structures of BamA from *N. gonorrhoeae* and *H. ducreyi* have been obtained (Fig. 1. 11, *93*). The POTRA domains of BamA adopt two different conformations in relation to the β-barrel in those structures (Fig. 1. 11A-C). The POTRA domain (P4 and P5, as P1-3 is deleted in this structure) of BamA from *H. ducreyi* (*Hd*BamAΔ3) turns away from the β-barrel, leaving the barrel in an "open" state, while the POTRA from *N. gonorrhoeae* (*Ng*BamA) interacts with periplasmic loops of BamA, resulting in a "closed" conformation in which the periplasmic opening of the β-barrel is blocked by the P5 domain. The difference in the conformation of POTRA domains may imply a gating mechanism by which access of the β-barrel is regulated by the POTRA domain.

Another interesting structural feature arising from the two BamA structures is the conformation of the last β-strand in relation to the first (Fig. 1. 11D, *93*). In *Hd*BamAΔ3, β strand

1 and 16 form multiple H-bonds, closing the barrel as expected, however, in *Ng*BamA, β strand 1 and 16 are connected by only two H-bonds, while a large part of β strand 16 is tucked inside the lumen of the barrel (Fig. 1. 11D, *93*). This part of a destabilized barrel could potentially provide a lateral gate like that in the Sec machinery which allows substrates to enter the lipid membrane, however, it is not clear at all whether this destabilized β strand interaction is physiologically relevant to the function of BamA.

It is note-worthy from the structure of BamA that the hydrophobic belt from the β-barrel is greatly reduced on the side of the β1-β16 compared to the other side (*93*). On the β1-β16 side of the barrel, the hydrophobic belt is about 9Å thick, while on the opposite side, it is about 20Å. This seems to suggest that the thickness of the lipid membrane is asymmetric around BamA. The side of β1-β16 has a much thinner hydrophobic membrane than the opposite side, implying that BamA may distort the topology of membrane around it. Whether the BamA induced membrane distortion facilitates OMP assembly is not known.

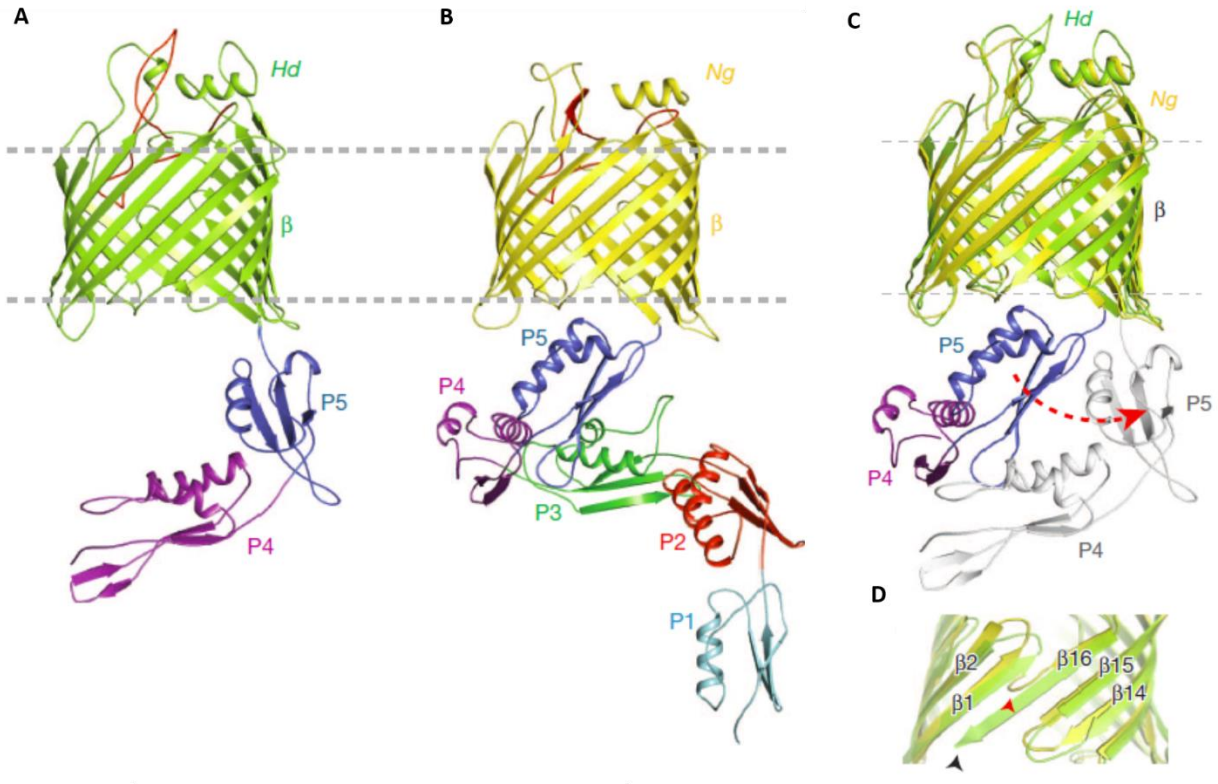

Figure 1.11. (Taken directly from ref. 93 with caption) Structure of BamA from *N. gonorrhoeae* and *H. ducreyi*. (A) The *Hd*BamAΔ3 crystal structure in cartoon representation showing the β-barrel (green) and POTRA domains 4 and 5 (purple and blue, respectively). (B) The *Ng*BamA crystal structure showing the β-barrel (gold) and POTRA domains 1–5 (cyan, red, green, purple and blue, respectively). (C) Alignment of *Hd*BamAΔ3 (green) and *Ng*BamA (gold) showing open and closed conformations for the POTRA domains, which may serve as a gating mechanism for regulating substrate access to the inside of the b-barrel. (D) Compared to *Hd*BamAΔ3 (green), β-strand 16 is disordered and tucked inside the b-barrel of *Ng*BamA (gold). Arrowheads indicate the location of the C-terminal strand in *Hd*BamA (black) and *Ng*BamA (red).

X-ray crystal structures of BamB, C, D, E were also obtained in recent years (*94-100*). However, how they function with BamA is still largely unknown.

1.1.4.4. Mechanistic studies of the Bam complex

How the Bam complex folds β-barrel proteins is still largely unknown. There are many challenges in trying to obtain a step-by-step mechanistic picture of β-barrel folding at the Bam machinery. It is difficult to observe intermediates during folding on the Bam complex as this is generally a highly efficient process, which means that half-finished products are extremely difficult to detect. We are going to discuss more about identifying and characterizing folding intermediate on the Bam complex in Chapter Three.

The Bam complex must recognize its substrates from the periplasm. It is believed that periplasmic chaperones, such as SurA, Skp, DegP and FkpA are responsible for maintaining unfolded β-barrel substrates in a folding competent state and delivering them to the Bam complex. SurA, the major chaperone in the periplasm, has been shown to chemically crosslink to BamA, suggesting that it directly interacts with BamA (*82, 101, 102*). Recently it has been shown that SurA interacts with P1 domain of BamA, which is consistent with its hypothesized role in delivering substrates to the periplasmic part of Bam complex (*101, 102*).

The process of Bam-assisted β-barrel assembly has recently been reconstituted from purified components in proteoliposomes (*91, 103, 104*). OmpT, an outer membrane protease was first used as a substrate for *in vitro* Bam-assisted β-barrel assembly in proteoliposome as it is convenient to take advantage of its protease activity as a reporter for β-barrel assembly (*91*). It was found that, when unfolded OmpT was pre-incubated with SurA and mixed with purified BamABCDE complex in a proteoliposome, the amount of folded OmpT increases with time (*91*). This process takes place without ATP or other energy source, which is consistent with the environment at the OM. It has also been demonstrated that the Bam complex was able to carry on multiple turnovers of the folding reaction, showing that this reconstituted folding process is also catalytic (*103*).

The assembly of BamA by the Bam complex has also been studied in proteoliposomes (*104*). In *E. coli*, there are only two essential β-barrel proteins at the OM, BamA and LptD; arguably, they are the most important substrates of the Bam complex. Interestingly, subcomponents of the Bam complex, some of which even without BamA, the central component, are able to assemble BamA into a membrane (*104*). Even a single lipoprotein, such as BamB, C, or D alone, are able to fold BamA, although less effectively than a complete Bam complex. Additionally, chaperones are not needed in BamA assembly as Bam complex is capable of inserting BamA into a membrane in the absence of SurA or any chaperone. These results indicate that BamA is a very special substrate of the Bam complex. We are going to characterize Bam assisted folding of LptD in Chaper Three.

1.2. Perspectives

In the past decade, the majority of, if not all, players in the LPS transport and OMP assembly pathways have been identified. Major achievements have been made in understanding how they function in the cell in the past few years during my PhD. Five years ago when I started my PhD, it was not at all clear how the Lpt machinery is assembled or how the Bam complex folds its substrates; as of now, we have yet to provide a complete answer to those questions but we have made significant progress towards answering them. Actually, structural and biochemical tools developed in recent years make us more powerful than ever in understanding how the OM is assembled.

This thesis describes the progress in trying to understand two central questions in OM biogenesis: 1. how does the biogenesis of the OM LPS translocon, the LptD/E complex take place

and, 2. how is the OM LPS translocon assembled by the Bam complex. We have extensively characterized the biogenesis pathway of the OM LPS translocon by identifying seven intermediates along the pathway, and further shown a different form of the Bam complex that is required in assembling the OM LPS translocon by characterizing folding intermediates on the Bam complex. These understandings may in the future allow the development of antibiotics that target these pathways to cure Gram-negative bacterial infections.

1.3. References

1. Nikaido H (2003) Molecular basis of bacterial outer membrane permeability revisited. *Microbiol Mol Biol Rev* 67:593-656.

2. Schulz GE (2002) The structure of bacterial outer membrane proteins. *Biochim Biophys Acta* 1565:308-317.

3. Sankaran K, Wu HC (1994) Lipid modification of bacterial prolipoprotein. Transfer of diacylglyeryl moiety from phosphatidylglycerol. *J Biol Chem* 269:19701-19706.

4. Hagan CL, Silhavy TJ, Kahne D (2011) β-Barrel membrane protein assembly by the Bam complex. *Annu Rev Biochem*. 80:189-210.

5. Ferguson AD, Deisenhofer J (2004) Metal import through microbial membranes. *Cell* 116:15-24.

6. Kostakioti M, Newman CL, Thanassi DG, Stathopoulos C (2005) Mechanisms of protein export across the bacterial outer membrane. *J Bacteriol* 187:4306-14.

7. Hinchliffe P, Symmons MF, Hughes C, Koronakis V (2013) Structure and operation of bacterial tripartite pumps. *Annu Rev Microbiol* 67:221-42.

8. Bos MP, Robert V, Tommassen J (2007) Biogenesis of the Gram-negative bacterial outer membrane. *Annu Rev Microbiol* 61:191-214.

9. Sankaran K, Wu HC (1994) Lipid modification of bacterial prolipoprotein. Transfer of diacylglyeryl moiety from phosphatidylglycerol. *J Biol Chem* 269:19701-19706.

10. Suzuki H, Nishimura Y, Yasuda S, Nishimura M, Yamada M, Hirota Y (1978) Murein-lipoprotein of *E. coli*: a protein involved in the stabilization of bacterial cell envelope. *Mol Gen Genet* 167:1-9.

11. Cascales E, Bernadac A, Gavioli M, Lazzaroni JC, Lloubes R (2002) Pal lipoprotein of *Escherichia coli* plays a major role in outer membrane stability. *J Bacteriol* 184:754-759.

12. Ruiz N, Kahne D, Silhavy TJ (2009) Transport of lipopolysaccharide across the cell envelope: the long road of discovery. *Nat Rev Microbiol* 7:677-683.

13. Bladen HA, Mergenhagen SE (1964) Ultrastructure of *Veillonella* and morphological correlation of an outer membrane with particles associated with endotoxic activity. *J Bacteriol* 88:1482–1492.

14. Raetz CRH, Whitfield C (2002) Lipopolysaccharide endotoxins. *Annu Rev Biochem* 71:635-700.

15. Mühlradt PF, Golecki JR (1975) Asymmetrical distribution and artifactual reorientation of lipopolysaccharide in the outer membrane bilayer of *Salmonella typhimurium*. *Eur J Biochem* 51:343-352.

16. Kamio Y, Nikaido H (1976) Outer membrane of *Salmonella typhimurium*: accessibility of phospholipid head groups to phospholipase C and cyanogen bromide activated dextran in the external medium. *Biochemistry* 15:2561-2570.

17. Funahara Y, Nikaido H (1975) Asymmetric localization of lipopolysaccharides on the outer membranes of *Salmonella typhimurium*. *J Bacteriol* 141:1463-1465.

18. Trent MS, Stead CM, Tran AX, Hankins JV (2006) Diversity of endotoxin and its impact on pathogenesis. *J Endotoxin Res* 12:205–223.

19. Raetz CR, Reynolds CM, Trent MS, Bishop RE (2007) Lipid A modification systems in Gram-negative bacteria. *Annu Rev Biochem* 76:295–329.

20. Sperandeo P et al. (2008) Functional analysis of the protein machinery required for transport of lipopolysaccharide to the outer membrane of Escherichia coli. *J Bacteriol* 190:4460–4469.

21. Ruiz N, Gronenberg LS, Kahne D, Silhavy TJ (2008) Identification of two inner-membrane proteins required for the transport of lipopolysaccharide to the outer membrane of *Escherichia coli*. *Proc Natl Acad Sci* USA 105:5537–5542.

22. Nishijima M, Raetz CR (1981) Characterization of two membrane-associated glycolipids from an Escherichia coli mutant deficient in phosphatidylglycerol. *J Biol Chem* 256:10690–10696.

23. Gioannini TL, Weiss JP (2007) Regulation of interactions of Gram-negative bacterial endotoxins with mammalian cells. *Immunol Res* 39:249-260.

24. Barb AW, Zhou P (2008) Mechanism and inhibition of LpxC: an essential zinc-dependent deacetylase of bacterial lipid A synthesis. *Curr Pharm Biotechnol* 9:9-15.

25. Cipolla L, Polissi A, Airoldi C, Galliani P, Sperandeo P, Nicotra F (2009) The Kdo biosynthetic pathway toward OM biogenesis as target in antibacterial drug design and development. *Curr Drug Discov Technol* 6:19-33.

26. Karow M, Georgopoulos C (1993) The essential *Escherichia coli msbA* gene, a multicopy suppressor of null mutations in the *htrB* gene, is related to the universally conserved family of ATP-dependent translocators. *Mol Microbiol* 7:69-79.

27. Zhou Z, White KA, Polissi A, Georgopoulos C, Raetz CRH (1998) Function of *Escherichia coli* MsbA, an essential ABC family transporter, in lipid A and phospholipid biosynthesis. *J Biol Chem* 273:12466-12475.

28. Doerrler WT, Gibbons HS, Raetz CRH (2004) MsbA-dependent translocation of lipids across the inner membrane of *Escherichia coli*. *J Biol Chem* 279:45102-45109.

29. Ward A, Reyes CL, Jodie Y, Roth CB, Chang G (2007) Flexibility in the ABC transporter MsbA: alternating access with a twist. *Proc Natl Acad Sci* USA 104:19005-19010.

30. Sperandeo P, Dehò G, Polissi A (2009) The lipopolysaccharide transport system of Gram-negative bacteria. *Biochim Biophy Acta* 1791:594-602.

31. Sperandeo P, Cescutti R, Villa R, di Benedetto C, Candia D, Dehò G, Polissi A (2007) Characterization of *lptA* and *lptB*, two essential genes implicated in lipopolysaccharide transport to the outer membrane of *Escherichia coli*. *J Bacteriol* 189:244-253.

32. Sperandeo P, Lau FK, Carpentieri A, de Castro C, Molinaro A, Dehò G, Silhavy TJ, Polissi A (2008) Functional analysis of protein machinery required for transport of lipopolysaccharide to the outer membrane of *Escherichia coli*. *J Bacteriol* 190:4460-4469.

33. Ruiz N, Gronenberg L, Kahne D, Silhavy TJ (2008) Identification of two inner-membrane proteins required for transport of lipopolysaccharide to the outer membrane of *Escherichia coli*. *Proc Natl Acad Sci* USA 105:5537-5542.

34. Narita S, Tokuda H (2009) Biochemical characterization of an ABC transporter LptBFGC complex required for the outer membrane sorting of lipopolysaccharides. *FEBS Lett* 583:2160-2164.

35. Gronenberg LS, Kahne D (2010) Development of an activity assay for discovery of inhibitors of lipopolysaccharide transport. *J Am Chem Soc* 132:2518-2519.

36. Sherman DJ, Okuda S, Denny WA, Kahne D (2013) Validation of inhibitors of an ABC transporter required to transport lipopolysaccharide to the cell surface in Escherichia coli. *Bioorg Med Chem.* 21(16):4846-51.

37. Sherman DJ, Ruiz N, Liu C, Kahne D (2014) *Proc Natl Acad Sci* USA *in press*.

38. Okuda S, Freinkman E, Kahne D (2012) Cytoplasmic ATP hydrolysis powers transport of lipopolysaccharide across the periplasm in E. coli. *Science*. 338(6111):1214-7.

39. Braun M, Silhavy TJ (2002) Imp/OstA is required for cell envelope biogenesis in *Escherichia coli*. *Mol Microbiol* 45:1289-1302.

40. Bos MP, Tefsen B, Geurtsen J, Tommassen J (2004) Identification of an outer membrane protein required for the transport of lipopolysaccharide to the bacterial cell surface. *Proc Natl Acad Sci* USA 101:9417-9422.

41. Wu T, McCandlish AC, Gronenberg LS, Chng SS, Silhavy TJ, Kahne D (2006) Identification of a protein complex that assembles lipopolysaccharide in the outer membrane of *Escherichia coli*. *Proc Natl Acad Sci* USA 103:11754-11759.

42. Chng SS, Ruiz N, Chimalakonda G, Silhavy TJ, Kahne D (2010) Characterization of the two-protein complex in *Escherichia coli* responsible for lipopolysaccharide assembly at the outer membrane. *Proc Natl Acad Sci* USA 107:5363-5368.

43. Ruiz N, Chng SS, Hiniker A, Kahne D, Silhavy TJ (2010) Non-consecutive disulfide bond formation in an essential integral outer membrane protein. *Proc Natl Acad Sci* USA. 107(27):12245-50.

44. Freinkman E, Chng S-S, Kahne D (2011). The complex that inserts lipopolysaccharide into the bacterial outer membrane forms a two-protein plug-and-barrel. *Proc Natl Acad Sci* USA. 108(6):2486-91.

45. Ma B, Reynolds CM, Raetz CR (2008) Periplasmic orientation of nascent lipid A in the inner membrane of an *Escherichia coli* LptA mutant. *Proc Natl Acad Sci* USA 105:13823-13828.

46. Suits MD, Sperandeo P, Dehò G, Polissi A, Jia Z (2008) Novel structure of conversed Gram-negative lipopolysaccharide transport protein A and mutagenesis analysis. *J Mol Biol* 380:476-488.

47. Tran AX, Trent MS, Whitfield C (2008) The LptA protein of *Escherichia coli* is a periplasmic lipid A-binding protein involved in the lipopolysaccharide export pathway. *J Biol Chem* 283:20342-20349.

48. Freinkman E, Okuda S, Ruiz N, Kahne D (2012) Regulated assembly of the transenvelope protein complex required for lipopolysaccharide export. *Biochemistry*. 51(24):4800-6
49. Chng SS, Gronenberg LS, Kahne D (2010) Proteins required for lipopolysaccharide assembly in *Escherichia coli* form a trans-envelope complex. *Biochemistry*, 49(22):4565-7

50. Sampson BA, Misra R, Benson SA (1989) Identification and characterization of a new gene of *Escherichia coli* K-12 involved in outer membrane permeability. *Genetics* 122:491-501.

51. Bos MP, Tefsen B, Geurtsen J, Tommassen J (2004) Identification of an outer membrane protein required for the transport of lipopolysaccharide to the bacterial cell surface. *Proc Natl Acad Sci* USA 101:9417-9422

52. Steeghs L, den Hartog R, den Boer A, Zomer B, Roholl P, van der Ley P (1998) Meningitis bacterium is viable without endotoxin. *Nature* 392:449-450

53. Serina S, Nozza F, Nicastro G, Faggioni F, Mottl H, Dehò G, Polissi A (2004) Scanning the *Escherichia coli* chromosome by random transposon mutagenesis and multiple phenotypic screening. *Res Microbiol* 155:692-701.

54. Sperandeo P, Pozzi C, Dehò G, Polissi A (2006) Non-essential KDO biosynthesis and new essential cell envelope biogenesis genes in the *Escherichia coli yrbG-yhbG* locus. *Res Microbiol* 157:547-558.

55. Meredith TC, Mamat U, Kaczynski Z, Lindner B, Holst O, Woodard RW (2007) Modification of lipopolysaccharide with colanic acid (M-antigen) repeats in *Escherichia coli*. *J Biol Chem* 282:7790-7798.

56. Bayer ME (1968) Areas of adhesion between wall and membrane of *Escherichia coli*. *J Gen Microbiol* 53:395-404.

57. Bayer ME (1991) Zones of membrane adhesion in the cryofixed envelope of *Escherichia coli*. *J Struct Biol* 107:268-280.

58. Mühlradt PF, Menzel J, Golecki JR, Speth V (1973) Outer membrane of *Samonella*: sites of export of newly synthesized lipopolysaccharide on the bacterial surface. *Eur J Biochem* 35:471-481.

59. Ishidate K, Creeger ES, Zrike J, Deb S, Glauner B, MacAlister TJ, Rothfield LI (1986) Isolation of differentiated membrane domains from *Escherichia coli* and *Salmonella typhimurium*, including a fraction containing attachment sites between the inner and outer membranes and the murein skeleton of the cell envelope. *J Biol Chem* 261:428-443.

60. Tefsen B, Geurtsen J, Beckers F, Tommassen J, de Cock H (2005) Lipopolysaccharide transport to the bacterial outer membrane in spheroplasts. *J Biol Chem* 280:4504-4509.

61. Tran AX, Dong C, Whitfield C. (2010) Structure and functional analysis of LptC, a conserved membrane protein involved in the lipopolysaccharide export pathway in Escherichia coli. *J Biol Chem.* 285(43):33529-39.

62. Hu KY, Saier MH Jr (2006) Bioinformatics analyses of Gram-negative bacterial OstA outer membrane assembly homologues. *Curr Genomics* 7:447-461.

63. Tokuda H (2009) Biogenesis of outer membranes in Gram-negative bacteria. *Biosci Biotechnol Biochem* 73:80778-1-9.

64. Tokuda H, Matsuyama S (2004) Sorting of lipoproteins to the outer membrane in *E. coli*. *Biochim Biophys Acta* 1694:IN1-9.

65. Driessen AJ, Nouwen N (2008) Protein translocation across the bacterial cytoplasmic membrane. *Annu Rev Biochem* 77:643-667.

66. Sankaran K, Wu HC (1994) Lipid modification of bacterial prolipoprotein. Transfer of diacylglyeryl moiety from phosphatidylglycerol. *J Biol Chem* 269:19701-19706.

67. Yakushi T, Yokota N, Matsuyama S, Tokuda H (1998) LolA-dependent release of a lipid-modified protein from the inner membrane of *Escherichia coli* requires nucleotide triphosphate. *J Biol Chem* 273:32576-32581.

68. Yakushi T, Masuda K, Narita S, Matsuyama S, Tokuda H (2000) A new ABC transporter mediating the detachment of lipid-modified proteins from membranes. *Nat Cell Biol* 2:212-218.

69. Ito Y, Kanamaru K, Taniguchi N, Miyamoto S, Tokuda H (2006) A ligand-bound ABC transporter, LolCDE, provides insights into molecular mechanisms underlying membrane detachment of lipoproteins. *Mol Microbiol* 62:1064-1075.

70. Matsuyama S, Tajima T, Tokuda H (1995) A novel periplasmic carrier protein involved in the sorting and transport of *Escherichia coli* lipoproteins destined for the outer membrane. *EMBO J* 14:3365-3372.

71. Yamaguchi K, Yu F, Inouye M (1988) A single amino acid determinant of the membrane localization of lipoproteins in *E. coli*. *Cell* 53:423-432.

72. Takeda K, Miyatake H, Yokota N, Matsuyama S, Tokuda H, Miki K (2003) Crystal structures of bacterial lipoprotein localization factors, LolA and LolB. *EMBO J* 22:3199-3209.

73. Okuda S, Tokuda H (2009) Model of mouth-to-mouth transfer of bacterial lipoproteins through inner membrane LolC, periplasmic LolA, and outer membrane LolB. *Proc Natl Acad Sci* USA 106:5877-82.

74. Taniguchi N, Matsuyama S, Tokuda H (2005) Mechanisms underlying energy-independent transfer of lipoproteins from LolA to LolB, which have similar unclosed β-barrel structures. *J Biol Chem* 280:34481-34488.

75. Driessen AJ, Nouwen N. 2008. Protein translocation across the bacterial cytoplasmic membrane. *Annu. Rev. Biochem*. 77: 643-67

76. Rapoport TA. 2007. Protein translocation across the eukaryotic endoplasmic reticulum and bacterial plasma membranes. *Nature.* 450: 663-9

77. Van den Berg B, Clemons WM, Jr., Collinson I, Modis Y, Hartmann E, et al. 2004. X-ray structure of a protein-conducting channel. Nature. 427: 36-44

78. Zimmer J, Nam Y, Rapoport TA. 2008. Structure of a complex of the ATPase SecA and the protein-translocation channel. Nature. 455: 936-43

79. Ureta AR, Endres RG, Wingreen NS, Silhavy TJ (2007) Kinetic analysis of the assembly of the outer membrane protein LamB in *Escherichia coli* mutants each lacking a secretion or targeting factor in a different cellular compartment. *J Bacteriol* 189:446-454.

80. Schäfer U, Beck K, Müller M (1999) Skp, a molecular chaperone of Gram-negative bacteria, is required for the formation of soluble periplasmic intermediates of outer membrane proteins. *J Biol Chem* 274:24567-24574.

81. Harms N, Koningstein G, Dontje W, Muller M, Oudega B, Luirink J, de Cock H (2001) The early interaction of the outer membrane protein PhoE with the periplasmic chaperone Skp occurs at the cytoplasmic membrane. *J Biol Chem* 276:18804-18811.

82. Sklar JG, Wu T, Kahne D, Silhavy TJ (2007) Defining the roles of the periplasmic chaperones SurA, Skp and DegP in *Escherichia coli*. *Genes Dev* 21:2473-2484.

83. Rizzitello AE, Harper JR, Silhavy TJ (2001) Genetic evidence for parallel pathways of chaperone activity in the periplasm of *Escherichia coli*. *J Bacteriol* 183:6794-6800.

84. Vertommen D, Ruiz N, Leverrier P, Silhavy TJ, Collet JF (2009) Characterization of the role of the *Escherichia coli* periplasmic chaperone SurA using differential proteomics. *Proteomics* 9:2432-2443.

85. Reumann S, Davila-Aponte J, Keegstra K (1999) The evolutionary origin of the proteintranslocating channel of chloroplastic envelope membranes: identification of a cyanobacterial homolog. *Proc Natl Acad Sci* USA. 96: 784-9.

86. Voulhoux R, Bos MP, Geurtsen J, Mols M, Tommassen J (2003) Role of a highly conserved bacterial protein in outer membrane protein assembly. *Science* 299: 262-5.

87. Wu T, Malinverni JC, Ruiz N, Kim S, Silhavy TJ, Kahne D (2005) Identification of a multi-component complex required for outer membrane biogenesis in *Escherichia coli*. *Cell* 121:235-245.

88. Ruiz N, Falcone B, Kahne D, Silhavy TJ (2005) Chemical conditionality: a genetic strategy to probe organelle assembly. *Cell* 121: 307-17.

89. Ruiz N, Wu T, Kahne D, Silhavy TJ (2006) Probing the barrier function of the outer membrane with chemical conditionality. *ACS Chem Biol* 1: 385-95.

90. Sklar JG, Wu T, Gronenberg LS, Malinverni JC, Kahne D, Silhavy TJ (2007) Lipoprotein SmpA is a component of the YaeT complex that assembles outer membrane proteins in *Escherichia coli*. *Proc Natl Acad Sci* USA 104: 6400-5.

91. Hagan CL, Kim S, Kahne D (2010) Reconstitution of outer membrane protein assembly from purified components. *Science* 328: 890-2.

92. Kim S, Malinverni JC, Sliz P, Silhavy TJ, Harrison SC, Kahne D (2007) Structure and function of an essential component of the outer membrane protein assembly machine. *Science* 317:961-964.

93. Noinaj N, Kuszak AJ, Gumbart JC, Lukacik P, Chang H, Easley NC, Lithgow T, Buchanan SK (2013) Structural insight into the biogenesis of β-barrel membrane proteins. *Nature.* 501(7467):385-90.

94. Noinaj N, Fairman JW, Buchanan SK (2011) The crystal structure of BamB suggests interactions with BamA and its role within the BAM complex. *J Mol Biol* 407:248–260.

95. Heuck A, Schleiffer A, Clausen T (2011) Augmenting β-augmentation: structural basis of how BamB binds BamA and may support folding of outer membrane proteins. *J Mol Biol* 406:659–666.

96. Kim KH, Aulakh S, Paetzel M (2011) Crystal structure of β-barrel assembly machinery BamCD protein complex. *J Biol Chem* 286:39116–39121.

97. Albrecht R, Zeth K (2011) Structural basis of outer membrane protein biogenesis in bacteria. *J Biol Chem* 286:27792–27803.

98. Sandoval CM, Baker SL, Jansen K, Metzner SI, Sousa MC (2011) Crystal structure of BamD: an essential component of the b-barrel assembly machinery of gram-negative bacteria. *J Mol Biol* 409:348–357.

99. Dong C, Hou, HF, Yang X, Shen YQ, Dong, YH (2012) Structure of *Escherichia coli* BamD and its functional implications in outer membrane protein assembly. *Acta Crystallogr D* 68, 95–101.

100. Knowles TJ et al (2011) Structure and function of BamE within the outer membrane and the beta-barrel assembly machine. *EMBO Rep* 12:123–128.

101. Bennion D, Charlson ES, Coon E, Misra R (2010) Dissection of β-barrel outer membrane protein assembly pathways through characterizing BamA POTRA 1 mutants of *Escherichia coli*. *Mol Microbiol* 77(5):1153-71.

102. Workman P, Heide K, Giuliano N, Lee N, Mar J, Vuong P, Bennion D, Misra R (2012) Genetic, biochemical, and molecular characterization of the polypeptide transport-associated domain of *Escherichia coli* BamA. *J Bacteriol* 194(13):3512-21.

103. Hagan CL, Kahne D (2011) The reconstituted Escherichia coli Bam complex catalyzes multiple rounds of β-barrel assembly. *Biochemistry* 50(35):7444-6.

104. Hagan CL, Westwood DB, Kahne D (2013) Bam Lipoproteins Assemble BamA in Vitro. *Biochemistry*.52(35):6108-13.

Chapter Two

Characterization of the Biogenesis Pathway of the Outer Membrane Lipopolysaccharide Translocon

Part of this chapter is adapted from
S. S. Chng*, **M. Xue***, R. A. Garner, H. Kadokura, D. Boyd, J. Beckwith, D. Kahne. *Science* **337**, 1665-1668 (2012). Disulfide Rearrangement Triggered by Translocon Assembly Controls Lipopolysaccharide Export

*: equal contribution

2.1. Introduction

As mentioned in Chapter One, the OM of Gram-negative bacteria, which is essential for survival, is an architecturally complex structure comprising an asymmetric bilayer that functions as a highly effective permeability barrier (*1*-*3*). The OM asymmetric bilayer cannot self-assemble but instead results from the operation of several sophisticated machines that span three compartments: the IM, the periplasm, and the OM itself. LPS, which is located exclusively in the outer leaflet of the OM, is the single most important determinant of the permeability barrier (*3*). LPS is placed on the cell surface by a translocon comprising two proteins, LptD and LptE (*4, 5*). LptD is a β-barrel protein that is folded and inserted into the outer membrane by the Bam machine (*6*); LptE is an OM lipoprotein that is sorted to the inner leaflet of the outer membrane by the Lol pathway (localization of lipoprotein) (*7*).

The two essential OM proteins, LptD and LptE, form a tightly associated plug-and-barrel structure (*8*). As the OM component of a seven-protein, trans-envelope structure that moves LPS from the IM to the OM, they serve together as the OM LPS translocon that facilitates the final insertion of LPS to the outer leaftlet of the OM (*8*-*10*). Depletion of any of the seven Lpt proteins leads to accumulation of LPS in the IM (*11*), suggesting that LPS export thus does not progress beyond a very early stage unless the entire Lpt machine is intact. How a cell assembles the seven-protein trans-envelope complex with components in three distinct compartments is unknown. Even assembly of the two-protein OM LPS translocon presents a challenging problem since the two proteins comprising the translocon are targeted via separate pathways and must form a plug-barrel architecture at the OM (*9*). Furthermore, the formation of proper disulfide bonds is required for this translocon to function (*9*).

This chapter describes our efforts in elucidating the oxidative assembly pathway of the OM LPS translocon, showing how cells use disulfide bond formation to coordinate LPS transport function with other processes in OM biogenesis. Using methods to identify different oxidized forms of LptD, we have extensively characterized its *in vivo* folding and assembly pathway in wild-type *E. coli*, and have studied a set of mutants containing defects in translocon assembly. We identified and characterized seven intermediates along the folding and assembly pathway of the translocon. In collaboration with Dr. Hiroshi Kadokura from the Beckwith Group, and Dr. Shu Sin Chng and Aaron Garner from our group, we demonstrate that a species with non-functional disulfide bonds that accumulates in mutants of defective LptD or LptE is an intermediate along the biogenesis of the LPS translocon. We further show that the rate limiting step of the biogenesis pathway is the folding and assembly of this intermediate. We also demonstrate that DsbA, a periplasmic oxidase, participates in this pathway during two different stages. This pathway includes unanticipated mechanisms for the formation of correct disulfide bonds in a protein.

2.2. Results and Discussion

2.2.1 A non-native disulfide-bonded intermediate (1) is observed during oxidative folding of LptD *in vivo*

As mentioned in Chapter One, *E. coli* LptD contains an N-terminal periplasmic domain (a.a. 25-202) and a C-terminal integral membrane β-barrel domain (a.a. 203-784) (*9*), which is folded and inserted into the OM by the Bam complex (β-barrel assembly machine) (*12-14*). LptD has four cysteines, two in the N-terminal domain at positions 31 and 173, and two very near the C-terminus at positions 724 and 725 (Fig. 2.1). In its mature form, LptD contains two long-range non-consecutive disulfide bonds connecting the N- and C-terminal domains, one between the first

and third cysteines (Cys_{31}-Cys_{724} or **[1-3]),** and the other between the second and fourth cysteines (Cys_{173}-Cys_{725} or **[2-4]**) (Fig. 1 and 2A) (*15*). However, either of these two disulfides is sufficient for LptD to function (*15*).

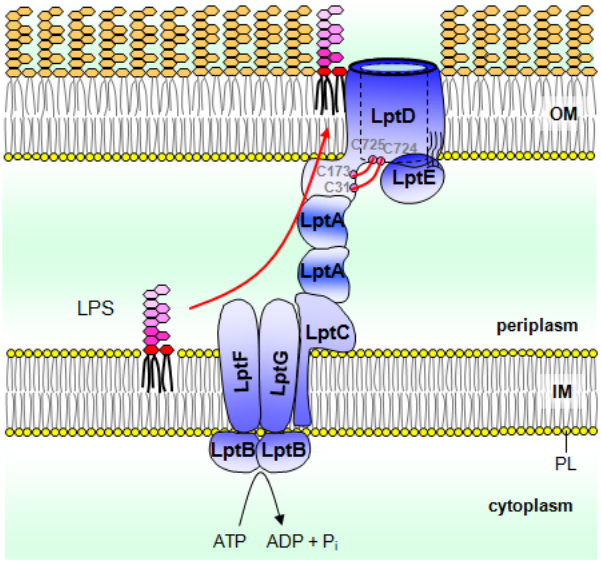

Figure 2.1. The Lpt machinery forms a trans-envelope bridge that exports LPS to the cell surface (*10*). LptBFGC forms an ABC transporter that releases LPS from the periplasmic side of the IM using ATP hydrolysis. LptD and LptE form the OM LPS translocon that inserts LPS into the outer leaflet of the OM. LptA presumably connects the IM ABC transporter to the OM LPS translocon, providing a path for LPS transit across the periplasm. LptD contains two non-consecutive disulfide bonds formed between its four cysteine residues as indicated.

To identify mechanisms that might trigger assembly of the functional OM LPS translocon, we examined the genesis of mature **[1-3][2-4]**-LptD and asked whether it would be possible to detect intermediate LptD species *in vivo*. Since we knew that LptE is required to produce mature LptD (*15*), we assumed it might be possible to accumulate an intermediate when LptE is the limiting reagent. Depletion of LptE results in cell death, so we chose to study LptD oxidation in viable strains that produce much lower levels of LptE compared to wild-type cells (Fig. 2.2) (*5*).

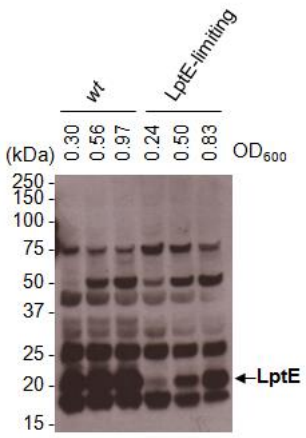

Figure. 2.2. A previously-reported LptE-limiting strain (*5*) makes different levels of LptE protein (lower than the wild-type strain) at various stages of growth even under non-depletion conditions. α-LptE immunoblot analysis of whole cell lysates obtained from wild-type (*wt*) or the LptE-limiting strain. Cells were sampled at early-, mid- and late-log phase (OD_{600} ~ 0.25, 0.5 and 0.9 respectively). Positions of relevant molecular weight markers are indicated in kDa.

OM fragments isolated from wild-type cells contain only mature LptD, which migrates more slowly during SDS-PAGE than reduced LptD (Fig. 2.3A) (*15*, *16*). In contrast, OM fragments from the LptE-limiting strain contain a new LptD species. In the absence of β-mercaptoethanol, this species migrates slightly faster than fully reduced LptD, suggesting that it is a disulfide-bonded form of LptD (Fig. 2.3A, compare lanes 1 and 2 with lanes 3 and 4). To assign the disulfide connectivity of this LptD species (intermediate **1**), we examined the SDS-PAGE migration patterns of the six LptD mutant proteins in which two of the cysteines were changed to serine (*15*). As might be expected for a protein containing only one disulfide between adjacent residues Cys_{724} and Cys_{725} (**[3-4]**) in the C-terminus, the mutant lacking the first two cysteines ($LptD_{SSCC}$) runs at the same position as reduced LptD (Fig. 2.4). Like wild-type LptD ($LptD_{CCCC}$), the other LptD mutants lacking two cysteines but are able to make disulfide bonds *between* the N- and C-terminal domains (e.g. $LptD_{SCSC}$ and $LptD_{CSCS}$) display slower mobility than reduced LptD on a gel (Fig. 2.4) (*15*). Only the mutant lacking the last two cysteines ($LptD_{CCSS}$), which can make

the Cys_{31}-Cys_{173} (**[1-2]**) disulfide bond *within* the N-terminal domain, exhibits faster mobility than reduced LptD (Fig. 2.3B and Fig. 2.4). Based on these results, we concluded that the LptD intermediate **1** that accumulates when LptE is limiting contains the consecutive **[1-2]** disulfide bond. As metioned below (section **2.2.6**), intermediate **1** may also contains the other consecutive **[3-4]** disulfide bond. Thus, the presence of LptE is required for the conversion of this intermediate to LptD with its native disulfide bonds.

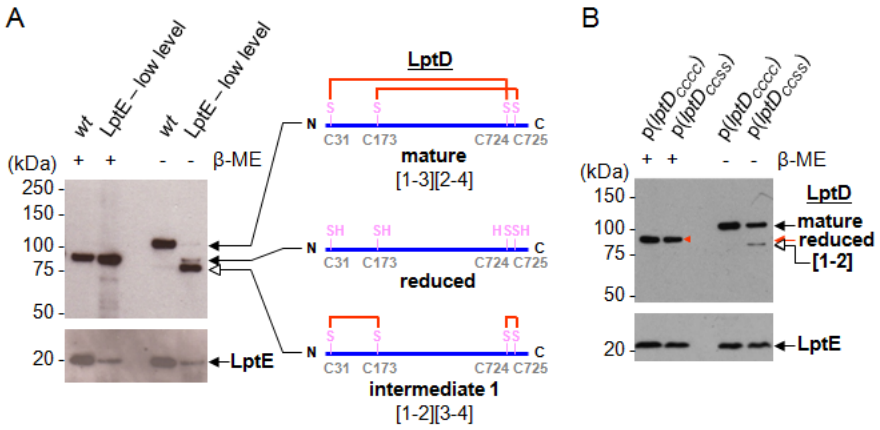

Figure 2.3. An LptD species containing non-functional disulfide bond is accumulated when LptE is limiting. (*A*) α-LptD and α-LptE immunoblot analyses of OM fragments obtained from wild-type cells (*wt*) or cells expressing low levels of LptE. OM fragments were isolated from cells grown to early-log phase (see Fig. 2.2). Three times more membranes from cells expressing low levels of LptE were loaded. Disulfide connectivity for each LptD species is shown on the right. (*B*) α-LptD and α-LptE immunoblot analyses of OM fragments obtained from *wt* cells expressing a second copy of LptD from a plasmid (p(*lptD*$_{CCCC}$) or p(*lptD*$_{CCSS}$)).

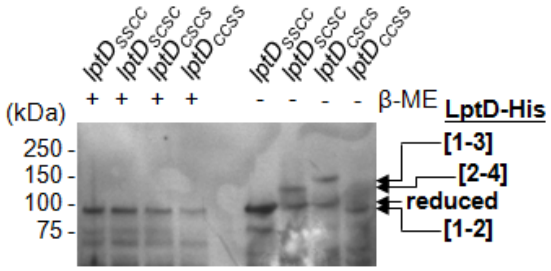

Figure. 2.4. The $LptD_{CCSS}$ double cysteine-less mutant protein migrates slightly faster than reduced LptD during non-reducing SDS-PAGE. α-His immunoblot analysis of OM fragments obtained from wild-type cells expressing $LptD_{SSCC}$-His, $LptD_{SCSC}$-His, $LptD_{CSCS}$-His or

$LptD_{CCSS}$-His (*15*). Where indicated, β-mercaptoethanol (β-ME) was used to reduce disulfide bonds.

2.2.2. Intermediate 1 is "on-pathway" to mature LptD

To determine whether the consecutive disulfide-bonded **[1-2][3-4]**-LptD (intermediate **1**) represents an on-pathway intermediate species produced during the assembly of mature LptD in the membrane, or a dead-end species that falls off-pathway as a product of the cellular condition where LptE is the limiting reagent, we carried out pulse-labeling experiments in a wild-type strain. We pulse-labeled $FLAG_3$-tagged LptD with [^{35}S]-methionine and monitored its progression to the mature form during a cold methionine chase. The predominant form at the start of the chase is **[1-2][3-4]**-LptD (intermediate **1),** which is slowly converted to the mature **[1-3][2-4]**-LptD species over time (Fig. 2.5A). Intermediate **1** cannot be chemically modified by thiol alkylating agents (e.g. poly(ethylene glycol) conjugated to maleimide, Fig. 2.5B), consistent with its having both the **[1-2]** and **[3-4]** disulfide bonds. The final distribution of LptD species at the end of the chase (~20 min) is identical to that at steady state, as detected in OM fragments (Fig. 2.6). This experiment establishes the intermediacy of a non-native disulfide-bonded species (intermediate **1**; **[1-2][3-4]**-LptD) along the oxidative folding pathway of LptD *in vivo*. Furthermore, the results imply that formation of the mature **[1-3][2-4]**-LptD species proceeds via disulfide bond rearrangement.

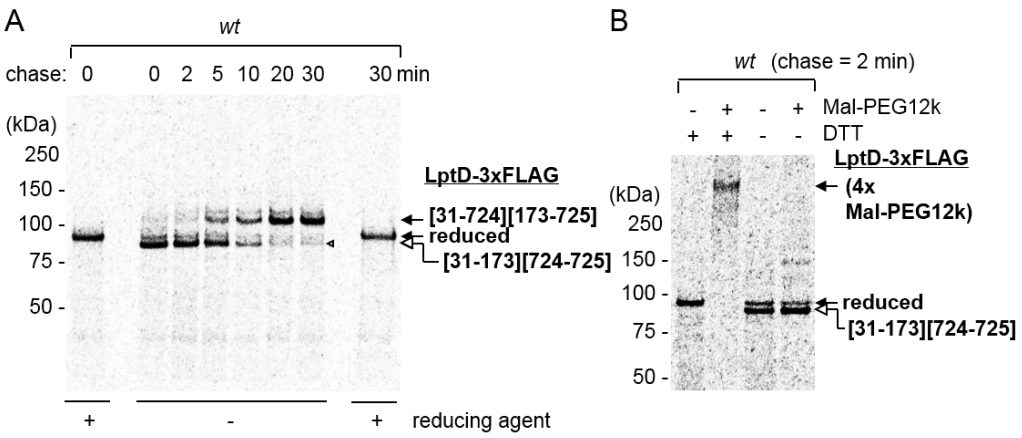

Figure 2.5. LptD containing the non-native Cys_{31}-Cys_{173} ([1-2]) and Cys_{724}-Cys_{725} ([3-4]) disulfide bonds (intermediate **1**) is an intermediate along the LptD assembly pathway *in vivo*. (*A*) [^{35}S]-Met pulse-chase of newly-synthesized LptD-$FLAG_3$ in a wild-type background. Wild-type cells expressing LptD-$FLAG_3$ were pulsed for 2 min with [^{35}S]-methionine and chased with cold methionine. The samples were NEM-alkylated, immunoprecipitated with α-FLAG antibody, and analyzed by SDS-PAGE/autoradiography. (*B*) Maleimidyl-PEG (Mal-PEG12k) alkylation of [^{35}S]-labeled intermediate **1** (**[1-2][3-4]**-LptD) from (*A*). Where indicated, β-mercaptoethanol (β-ME) or dithiothreitol (DTT) was used to reduce disulfide bonds. Positions of relevant molecular weight markers are indicated in kDa.

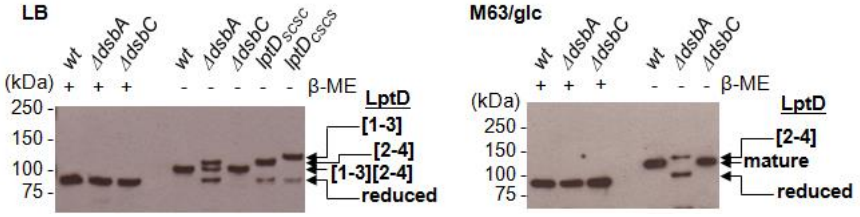

Figure. 2.6. LptD containing the non-consecutive Cys_{173}-Cys_{725} (**[2-4]**) disulfide bond accumulates in the absence of DsbA. α-LptD Immunoblot analysis of OM fragments obtained from *wt*, *ΔdsbA* and *ΔdsbC* cells grown in rich (LB) or minimal media (M63/glc). OM fragments from $lptD_{SCSC}$ and $lptD_{CSCS}$ (*15*) were loaded as position markers for LptD species containing either the Cys_{173}-Cys_{725} (**[2-4]**) or Cys_{31}-Cys_{724} (**[1-3]**) disulfide bonds, respectively.

2.2.3. Folding of the β-barrel domain is slow and precedes disulfide bond rearrangement

The Bam machine must assemble the β-barrel domain of LptD in the OM compartment (*12-14*). We asked whether formation of the disulfide bonds in mature LptD occurs before β-barrel folding, or vice versa. To address this question, we performed pulse-chase experiments under

different conditions that do not denature a folded β-barrel so we could analyze the folded states of the disulfide-bonded LptD species. Two different measures of structure have been developed for β-barrel proteins; folding of β-barrel membrane proteins can be followed by detecting changes in SDS-PAGE mobility upon heat denaturation (heat modifiability) or by monitoring protease susceptibility (*9*). Using a "seminative" SDS-PAGE, we observed that without heating, the β-barrel domain of wild-type mature **[1-3][2-4]**-LptD remains folded and the protein migrates as a broad band that has faster gel mobility than the unfolded mature form (Fig. 2.7A, compare *wt* "–" with "+" heat) (*9*). The amount of folded **[1-3][2-4]**-LptD increases with time (beginning around t = 2 min) and persists throughout the chase. Interestingly, a new long-lived fast-migrating LptD species, appearing at t = 0 min and chasing away by t = 20 min, can be detected (Fig. 2.7A, *wt* "–" heat, double open arrowhead). This species is also heat modifiable (absent in *wt* "+" heat) and it runs at the same position as the major band in the $LptD_{CCSS}$ sample containing the **[1-2]** disulfide bond (Fig. 2.7A, $lptD_{CCSS}$ "–" heat, double asterisks). We assign this LptD species as intermediate **1** (**[1-2][3-4]**-LptD) containing a folded β-barrel. Since the folded form of intermediate **1** chases to folded mature **[1-3][2-4]**-LptD, we conclude that the Bam machine folds the β-barrel domain of LptD before the disulfide rearrangement occurs. Because this **[1-2][3-4]**-LptD species never substantially accumulates during the chase, we conclude that folding is slower than rearrangement.

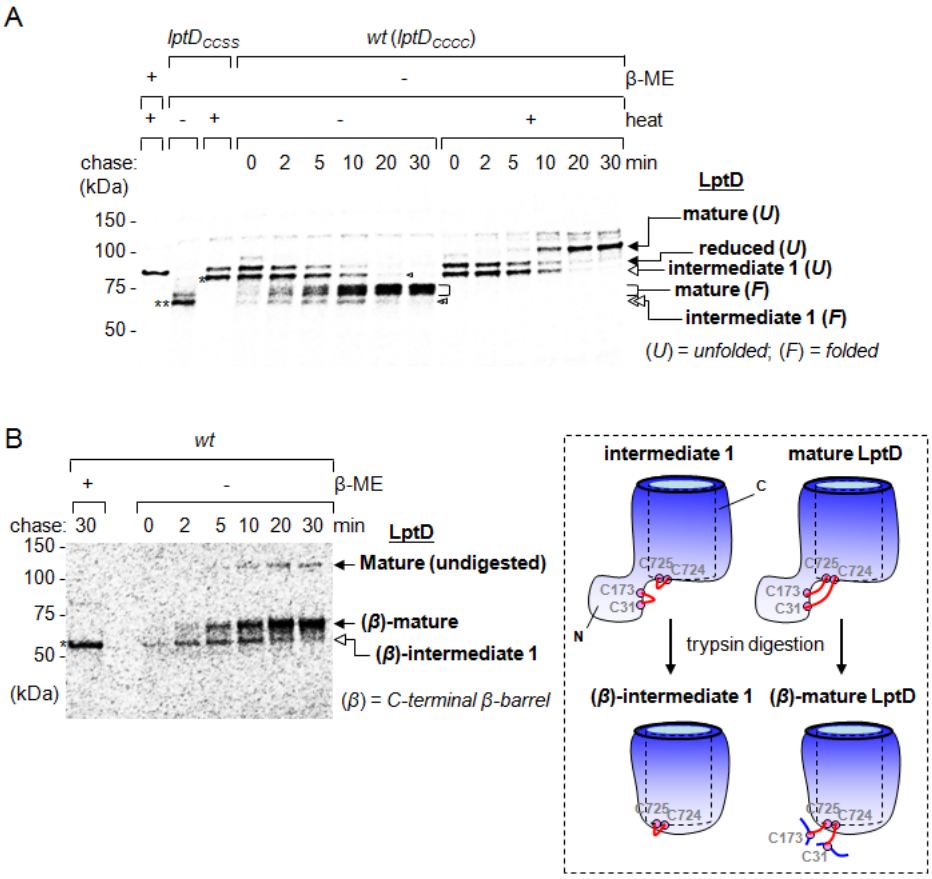

Figure 2.7. Folding of the LptD β-barrel domain is slow and precedes disulfide bond rearrangement. (*A*) Seminative [^{35}S]-Met pulse-chase of newly-synthesized LptD-FLAG$_3$ in a wild-type background. Samples were processed using non-denaturing conditions and analyzed by seminative SDS-PAGE that preserve (- heat) or denature (+ heat) the β-barrel fold. Pulse-labeled LptD$_{CCSS}$-FLAG$_3$ was used as a control to indicate the positions of unfolded (asterisk) and folded (double asterisks) LptD containing the **[1-2]** disulfide bond. (*B*) Samples from (*A*) were subjected to limited trypsin digestion and analyzed by denaturing SDS-PAGE. Graphical representations of LptD species before or after trypsin digestion are shown on the right.

To provide further evidence that folding and membrane insertion of **[1-2][3-4]**-LptD precedes disulfide bond rearrangement, we examined susceptibility of LptD to trypsin digestion during pulse-chase. We observed that a stable fragment resistant to trypsin digestion appears early during the chase, and disappears with the concomitant appearance of a second slightly larger trypsin-stable fragment (Fig. 2.7B) (*9*). The time-dependent appearance of the two trypsin-stable fragments is consistent with formation first of a folded intermediate **1** creating a trypsin-resistant

β-barrel domain ((*β*)-intermediate **1**) which, because it does not contain disulfide bonds that connect the N- and C- domains of LptD (see Fig. 2.7B, *right*), is of smaller size than the LptD fragment ((*β*)-mature) produced by treatment with trypsin after disulfide bond rearrangement. Again it can be seen that the trypsin fragment produced from the intermediate **1** (**[1-2][3-4]**-LptD) does not accumulate substantially, suggesting that rearrangement of the folded **[1-2][3-4]**-LptD to folded **[1-3][2-4]**-LptD is faster than folding of the unfolded **[1-2][3-4]**-LptD. Our studies have established that the rate-determining step in translocon assembly is folding of LptD into a β-barrel. Folding is remarkably slow, taking approximately 20 minutes, or one-third of the cell cycle, under the conditions studied (growth in minimal media at 37 ºC). Typical β-barrel proteins such as LamB fold several orders of magnitude faster than LptD (*17*). LptD folding may be slow because the protein must wrap around LptE, forming a β-barrel that also contains a plug (*8, 9*).

2.2.4. Wild-type LptD can only assemble efficiently if folding proceeds through intermediate 1

Disulfide bonds in *E. coli* envelope proteins are introduced by the periplasmic oxidase DsbA (*18*). LptD has previously been shown to be a substrate of DsbA (*19*) and oxidation of LptD is impaired in strains lacking DsbA (*15*, *16*). Given that the formation of mature **[1-3][2-4]**-LptD proceeds via intermediate **1** (**[1-2][3-4]**-LptD), we sought to elucidate the role of DsbA in introducing the initial non-native disulfide bonds in LptD. Cells lacking DsbA grown in minimal media accumulate mainly reduced LptD in the OM at steady state but also produce a small amount of an LptD species (intermediate **2**) containing only the **[2-4]** disulfide bond (Fig. 2.6 and 2.8A). When we [^{35}S]-pulse-label this same strain, newly-synthesized LptD remains in a reduced state throughout the chase with only a small amount of intermediate **2** appearing (Fig. 2.8B).

Furthermore, reduced LptD that accumulates in the absence of DsbA can be completely alkylated (Fig. 2.8C), indicating that all four Cys remain as free thiols and that the **[1-2]** and **[3-4]** disulfide bonds cannot be formed in the absence of DsbA. Therefore, DsbA is required for the formation of intermediate **1** (**[1-2][3-4]**-LptD). In fact, neither intermediate **1** nor mature LptD is detected in these experiments (Fig. 2.8A and B). Although cells lacking DsbA do make a small amount of a functional LptD (intermediate **2**; **[2-4]**-LptD), these cells do not grow well. It is clear that without formation of the **[1-2][3-4]**-LptD intermediate, the pathway to form mature **[1-3][2-4]**-LptD is extremely inefficient.

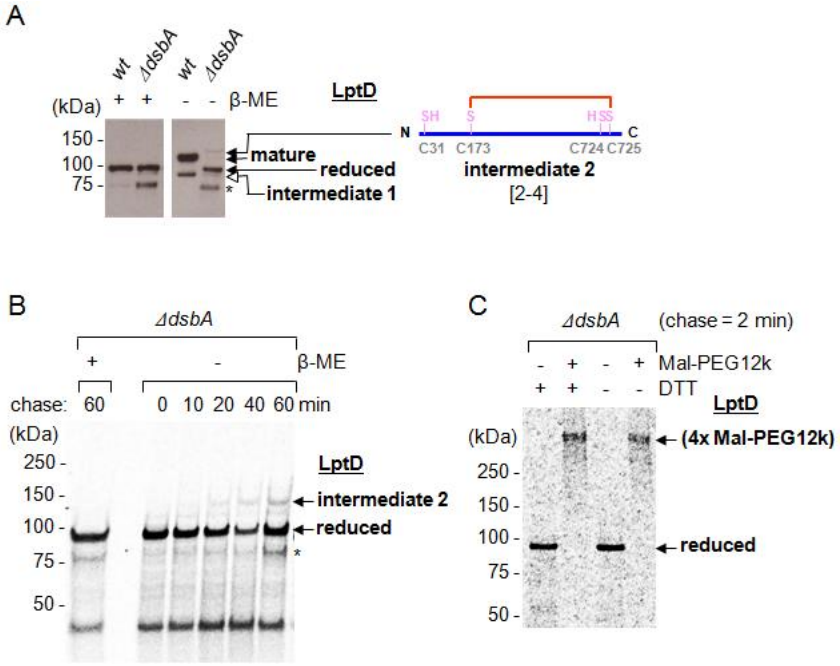

Figure 2.8. DsbA is required for efficient assembly of mature LptD through intermediate **1**. (*A*) α-FLAG immunoblot analysis of OM fragments obtained from *wt* and *ΔdsbA* strains containing pET23/42*lptD-FLAG*$_3$ grown in minimal media. Disulfide connectivity for relevant LptD species is shown on the right. (*B*) [^{35}S]-Met pulse-chase of newly-synthesized LptD-FLAG$_3$ in a *ΔdsbA* background. (*C*) Maleimidyl-PEG (Mal-PEG12k) alkylation of [^{35}S]-labeled reduced-LptD from (*B*). Bands denoted by asterisks represent LptD degradation products.

2.2.5. A disulfide bond between Cys$_{724}$ and Cys$_{725}$ ([3-4]) is likely formed in intermediate 1

To determine if the **[3-4]** disulfide bond is formed, we examined whether the cysteines in

intermediate **1** could be labeled by thiol-alkyating agents. Intermediate **1** cannot be chemically modified by maleimidyl-poly(ethylene glycol) (Mal-PEG) unless it has been pre-treated with reducing agent DTT (Fig. 2.5B and 2.8C). To rule out the possibility that the 3rd and 4th cysteines in intermediate **1** were not reactive due to steric inaccessibility (even under reducing conditions), we also performed alkylating experiments with the C-terminal domain of LptD (C-LptD) alone, which contains only these two cysteines. We found that the C-LptD protein can be modified by Mal-PEG when pre-treated with DTT (Fig. 2.9A). Taken together, these results suggest that intermediate **1** likely contains both the **[1-2]** and **[3-4]** disulfide bonds.

Intermediate **1** must convert to **[2-4]**-LptD during oxidative assembly of LptD (Fig. 2.5A). If intermediate **1** contains both the **[1-2]** and **[3-4]** disulfide bonds, one of these bonds would need to be reduced prior to rearrangement to the **[2-4]** bond. To determine if the periplasmic disulfide isomerase DsbC could serve as a reductant in the pathway, we conducted pulse-chase experiments to follow the biogenesis of wild-type LptD proteins in a strain lacking DsbC. We found that removing DsbC significantly slows down the rate of disulfide bond rearrangement from intermediate **1** to the mature form of wild-type LptD (Fig. 2.9B); in the presence of DsbC, this conversion takes ~20 min (Fig. 2.5A), while in the absence of DsbC, it takes ~2-3 times (40-60 min) longer (Fig. 2.9B). We also examined the biogenesis of the LptD$_{CCSC}$ mutant protein in the absence of DsbC, and found that the rate of disulfide bond rearrangement from the **[1-2]**-LptD$_{CCSC}$ species to the **[2-4]**-LptD$_{CCSC}$ species now occurs ~20 min (Fig. 2.9C), comparable to the rearrangement in wild-type LptD$_{CCCC}$ in the presence of DsbC (Fig. 2.5A). Since the LptD$_{CCSC}$ does not (cannot) contain the **[3-4]** bond, these data suggest that DsbC may be involved in reducing that disulfide bond in wild-type intermediate **1** (likely **[1-2][3-4]**-LptD) in order to allow rearrangement to take place.

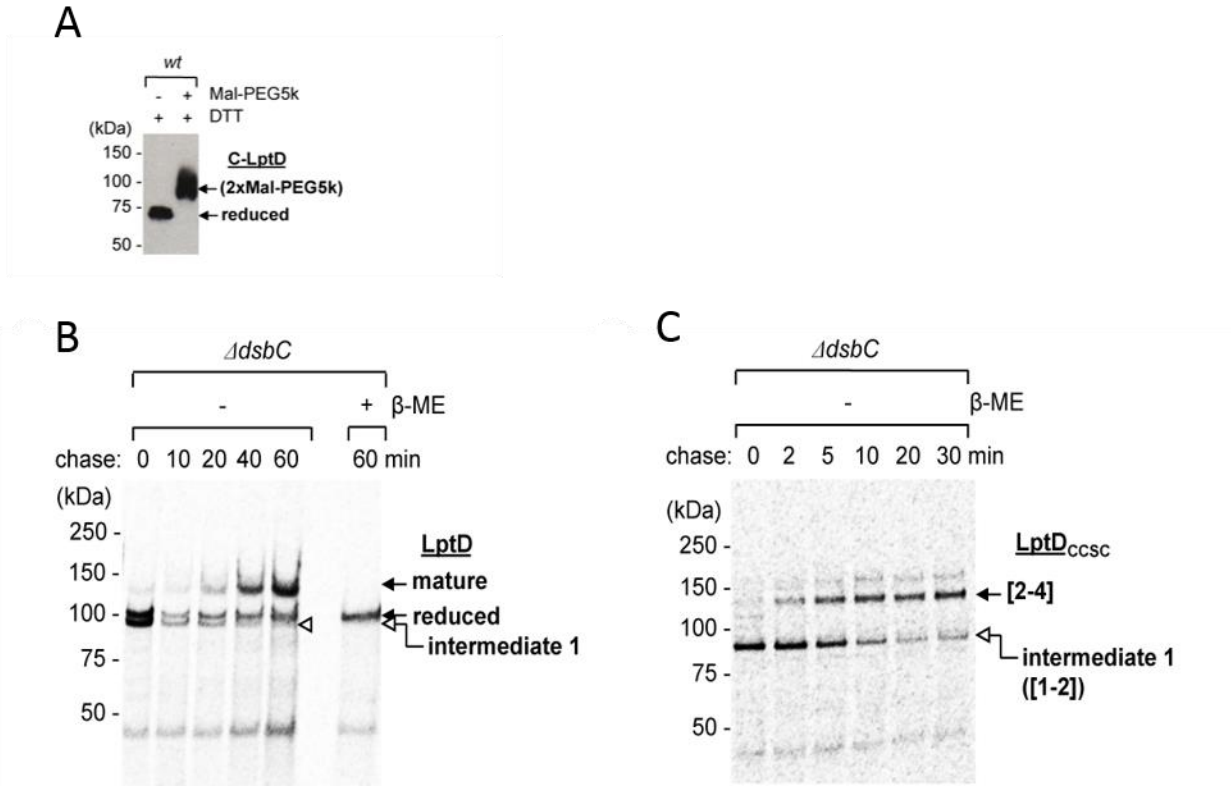

Fig. 2.9. A disulfide bond between Cys_{724} and Cys_{725} may be formed in intermediate **1**. (*A*) Maleimidyl-PEG (Mal-PEG5k) alkylation of C-LptD-$FLAG_3$ in a wild-type background. (*B*) [^{35}S]-Met pulse-chase of newly-synthesized LptD-$FLAG_3$ in a *ΔdsbC* background. (*C*) [^{35}S]-Met pulse-chase of newly-synthesized $LptD_{CCSC}$-$FLAG_3$ in a *ΔdsbC* background. Where indicated, β-mercaptoethanol (β-ME) or dithiothreitol (DTT) were used to reduce disulfide bonds.

The assumption that the **[3-4]** disulfide bond forms in this pathway remains an open question. Whether the **[3-4]** bond exists, however, does not affect our proposed pathway (since subsequent reduction of this disulfide bond is a prerequisite for rearrangement). It is also true that while we were able to observe DsbA adducts responsible for the formation of **[1-2]** and **[1-3]** disulfide bonds (Fig. 2.10), we were not able to detect a DsbA adduct (with either the 3rd or 4th Cys of LptD) that would allow formation of the **[3-4]** disulfide bond.

2.2.6. LptD intermediates containing mixed-disulfide adducts with DsbA can be detected *in vivo* allowing the complete oxidative folding pathway for LptD to be delineated

We used a $DsbA_{P151T}$ mutant that forms kinetically stable mixed-disulfide intermediates with substrate proteins to see if we could accumulate cross-linked adducts between LptD and DsbA (*19*). We observed two LptD species that also contain DsbA (Fig. 2.10A). These new bands can be assigned as mixed-disulfide intermediates linking DsbA to Cys_{31} of reduced LptD (DsbA adduct **A**; **[1-DsbA]**) and to Cys_{31} of **[2-4]**-LptD (DsbA adduct **B**; **[2-4][1-DsbA]**) by comparing to adducts observed with LptD using Cys-to-Ser mutants (Fig. 2.10A, C and 2.11). DsbA adduct **A** likely corresponds to the first-formed intermediate between LptD and DsbA leading to the formation of the **[1-2]** disulfide bond (Fig. 2.10C). In fact, when pulse-chase analysis is carried out in the $dsbA_{P151T}$ strain, we detect [^{35}S]-labeled DsbA adduct **A** at early time points (t = 0-2 min, Fig. 2.10B), consistent with this interpretation. We also observe the appearance of DsbA adduct **B** (**[2-4][1-DsbA]**-LptD) at t = 2 min, which chases by t = 40 min. The fact that this species appears before (and chases into) final mature LptD (**[1-3][2-4]**-LptD) is strong evidence that DsbA adduct **B** is also a true species along the assembly pathway and suggests that DsbA directly introduces the **[1-3]** disulfide bond in LptD after the **[2-4]** disulfide is already formed (Fig. 2.10C). Therefore, DsbA makes both the **[1-2]** and the **[1-3]** disulfide bonds in LptD at different stages of assembly.

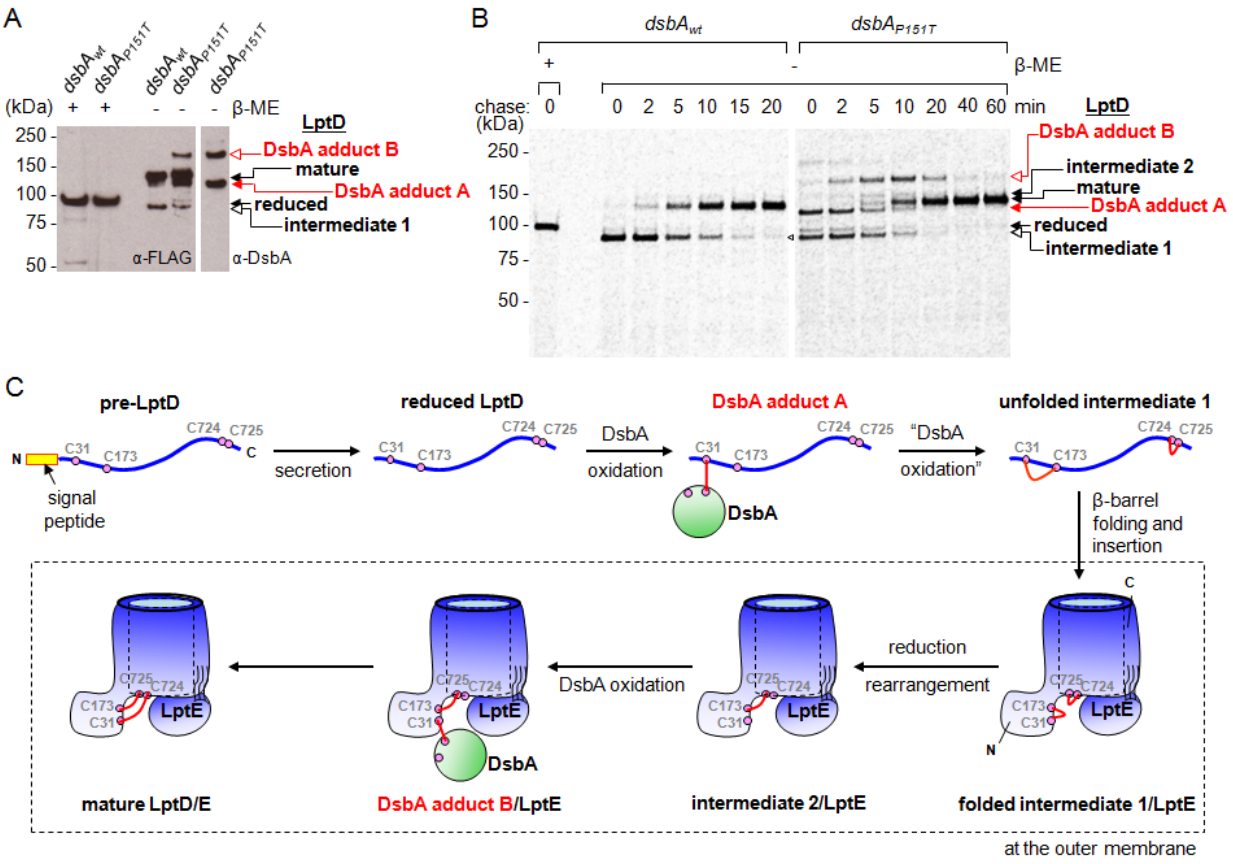

Figure 2.10. LptD intermediates containing mixed-disulfide adducts with DsbA can be detected *in vivo*. (*A*) α-FLAG immunoprecipitation using *wt* or *dsbA*$_{P151T}$ cells containing pET23/42*lptD-FLAG*$_3$. Samples were analyzed by α-FLAG and α-DsbA immunoblots. (*E*) [^{35}S]-Met pulse-chase of newly-synthesized LptD-FLAG$_3$ in *wt* and *dsbA*$_{P151T}$ backgrounds. (*C*) The seven intermediate LptD species observed experimentally (including the final mature form) are depicted as they appear after secretion across the IM during oxidative assembly of the OM LPS translocon. The precursor of LptD (pre-LptD) containing its signal peptide (prior to secretion) is also shown. Introduction of the **[3-4]** disulfide bond, presumably following **[1-2]** disulfide formation, is likely also dependent on DsbA.

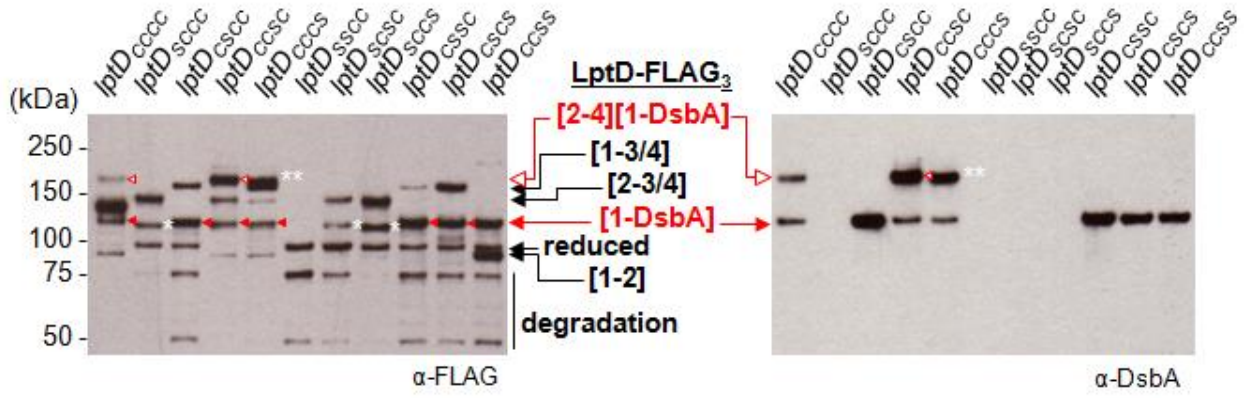

Fig. 2.11. The *dsbA*$_{P151T}$ mutation results in the accumulation of mixed-disulfide adducts between DsbA and Cys$_{31}$ of LptD. α-FLAG immunoprecipitation using *dsbA*$_{P151T}$ cells containing pET23/42*lptD-FLAG*$_3$ or single/double Cys mutants. Samples were analyzed by α-FLAG and α-DsbA immunoblot under non-reducing conditions. All LptD Cys mutant proteins that contain Cys$_{31}$ can be trapped in an intermediate with DsbA (**[1-DsbA]**-LptD, closed red arrowheads). The LptD$_{CCSC}$ and LptD$_{CCCS}$ proteins are also trapped in a second DsbA adduct via Cys$_{31}$. LptD$_{CCSC}$ exists predominantly as **[2-4]**-LptD in a wild-type *dsbA* background (*15*), which becomes cross-linked to DsbA in a *dsbA*$_{P151T}$ background (**[2-4][1-DsbA]**-LptD, open red arrowhead). In addition to **[1-3]**-LptD, LptD$_{CCCS}$ also exist as **[2-3]**-LptD in a wild-type DsbA background (*15*), which becomes cross-linked to DsbA in a *dsbA*$_{P151T}$ background (**[2-3][1-DsbA]**-LptD, double asterisks). Single asterisks denote degradation products from LptD containing one disulfide bond.

The ability to detect several DsbA adducts with LptD during pulse-chase allows us to describe the sequence of events leading to the assembly of a functional OM LPS translocon. Taken together we can assign seven distinct species along the oxidative folding pathway of LptD *in vivo* (Fig. 2.10C). The first non-consecutive disulfide bond is formed between Cys$_{173}$ and Cys$_{725}$ (**[2-4]**), presumably via reduction of one of the consecutive disulfides of **[1-2][3-4]**-LptD, followed by disulfide bond rearrangement. Since it has been established that either of the two non-consecutive disulfide bonds is sufficient for the proper function of LptD (*15*), the **[2-4]**-LptD species (intermediate **2**) represents the first functional form of LptD assembled in the cell. In this regard, it is important to point out that cysteines corresponding to both Cys$_{173}$ and Cys$_{725}$ are present in >95% of over one thousand Gram-negative LptD proteins that have non-identical sequences (Fig.

2.12, *16*), suggesting that the **[2-4]** disulfide bond plays a critical structural role in the function of the OM LPS translocon.

A

Cysteine motifs in LptD	Cys_{31}	Cys_{173}	Motifs at $Cys_{724/5}$	
			CysCys/ CysXaaCys	Single Cys
Present	236	1028	491	526
Missing	820	28	39	
Total	1056			

B

Organisms	Cys_{31}	Cys_{173}	$Cys_{724/5}$
Candidatus Solibacter usitatus	ILAVSAAAQVN	GFVTNCK---MPQ	VQYNTN--CCGF--SV
Campylobacter jeluni	-------MLGT	SAVSSCN---VED	YTYQRK--CWNY--SL
Helicobacter pylori	-----GALDAK	MSASGCS---IDN	ANYQRK--FLSF--NL
Candidatus Liberibacter solanacearum	--ETSSNKKVI	GTYTACAKCVQSP	LSYQND--CTTF--NI
Mariprofundus ferrooxydans	-----MLLLLH	VLYSTCP---ADE	LQYKHP--CWTA--GV
Candidatus Odyssella thessalonicensis	---SASVNAQP	GVYSPCDVCKADP	LRHTNE--CLVT--TF
Oceanibulbus indolifex	------ALCVA	AAVTSCKVCEDGE	LSYNNE--CVQV--DL
Asticcacaulis excentricus	FFADETDLTAP	ALFTPCQLCVKNN	VIYKDD--CARF--EL
Sphingomonas sp.	--AQQLNEPQT	AAYTGCSV--EDS	IAYEDD--CLTL--GF
Roseomonas cervicalis	----------	VLYSACDLCAEDP	LTYEDE--CLIF--DT
Francisella cf._novicida	KALADDLAWVK	GYITSGD---PYD	LQYNAK--SWAV--RA
Marinomonas sp.	--SATELDWFP	GFYTTCE---PGS	IGFENC--CVKA--QF
Candidatus Blochmannia floridanus	DNSHKYSDHAP	GKFSTCT---IDN	IQYFTP--CWIF--SI
Acinetobacter sp.	IKEAYPGQEFF	ATYTTCP---PGQ	VNYESC--CWGI--SV
Escherichia coli	--ASQCMLGVP	GSFTSCL---PGS	VQYSSC--CYAI--RV
Pseudomonas aeruginosa	SADYSHLDWIP	GTYTRCE---PSS	FEYDSC--CWKL--RL
Polynucleobacter necessarius	SANTVLLPDRG	ATYSTCT---PQN	LEWNRD--CWTF--RG
Lautropia mirabilis	----MPLQLAP	GSFTSCK---PDD	VEYARD--CWAV--RV
Bdellovibrio bacteriovorus	------TVMSS	ADYTACT---NCP	AQFKPPGDCMMI--TF
Thermodesulfovibrio yellowstonii	-----FFIARI	ATFSTCE---PEP	IKYTQS--CWAT--NI
uncultured_Desulfobacterales bacterium	SNESLSMPQAL	GHFTTCE---GIL	ILYDNPCKCWGF--NL
Sulfurihydrogeninium yellowstonense	----------	GEFSGCP---FDQ	FDWNRG--CWSL--SF
Hydrogenobacter thermophilus	------MILSA	GDITTCP---PDK	LDYTGA--CWSL--GV
Thermovibrio ammonificans	--MRIGLPTVT	GEYTPCS---HSC	LTVNRG--CWSG--VL
Calditerrivibrio nitroreducens	------LLLQP	ATISACS---GDV	ILYKSE--CWNL--GF
Hippea maritima	------LLLFI	GIITTCK---CQD	FLYQED--CWGI--GL
Geobacter metallireducens	------APVFL	GTFTTCD---AER	VEYRHQ--CWSV--SV
Thermodesulfatator indicus	------ILVCP	TTITTCDICKNGK	FEYRTK--CWWG--VI
Desulfobacca acetoxidans	--WAEEVEIFK	CVVTTCD---ADR	LIFQRQ--CWGV--SL
Desulfobulbus propionicus	RYENPPRIEAE	GWVVTCKLHPGEV	LRYIQP--CWSV--EV
Desulfatibacillum alkenivorans	--WALTVLLFA	ASLTTCD---PDD	LIYEAA--CWAI--DL
Desulfovibrio sp.	--GGAHAQQPQ	AKITVCD---GDT	IIYNHQ--CFKVIGRT

Fig. 2.12. Cys_{173} and Cys_{725} are very highly conserved among LptD homologs. (*A*) Conservation of the four cysteine residues in *E. coli* LptD across 1056 LptD homologs that are non-identical. (*B*) Sequence alignments of 32 LptD homologs that are <30% identical depicting only the regions around the cysteine residues in *E. coli* LptD. *E. coli* LptD is shown in green.

2.2.7. Disulfide rearrangement of intermediate 1 is triggered by LptE to activate the OM translocon for LPS export

We have shown that LptD accumulates in the form of intermediate **1** (**[1-2][3-4]**-LptD) when LptE is limiting (Fig. 2.3A). Restoring LptE levels should rescue this defect by allowing

the conversion of the accumulated **[1-2][3-4]**-LptD species to mature LptD. We discovered that a previously described LptE-depletion strain produces increasing levels of LptE as the cells progress through exponential growth phase (Fig. 2.4) (*5*). This offers the possibility for us to watch how LptD assembly progresses as LptE levels increase. At early log phase, LptD intermediate **1** accumulates because LptE levels are limiting (Fig. 2.3A and 2.13A). As we examined these cells at mid-log phase, when levels of LptE have increased substantially, we observed a corresponding conversion of previously accumulated intermediate **1** to the mature LptD species (Fig. 2.13A). As a component of the LptD/E complex, LptE is, by definition, required for the formation of the non-functional OM LPS translocon (intermediate **1**/LptE, "INACTIVE" state) in the OM (Fig. 2.13C). Our results show that by changing the levels of LptE, the cell can also control the levels of activated translocon (**[1-3][2-4]**-LptD/E, "ACTIVE" state) in the OM. Therefore, assembly of the LptD/E complex controls activation of the translocon; only when the non-functional OM translocon is properly formed does disulfide bond rearrangement take place efficiently to activate LPS transport at the OM (Fig. 2.13C).

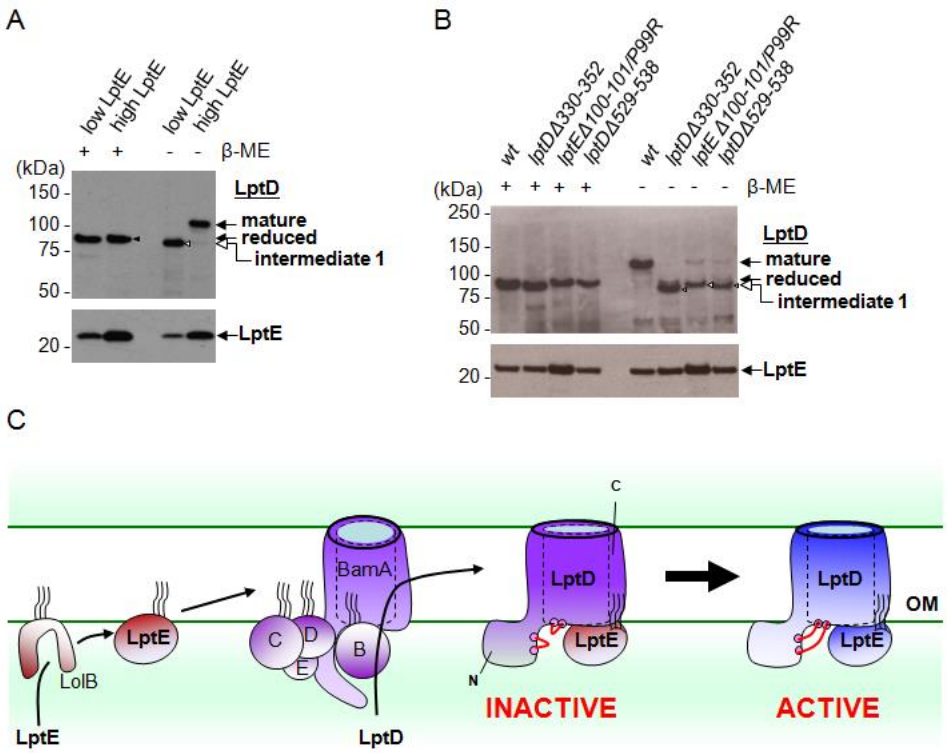

Figure 2.13. Formation of the mature functional OM LPS translocon proceeds via pre-assembly of a non-functional LptD/E intermediate that is activated via disulfide bond rearrangement. (*A*) α-LptD and α-LptE immunoblot analyses of OM fragments obtained from cells that express different levels of LptE according to the growth phase. OM fragments were isolated from cells grown to early-log phase (low LptE) and mid-log phase (high LptE) (see Fig. 2.4). (*B*) α-LptD and α-LptE immunoblot analyses of OM fragments obtained from *wt*, *lptD*$_{\Delta 330\text{-}352}$, *lptE*$_{\Delta 100\text{-}101/P99R}$ and *lptD*$_{\Delta 529\text{-}538}$ strains. Open arrowheads indicate the position of **[1-2][3-4]**-LptD in each strain. (*C*) Folding (pre-assembly) and rearrangement (activation) of the OM LPS translocon coordinate all three OM biogenesis pathways (Bam, Lol, and Lpt) so that they converge on the single most important process, LPS export, in establishing the barrier function of the OM.

2.2.8. OM LPS translocon mutants have defective triggering mechanisms

We have shown that the maturation of a functional OM LPS translocon is a two-step process involving a folding/insertion step followed by disulfide rearrangement. Useful mutants having defects in the OM LPS translocon have proven difficult to isolate. The first, identified more than twenty years ago, contains a 23-amino acid deletion (**Δ**330-352) in the β-barrel domain of LptD (LptD$_{\Delta 330\text{-}352}$, known as LptD4213) (*20*). Since that time very few other useful mutants have been reported. One contains a 10-amino acid deletion (**Δ**529-538) in the LptD β-barrel

(LptD$_{\Delta 529\text{-}538}$) (*8*), and another contains a two-amino acid deletion (**Δ**100-101/P99R) in LptE (LptE$_{\Delta 100\text{-}101/P99R}$) (*21*). We analyzed the LptD oxidation states for all three mutants in the OM fractions and found that each of the mutations results in substantial accumulation of intermediate **1** (**[1-2][3-4]**-LptD) (Fig. 2.13B), similar to what occurs under LptE-limiting conditions (Fig. 2.3A and 2.13A). Therefore, for these three mutants, progression along the oxidative folding pathway of LptD from intermediate **1** to the mature form is arrested. Since the disulfide bonds in the mature form of LptD are between pairs of cysteines that are far apart on the primary sequence of the protein (Cys$_{31}$-Cys$_{724}$ and Cys$_{173}$-Cys$_{725}$), conversion of intermediate **1** (**[1-2][3-4]**-LptD) to mature LptD (**[1-3][2-4]**-LptD) likely requires that all the cysteines be in close spatial proximity. Inefficient formation of mature LptD in the mutants suggests that the alignment of the non-native disulfides in intermediate **1** is not optimal. In fact, we can show that with one of the LptD mutants (LptD$_{\Delta 330\text{-}352}$), LptD still interacts with LptE (Fig. 2.14). This mutant LptD can fold and assemble with LptE to form the non-functional intermediate **1** ("INACTIVE" state) in the OM, but it appears as though the cysteines are not correctly positioned for rearrangement to activate the translocon.

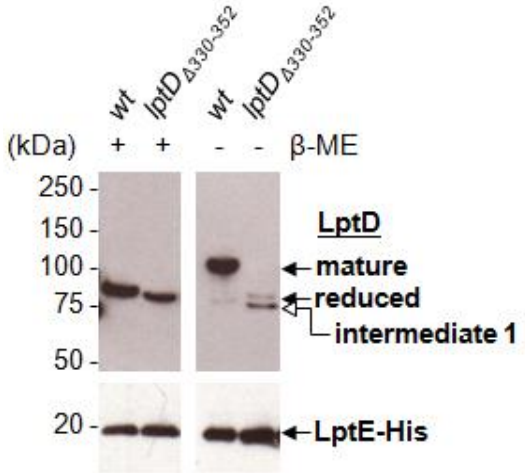

Fig. 2.14. The **[1-2][3-4]**-LptD$_{\Delta 330\text{-}352}$ mutant protein can assemble with LptE, but is defective in disulfide bond rearrangement to form mature LptD. Ni-NTA affinity purification using *wt* or *lptD$_{\Delta 330\text{-}352}$* cells containing pET23/42*lptE-His*. Samples were analyzed by α-LptD and α-His immunoblots.

Producing nonfunctional intermediate **1** before activation via disulfide bond rearrangement also provides a mechanism for quality control to ensure that the trans-envelope LPS exporter is assembled with only a functional OM translocon. Proper disulfide bonds in LptD are required for the trans-envelope Lpt bridge to form via interactions between LptA and LptD (*22*). The triggering strategy prevents a defective OM translocon from achieving the correct disulfide bond configuration, thereby preventing formation of a nonfunctional trans-envelope LPS exporter that might release LPS into an inappropriate compartment.

2.3. Conclusion and Future Work

In this chapter, we extensively characterized the biogenesis pathway of LptD. LptD has two non-consecutive disulfide bonds (**[1,3]** and **[2,4]**) that connect the N-terminal periplasmic domain to the C-terminal β-barrel domain in the mature form (*15*). A non-functional disulfide bonded species of LptD, **[1,2][3,4]**-LptD accumulates when LptE is limiting. This **[1,2][3,4]**-LptD also accumulates when there are defects in LptD or LptE. We demonstrate that this species is an on-pathway intermediate towards the assembly of LPS translocon, and the folding of this species by the Bam machine is the rate determining step of the biogenesis pathway of the LptD/E complex. We also show that although this **[1,2][3,4]**-LptD is not a required intermediate towards function translocon in mutants like *dsbA*$^{-}$, the efficiency of translocon assembly is largely deterred when this intermediate is not able to form. Using a mutant that allows accumulation of DsbA-substrate during oxidation, we demonstrate that two separate oxidation steps by the periplasmic oxidase DsbA take place during the assembly of the LptD/E complex. DsbA is required for the formation of **[1,2][3,4]**-LptD in the periplasm and, later at the OM after disulfide rearrangement, to make the

[1,3] disulfide bond. Given that a functional translocon with proper disulfide bond is a prerequisite to the formation of the seven-protein trans-envelop LPS transporter, the oxidative assembly pathway of LptD ensures that only the functional translocons are employed to form the Lpt machine.

To understand the molecular mechanism of how the LPS translocon functions requires detailed structural information of the complex. Dr. Goran Malojcic and Aaron Garner have been working closely to obtain X-ray crystallographic information of the β-barrel structure of the LptD/E complex. In lieu of a molecular structure, Dr. Suguru Okuda, a former postdoc in our group and Alex George have appled the photo-activatable unnatural amino acid crosslinking technique to capture LPS molecules that are being transported by the translocon on their way to the final destination.

Our long-term goal is to understand Bam-mediated assembly of β-barrel proteins (*6*). LptD is an important substrate for the Bam machine since it is the only essential β-barrel protein in *E. coli* besides BamA, the β-barrel component of the Bam complex itself. We propose that LptD would be an ideal system in which to study β-barrel assembly *in vivo* since seven intermediates have been identified along its assembly pathway (see Chapter Three). Additionally, LptD β-barrel folding is extremely slow and precedes disulfide rearrangement; this allows us to monitor folding intermediates during β-barrel folding using different disulfide-bonded states. Our ability to visualize and accumulate different oxidation states of LptD allows us to extend to membrane proteins the classic approach of using disulfide bonds to study the folding of soluble proteins *in vivo* (*23*, *24*). Combined with our *in vitro* reconstitution of Bam-mediated folding (*25*), it may be possible to dissect β-barrel protein folding into individual steps. It is too early to tell whether it will be possible to use the information concerning assembly of the translocon to break the machine

responsible for LPS export. We are encouraged by the fact that small molecules that target LptD in *Pseudomonas aeruginosa* have recently been described (*26*). Given the slow rate of LptD folding, we might be able to design inhibitors against the long-lived non-functional states of the OM LPS translocon, and thus prevent its activation.

2.4. Materials and Methods

2.4.1. Bacterial strains

For most experiments, the wild-type strain used is MC4100 [*F⁻ araD139 Δ(argF-lac) U169 rpsL150 relA1 flbB5301 ptsF25 deoC1 ptsF25 thi*]. The LptE-depletion strain used that makes varying levels of LptE according to growth phase is AM689 [MC4100 *ara⁺ lptE::kan* λ_{att}*(*P_{BAD}*-lptE)*] (*5*). The *lptD*$_{\Delta 330\text{-}352}$ (*lptD4213*), *lptE*$_{\Delta 100\text{-}101/P99R}$ (*lptE6*) and *lptD*$_{\Delta 529\text{-}538}$ mutant strains used are NR698 (*20*), GC190 [MC4100 *ara⁺ ΔlptE2::kan* pBAD18*lptE*] (*21*) and MC4100 *ΔlptD2::kan* pET23/42*lptDΔ529-538* (*8*), respectively. The *ΔdsbA* and *ΔdsbC* strains used are NR1216 and NR1217 (*15*), respectively. For experiments involving the *dsbA*$_{P151T}$ mutant, the wild-type strain used is HK295, a MC1000 derivative [*F⁻ Δara714 galU galK Δ(lac)X74 rpsL thi*] and the *dsbA*$_{P151T}$ mutant used is HK348 [HK295 *zin::Tn10 dsbA*$_{P151T}$] (*19*). Luria-Bertani (LB) broth and M63/glucose minimal broth and agar were prepared as described previously (*27*). Arabinose (0.2% w/v) was added for the growth of AM689 (*5*) and GC190 (*21*). Growth of strains was carried out at 37 ^{o}C unless explicitly indicated. When appropriate, kanamycin (25 μg/ml) and carbenicillin (50 μg/ml) were added. Amino acids were added at 50 μg/ml when indicated.

2.4.2. Plasmid construction

To construct pET23/42*lptD-FLAG*$_3$, a cassette containing the coding sequence of the $FLAG_3$ tag was inserted into pET23/42*lptD-His* (*5*) to replace the original His_8 tag. Briefly, the entire pET23/42*lptD-His* template was amplified by PCR (using primers 5'-AGATCATGATATCGACTATAAAGACGATGATGACAAATAATTGATTAATACCTAGGCTGC-3' and 5'-ATAGTCGATATCATGATCTTTGTAGTCGCCGTCGTGATCTTTATAATCGCGCGCCAAG GC-3') and the resulting PCR product mixture digested with DpnI for > 1 h at 37 ^{o}C. NovaBlue (Novagen) cells were transformed with 1 μl of digested PCR product and plated onto LB plates containing 50 μg/ml carbenicillin. For each construct, plasmids from six colonies were isolated and sequenced.

To generate LptD Cys mutant constructs containing the $FLAG_3$ tag, pET23/42*lptD*$_{XXXX}$*-His* constructs were first made via site-directed mutagenesis using relevant primers (*15*) and pET23/42*lptD-His* (*5*) as the initial template. Briefly, the entire template was amplified by PCR and the resulting PCR product mixture digested with DpnI for > 1 h at 37 ^{o}C. NovaBlue (Novagen) cells were transformed with 1 μl of digested PCR product and plated onto LB plates containing 50 μg/ml carbenicillin. For each construct, plasmids from six colonies were isolated and sequenced. The resulting pET23/42*lptD*$_{XXXX}$*-His* constructs were used in the same protocol above to generate pET23/42*lptD*$_{XXXX}$*-FLAG*$_3$ constructs.

2.4.3. Growth of AM689 for OM analysis

10-ml cultures were grown overnight at 30 ^{o}C in LB broth containing 0.2% arabinose. Cultures were pelleted and washed twice in equal volume of LB broth. Fresh LB cultures (1.5-l) either containing 0.2% arabinose were inoculated with the washed cells to an initial OD_{600} of ~0.01 and were grown at 30 ^{o}C until OD_{600} reaches ~0.25 (~4 h) and ~0.5 (~5 h). The amount of cells

equivalent to that in a 500-ml culture of OD_{600} ~0.5 was pelleted by centrifugation at 5000 x *g* for 20 min and subjected to OM analysis (see below).

2.4.4. Isolation of OM for analysis of LptD oxidation states

Strains MC4100, AM689, NR1216, NR1217, NR698, GC190 and MC4100 *ΔlptD2::kan* pET23/42*lptDΔ529-538* were used for OM analysis. These strains contain a single copy of *lptD* expressed from the chromosome or plasmid. Strains MC4100 containing p($lptD_{CCCC}$) or p($lptD_{CCSS}$) (pET23/42*lptD* or pET23/42$lptD_{CCSS}$, respectively (*15*)), MC4100, NR1216, HK295 and HK348 containing pET23/42*lptD-*$FLAG_3$ were also used for OM analysis experiments. These strains contain two copies of *lptD,* one expressed from the chromosome and the other expressed from pET23/42. OM analysis is performed as previously described (*15*).

2.4.5. Pulse-chase analysis

Strains MC4100, NR1216, HK295 and HK348 containing pET23/42*lptD-*$FLAG_3$ were used in pulse-chase experiments. Pulse-chase experiments were essentially carried out according to published protocols (*23*). Briefly, a 5-ml culture was grown to OD_{600} ~0.5 in M63/glucose minimal media supplemented with eighteen amino acids (minus methionine and cysteine) at 37 ^{o}C. The culture was pulse-labeled with [^{35}S]-methionine (100 μCi/ml final concentration) (American Radiochemicals) for 2 min and then chased with cold methionine (5 mM) at 37 ^{o}C. At the indicated time point during the chase, a 800 μl culture aliquot was transferred to a 1.5-ml tube containing 80 μl of trichloroacetic acid (TCA, 70% in water), incubated on ice for 20 min. Precipitated proteins were pelleted at 18,000 x *g* for 10 min at 4 ^{o}C, washed with 700 μl ice-cold acetone, and then solubilized in 80 μl 100 mM Tris.HCl, pH 8.0 containing 1% SDS and 20 mM *N*-ethylmaleimide

(NEM, Sigma). The sample was sonicated for 30 s to aid solubilization. Following that, 800 µl of ice-cold IP buffer (50 mM Tris.HCl, pH 8.0 containing 150 mM NaCl, 2% Triton X-100, 1 mM EDTA) was added and the sample was centrifuged at 18,000 x *g* for 10 min at 4 ºC. 700 µl of the supernatant was transferred to another 1.5-ml tube containing 2.5 µl of anti-FLAG® M2 magnetic beads (Sigma). The beads were washed and pre-equilibrated with 3 x 1 ml IP buffer before use. The mixture was incubated on a rotary shaker for 1 h at 4 ºC, and the beads were washed with 3 x 800 µl of ice-cold high salt buffer (50 mM Tris.HCl, pH 8.0 containing 1 M NaCl, 1% Triton X-100, 1 mM EDTA) and 1 x 800 µl ice-cold 10 mM Tris.HCl, pH 8.0 using a magnetic separation rack (New Englands Biolabs). 60 µl 2X SDS non-reducing sample buffer was then added to the beads and the mixture heated for 10 min at 100 ºC to elute the bound proteins. 15 µl of eluted sample was applied to SDS-PAGE directly. For reduction of disulfide bonds, 0.5 µl β-mercaptoethanol (β-ME, Sigma) was added to 20 µl eluted sample and heated for 5 min at 100 ºC before loading. 4-20% Tris.HCl polyacrylamide gels were used (running conditions: 150 V for 120 min). The gel was then dried and exposed to phosphor storage screens for autoradiography.

2.4.6. Maleimide-PEG (Mal-PEG12k) alkylation of [^{35}S]-pulse-labeled samples

Alkylation was carried out according to published protocols (*23*). Following the acetone wash step as outlined in the pulse-chase analysis protocol above, TCA-precipitated proteins were either directly subjected to alkylation or first reduced before alkylation. For reduction of disulfide bonds, TCA-precipitated proteins were incubated in 100 µl 100 mM Tris.HCl, pH 8.0 containing 0.1% SDS and 100 mM dithiothreitol (DTT, Invitrogen) for 30 min at room temperature. 700 µl M63 media was added and the reduced proteins were re-precipitated with TCA and further washed with acetone. Precipitated proteins (reduced or not) were then solubilized in 80 µl 100 mM

Tris.HCl, pH 6.8 containing 1% SDS and 5 mM Mal-PEG12k (Sunbright ME-120MA, NOF). The mixture was gently vortexed for 20 min at room temperature, and subsequently incubated for 30 min at 37 ºC. 800 µl of ice-cold IP buffer was added and the sample was subjected to immunoprecipitation as outlined in the pulse-chase analysis protocol.

2.4.7. Seminative pulse-chase analysis

Strain MC4100 containing pET23/42*lptD-FLAG*$_3$ was used in seminative pulse-chase experiments. A 5-ml culture was grown to OD_{600} ~0.5 in M63/glucose minimal media supplemented with eighteen amino acids (minus methionine and cysteine) at 30 ºC. The culture was pulse-labeled with ^{35}S-methionine (100 µCi/ml final concentration) (American Radiochemicals) for 2 min and then chased with cold methionine (5 mM) at 37 ºC. At the indicated time point during the chase, a 800 µl culture aliquot was transferred to a 1.5-ml tube and pelleted at 18,000 x *g* for 1 min at 4 ºC. The cell pellet was resuspended in 100 µl lysis buffer (20 mM Tris.HCl, pH 8.0 containing 150 mM NaCl, 1% SDS, 0.5 mg/ml lysozyme, 1 mM phenylmethylenesulfonylfluoride (PMSF, Sigma), 1 mM EDTA and 40 mM NEM). After incubated for 2.5 min at room temperature, 1 ml of ice-cold IP-2 buffer (50 mM Tris.HCl, pH 8.0 containing 150 mM NaCl, 2% n-octyl-β-glucoside (OG, Anatrace), 1 mM EDTA) was added and the sample was centrifuged at 18,000 x *g* for 30 min at 4 ºC. 950 µl of the supernatant was transferred to another 1.5-ml tube containing 2.5 µl of anti-FLAG® M2 magnetic beads (Sigma). The beads were washed and pre-equilibrated with 3 x 1 ml IP-2 buffer before use. The mixture was incubated on a rotary shaker for 2 h at 4 ºC, and the beads were washed with 4 x 800 µl of ice-cold wash buffer (50 mM Tris.HCl, pH 8.0 containing 1 M NaCl, 2% OG, 1 mM EDTA) using a magnetic separation rack (New Englands Biolabs). 30 µl of ice-cold elution buffer (50 mM

Tris.HCl, pH 8.0 containing 1 M NaCl, 2% OG, 1 mM EDTA, 250 μg/ml $FLAG_3$ peptide (Sigma)) was then added to the beads and the mixture incubated for 10 min at 4 ^oC to elute the bound proteins. An equal volume of 2X SDS non-reducing sample buffer was added and the sample split into two – one applied to seminative SDS-PAGE directly and the other heated for 10 min at 100 ^oC before loading. 10% Tris.HCl polyacrylamide gels were used (Running conditions: 150 V for 75 min, 4 ^oC). The gel was then dried and exposed to phosphor storage screens for autoradiography.

2.4.8. Trypsin digestion following seminative pulse-chase experiment

Trypsin digestion was performed according to published protocols (*9*). Samples that were eluted off the M2 magnetic beads were treated with 50 μg/ml trypsin for 4 h at room temperature. An equal volume of 2X SDS non-reducing sample buffer was added and the samples heated for 10 min at 100 ^oC before SDS-PAGE. 4-20% Tris.HCl polyacrylamide gels were used (running conditions: 150 V for 120 min). The gel was then dried and exposed to phosphor storage screens for autoradiography.

2.4.9. Affinity purification

Strains MC4100 and NR698 containing pET23/42*lptE-His* (*9*) was used in affinity purification experiments. Affinity purification experiments were performed as previously described (*9*).

2.4.10. Bioinformatics

The list of non-identical LptD sequences was collected by BLAST. Using the *E. coli* LptD sequence as a start, an initial BLAST hit list was collected. The weak hits were then used as the new reference sequence to BLAST search for more LptD sequences. By doing this recursively for

over 20 rounds, thousands of LptD sequences were collected. This initial list was then filtered to remove identical sequences and partial genes (usually containing deletions on one or the other end of the gene). The final list contains 1056 non-identical LptD sequences.

2.4.11. Antibodies

Monoclonal α-His conjugated to horseradish peroxidase was purchased from Qiagen. Monoclonal α-FLAG conjugated to horseradish peroxidase was purchased from Sigma. α-LptD (*16*), α-LptE (*9*) and α-DsbA (*28*) antiserum were already described.

2.5. References

1. Raetz CRH, Whitfield C (2002) Lipopolysaccharide endotoxins. *Annu Rev Biochem* 71:635-700.

2. Mühlradt PF, Golecki JR (1975) Asymmetrical distribution and artifactual reorientation of lipopolysaccharide in the outer membrane bilayer of *Salmonella typhimurium*. *Eur J Biochem* 51:343-352.

3. Nikaido H (2003) Molecular basis of bacterial outer membrane permeability revisited. *Microbiol Mol Biol Rev* 67:593-656.

4. Ruiz R, Kahne D, Silhavy TJ (2009) Transport of lipopolysaccharide across the cell envelope: the long road of discovery. *Nat Rev Microbiol* 7:677-683.

5. Wu T, McCandlish AC, Gronenberg LS, Chng SS, Silhavy TJ, Kahne D (2006) Identification of a protein complex that assembles lipopolysaccharide in the outer membrane of *Escherichia coli*. *Proc Natl Acad Sci* USA 103:11754-11759.

6. Hagan CL, Silhavy TJ, Kahne D (2011) β-Barrel membrane protein assembly by the Bam complex. *Annu Rev Biochem* 80:189-210.

7. Tokuda H (2009) Biogenesis of outer membranes in Gram-negative bacteria. *Biosci Biotechnol Biochem* 73:465-473.

8. Freinkman E, Chng SS, Kahne D (2011) The complex that inserts lipopolysaccharide into the bacterial outer membrane forms a two-protein plug-and-barrel. *Proc Natl Acad Sci* USA 108:2486-2491.

9. Chng SS, Ruiz N, Chimalakonda G, Silhavy TJ, Kahne D (2010) Characterization of the two-protein complex in Escherichia coli responsible for lipopolysaccharide assembly at the outer membrane. *Proc Natl Acad Sci* USA 107:5363-5368.

10. Chng SS, Gronenberg LS, Kahne D (2010) Proteins required for lipopolysaccharide assembly in Escherichia coli form a transenvelope complex. *Biochemistry* 49:4565-4567.

11. Sperandeo P, Lau FK, Carpentieri A, De Castro C, Molinaro A, Dehò G, Silhavy TJ, Polissi A (2008) Functional analysis of the protein machinery required for transport of lipopolysaccharide to the outer membrane of *Escherichia coli*. *J Bacteriol* 190:4460-4469.

12. Eggert US, Ruiz N, Falcone BV, Branstrom AA, Goldman RC, Silhavy TJ, Kahne D (2001) Genetic basis for activity differences between vancomycin and glycolipid derivatives of vancomycin. *Science* 294 :361-364.

13. Wu T, Malinverni J, Ruiz N, Kim S, Silhavy TJ, Kahne D (2005) Identification of a multicomponent complex required for outer membrane biogenesis in *Escherichia coli*. *Cell* 121 :235-245.

14. Sklar JG, Wu T, Gronenberg LS, Malinverni JC, Kahne D, Silhavy TJ (2007) Lipoprotein SmpA is a component of the YaeT complex that assembles outer membrane proteins in *Escherichia coli*. *Proc Natl Acad Sci* USA 104:6400-6405.

15. Ruiz N, Chng SS, Hiniker A, Kahne D, Silhavy TJ (2010) Nonconsecutive disulfide bond formation in an essential integral outer membrane protein. *Proc Natl Acad Sci* USA 107:12245-12250.

16. Braun M, Silhavy TJ (2002) Imp/OstA is required for cell envelope biogenesis in *Escherichia coli*. *Mol Microbiol* 45:1289-1302.

17. Ureta AR, Endres RG, Wingreen NS, Silhavy TJ (2007) Kinetic analysis of the assembly of the outer membrane protein LamB in *Escherichia coli* mutants each lacking a secretion or targeting factor in a different cellular compartment. *J Bacteriol* 189:446-454.

18. Kadokura H, Beckwith J (2010) Mechanisms of oxidative protein folding in the bacterial cell envelope. *Antioxid Redox Signal* 13:1231-1246.

19. Kadokura H, Tian H, Zander T, Bardwell JC, Beckwith J (2004) Snapshots of DsbA in action: detection of proteins in the process of oxidative folding. *Science* 303:534-537.

20. Sampson BA, Misra R, Benson SA (1989) Identification and characterization of a new gene of *Escherichia coli* K-12 involved in outer membrane permeability. *Genetics* 122:491-501.

21. Chimalakonda G, Ruiz N, Chng SS, Garner RA, Kahne D, Silhavy TJ (2011) Lipoprotein LptE is required for the assembly of LptD by the beta-barrel assembly machine in the outer membrane of *Escherichia coli*. *Proc Natl Acad Sci* USA 108:2492-2497.

22. Freinkman E, Okuda S, Ruiz N, Kahne D (2012) Regulated assembly of the transenvelope protein complex required for lipopolysaccharide export. *Biochemistry* 51:4800-4806.

23. Kadokura H, Beckwith J (2009) Detecting folding intermediates of a protein as it passes through the bacterial translocation channel. *Cell* 138:1164-1173.

24. Jansens A, van Duijn E, Braakman I (2002) Coordinated nonvectorial folding in a newly synthesized multidomain protein. *Science* 298:2401–2403.

25. Hagan CL1, Kim S, Kahne D (2010) Reconstitution of outer membrane protein assembly from purified components. *Science* 328:890-892.

26. Srinivas N, Jetter P, Ueberbacher BJ, Werneburg M, Zerbe K, Steinmann J, Van der Meijden B, Bernardini F, Lederer A, Dias RL, Misson PE, Henze H, Zumbrunn J, Gombert FO, Obrecht D, Hunziker P, Schauer S, Ziegler U, Käch A, Eberl L, Riedel K, DeMarco SJ, Robinson JA (2010) Peptidomimetic antibiotics target outer-membrane biogenesis in *Pseudomonas aeruginosa*. *Science* 327:1010-1013.

27. Silhavy TJ, Berman ML, Enquist LW (1984) *Experiments with gene fusions* (Cold Spring Harbor Laboratory Press, Plainview, NY)

28. Kadokura H, Beckwith J (2002) Four cysteines of the membrane protein DsbB act in concert to oxidize its substrate DsbA. *EMBO J* 21:2354-2363.

Chapter Three

Characterization of Lipopolysaccharide Translocon Folding by the Bam Complex

3.1. Introduction

In Chapter Two, we demonstrated that we were able to see seven intermediates along the biogenesis pathway of LptD, in which folding of the β-barrel is the rate-limiting step (*1*). Since folding of the β-barrel takes ~20 min for LptD/E, we wondered if we could characterize this process further. In this chapter, we study how the Bam complex folds LptD.

One of the most important functions of the Bam complex is to fold LptD as LptD, together with lipoprotein LptE, facilitates the final insertion of LPS into the OM. Among all the β-barrel substrates of Bam complex, only two of them are essential: BamA, the β-barrel component of the Bam complex itself and LptD, the β-barrel portion of the OM LPS translocon (*2, 3*).

Folding of general β-barrel proteins by the Bam machinery is rapid (*4*). For example, a typical β-barrel protein, LamB, folds in a matter of seconds (*4*). The rapid nature of this general folding process complicates study, since it is unlikely that folding intermediates could be observed during such a short time frame. For this reason, LptD is an ideal substrate to study Bam assisted protein folding, because the long folding process greatly increases the likelihood of observing distinct intermediates on the Bam complex.

Folding of LptD is a challenging task. In its folded form, LptD forms a tight plug-and-barrel complex with the lipoprotein LptE (*5, 6*). As an lipoprotein, LptE arrives at the OM via a separate Lol pathway. How the two proteins that are directed to the OM by separate means fold into a tight complex with one sitting inside of the other poses a challenging question.

This chapter describes our efforts to characterize Bam assisted LptD folding by studying folding intermediates on the Bam complex. We employed a chemical crosslinking technique in both steady state and radioactive methionine pulse labeled cells to trap substrates on the Bam

complex. In collaboration with two geneticists, Prof. Thomas Silhavy at Princeton University and Prof. Natividad Ruiz at Ohio State Univeristy, and with Dr. Joseph Wzorek in our group, we first demonstrated that an LptD mutant can be chemically crosslinked to BamA. We further characterized this trapped LptD mutant species and found that it is a species that we have seen before; a species that has a characteristic **[1,2]** disulfide bond which indicates that it is an intermediate on the assembly pathway of LptD. We demonstrated that this trapped species on the Bam complex is a folding intermediate when all four essential OM proteins (BamA/D, LptD/E) are making contacts with each other. We also found that the lipoprotein LptE is part of the Bam complex when folding LptD, and it mediates the interaction between an essential Bam lipoprotein and LptD. Additionally, we demonstrated that LptE and BamA can be purified as a stable complex, and the presence of LptE enhances the activity of the machine when folding a β-barrel substrate.

3.2. Results and Discussion

3.2.1. LptD and LptE can be chemically crosslinked to BamA *in vivo*

LptD is a slow folding substrate on the Bam complex (*1*). We wondered if it is sufficiently slow that we could see a folding substrate on the Bam machine. We first analyzed the folding of wild-type LptD, a defective mutant *lptD4213* and its intragenic suppressor *lptD61* by looking at dithiobis[succinimidyl propionate] (DSP) crosslinking between LptD and BamA. *LptD4213* harbors a 23 amino acid deletion in one of the putative extra-cellular loops, which results in the accumulation of a LptD species that has intermediary disulfide bonds (see Chapter Two) and *lptD61* has an additional N274I mutation that restores the majority of LptD back to the functional form (Fig 3.1A). DSP, a thiol cleavable crosslinking reagent, has two amine-reactive groups at

each end of a spacer arm that can react with proteins that physically interact. At steady state, we observed little to no wild type LptD crosslinked to BamA (Fig. 3.1B, lane 1). However, a large amount of LptD4213 crosslinked to BamA can be found (Fig. 3.1B, lane 2). The intragenic suppressor, *lptD61*, reduced the amount of crosslinking significantly (Fig. 3.1B, lane 3). These results suggest that mutant LptD can be trapped on BamA *in vivo*.

We wondered what else was also attached to BamA when LptD4213 accumulated on it. We found that another essential lipoprotein is associated with BamA (Fig. 3.1B); that lipoprotein is LptE, the lipoprotein that resides inside the lumen of the β-barrel of LptD. It suggests that LptE is present on the Bam complex when folding LptD.

Genetic evidence arising from a mutant-suppressor pair of LptE and BamA also suggests that LptE is involved in the Bam mediated folding of the LptD/E complex (*8*). LptE6, a defective LptE mutant that harbors a two-amino acid deletion (**Δ**100-101/P99R) which causes accumulation of **[1,2][3,4]**-LptD (*1, 8*), can be rescued by a suppressor found in BamA ($BamA_{P159L}$) (*8*). How $BamA_{P159L}$ rescues LptE6 remains unknown.

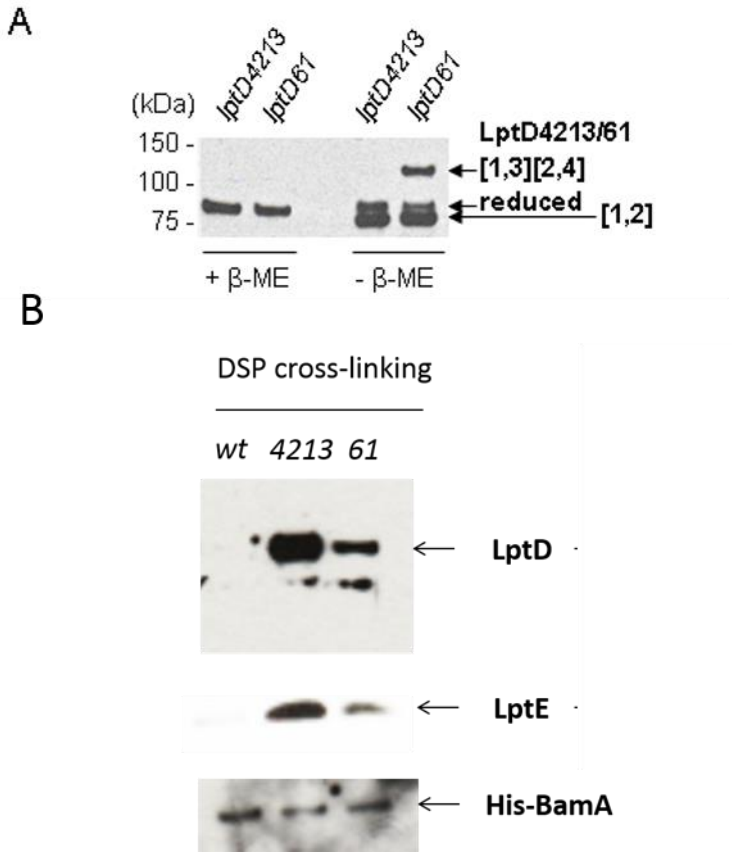

Figure 3.1. LptD and LptE can accumulates on BamA in an LptD mutant. (*A*) α-LptD immunoblot analysis of OM fragments obtained from *wt*, *lptD4213* and *lptD61* strains. (*B*) *wt*, *lptD4213* and *lptD61* strains expressing his-BamA were crosslinked with DSP, affinity purified with Ni-NTA column and analyzed by α-LptD and α-LptE immunoblot under reducing condition.

3.2.2. The chemically trapped LptD on BamA is a characterized intermediate along the LptD biogenesis pathway

LptD undergoes specific oxidative rearrangement of disulfides during its biogenesis (*1*, see Chapter Two). We wondered if the crosslinked species was a species that was slower to assemble, and we were crosslinking a folding intermediate. To address this question, we investigated the oxidation states of the crosslinked LptD4213 species.

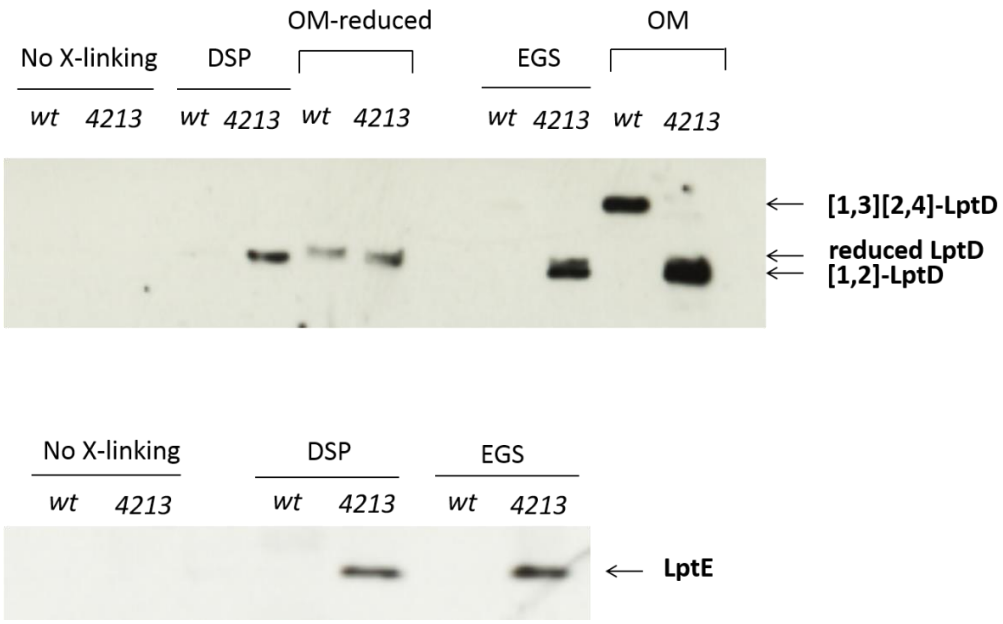

Figure 3.2. The mutant that accumulates on BamA is a characterized intermediate on the assembly pathway of LptD. *wt* and *lptD4213* cells expressing his-BamA were crosslinked with DSP or EGS and affinity purified with a Ni-NTA column. Crosslinkers were subsequently cleaved by treatment with β-mercaptoethanol (in the case of DSP) or hydroxylamine (in the case of EGS). Samples are subjected to α-LptD and α-LptE immunoblot analyses. Outer membrane fragment of the same cells are used as internal markers.

In order to analyze the oxidation states of crosslinked intermediates, we switched to a different crosslinking reagent, ethylene glycol bis[succinimidylsuccinate] (EGS), which, unlike DSP, could be cleaved under non-reducing condition that allows the assessment of disulfide bond configurations. We found that the trapped LptD substrates on BamA were indeed in the **[1,2]** disulfide bonded state by comparing SDS–polyacrylamide gel electrophoresis (PAGE) mobility to authentic standards isolated from outer membranes of respective strains (Fig. 3.2). This shows that the accumulated species that we trapped on BamA is an intermediate that we have observed before (see Chapter Two) (*1*). It is a species that is an intermediate on the assembly pathway of LptD and it has not yet finished assembly (*1*). We conclude that *lptD4213* is a mutation that leads to an assembly defective substrate that accumulates on the Bam complex.

3.2.3. LptD can be trapped by chemical crosslinking during folding on BamA as on-pathway folding intermediates

We wondered if the crosslinked species that we observed represents an accumulated on-pathway folding intermediate of LptD on BamA. We have previously developed a S^{35}-methionine pulse-chase method that allows us to observe seven intermediates along the biogenesis pathway of LptD (see Chapter Two) (*1*). We wondered if we could extend and modify this method to allow crosslinking reaction during the process of folding to determine if the crosslinked species observed occurs at the Bam complex during β-barrel assembly. We performed DSP crosslinking on [^{35}S]-methionine pulse-labeled Myc_3-tagged LptD at different time points during the folding process and monitored the amount of crosslinked LptD on $FLAG_3$-tagged BamA. Both Myc_3-tagged LptD and $FLAG_3$-tagged BamA are functional and can fully complement their respective chromosomal copy. We observed a band corresponding to wild type LptD at time points from 0 to 10 min, which subsequently disappeared by 20 min (Fig. 3.3A). The time-dependent crosslinking observed is consistent with the fact that wild type LptD does not crosslink to BamA at steady state (Fig. 3.1, 3.2). Presumably the folding reaction occurred rapidly enough that wild type LptD does not accumulate on BamA to a significant level at steady state.

When the mutant LptD, LptD4213, was subject to the same crosslinking during pulse-chase analysis, we observed that the amount of LptD4213 that crosslinked to BamA did not change over time (Fig. 3.3B). Moreover, it appeared that a much larger percentage of the mutant substrate was crosslinked to BamA that that of the wild type substrate.

We wondered if the mutant substrate that appears to be stably associated with BamA implies that the mutant is jammed on the Bam machine. There is a single point mutant of LptD4213 at N274I that suppresses the phenotypes associated with the defective substrate. We

examined this mutant, LptD61, in a similar pulse-chase crosslinking experiment. We found that the LptD61 mutant showed time-dependent crosslinking to BamA that was similar to wild type (Fig. 3.3C). Given that the only chemical difference between LptD4213 and LptD61 is a single amino acid substitution, we conclude that LptD4213 represents an on-pathway folding intermediate on the Bam complex.

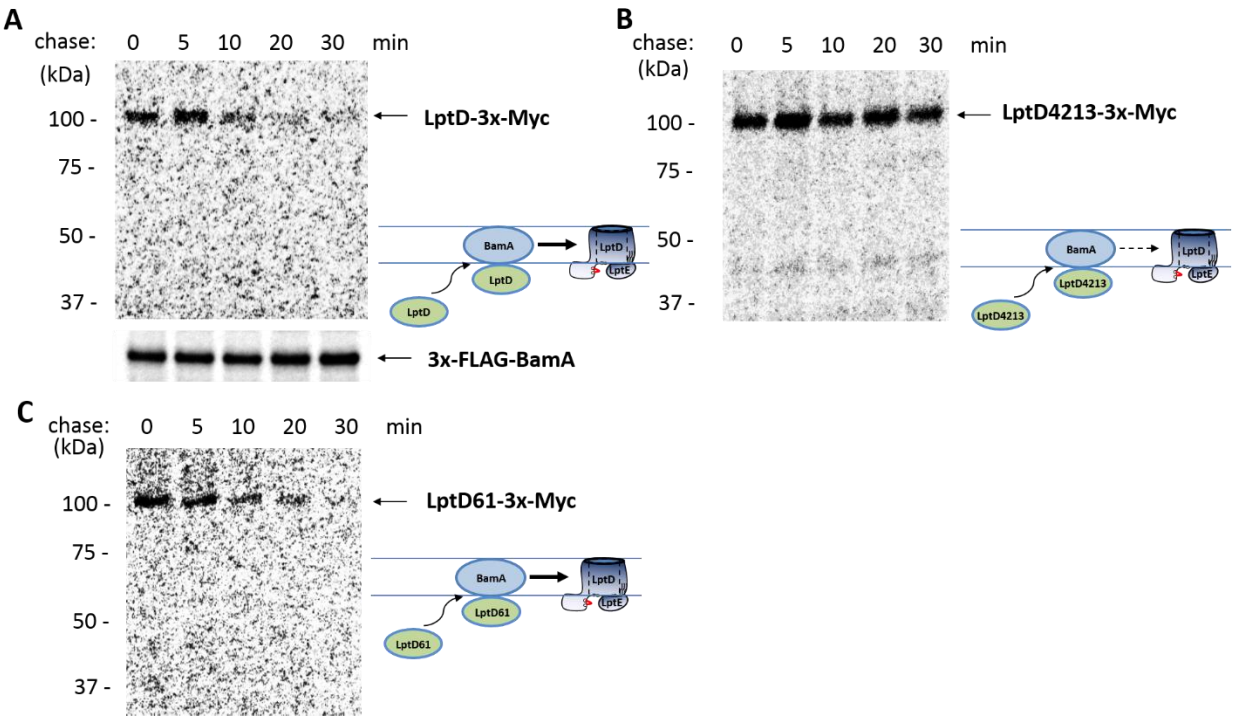

Figure 3.3. LptD can be trapped by chemical crosslinking during folding on BamA. (A-C) Cells expressing 3x-FLAG-BamA and LptD(wt/4213/61)-3x-Myc were pulsed with [^{35}S]-methionine and chased with cold methionine. The samples were washed, crosslinked with DSP, immunoprecipitated with α-FLAG antibody, and analyzed by SDS-PAGE / autoradiography. A second immunoprecipitation with α-Myc antibody enriched BamA-LptD complex.

3.2.4. Loading of LptD to BamA is independent of LptE

We next wondered if defects in the Bam machine would slow the folding of wild type LptD substrates to allow trapping during folding. We have shown that LptE is present at the Bam complex during the folding of LptD (Fig. 3.1 and 3.2). A very challenging part of LptD/E assembly is that both polypeptide chains are delivered to the OM via different pathways and yet are seemingly assembled simultaneously at the Bam complex. There are a couple of hypotheses on how LptD and LptE reach the Bam complex. One hypothesis is that LptD and LptE go to the Bam complex independent of each other. A second hypothesis is that they form a pre-complex in the periplasm prior to folding. This complex is then delivered to the Bam complex. A third hypothesis is that LptE is required for LptD to be loaded to Bam. Lastly, a fourth hypothesis is the opposite of the third, meaning that LptD is required for LptE to be recruited to Bam.

In order to test the above hypotheses, we used a strain that conditionally expresses very low levels of LptE and tested whether we could trap stalled wild type LptD on BamA. When LptE became the limiting reagent (Fig. 3.4, left panel), we saw significant accumulation of wild type LptD on BamA, comparable to the amount of LptD in *lptD4213* mutant that was trapped during folding (Fig. 3.4, right panel). The accumulated LptD on BamA can be subsequently rescued when LptE was no longer limiting, restoring the system back to a state that is similar to wild type (Fig. 3.4, right panel). This shows that wild type LptD can interact with BamA independent of LptE. However, earlier recruited LptD substrate was folded by the Bam complex only when LptE was sufficiently provided.

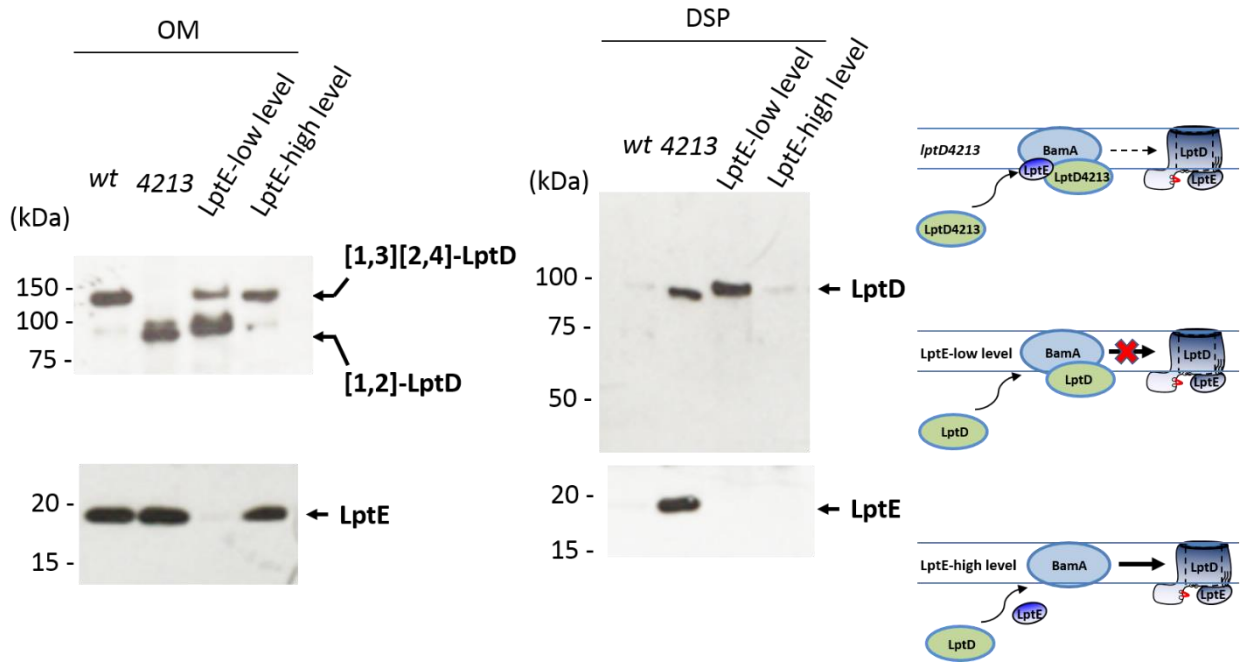

Figure 3.4. Loading of LptD to BamA is independent of LptE. α-LptD and α-LptE immunoblot analysis of OM fragments obtained from *wt, lptD4213* and LptE-limiting strains expressing his-BamA. Both early log (OD = 0.22) and mid log (OD = 0.66) phase cells for the LptE-limiting strain are analyzed. The same strains were crosslinked with DSP, affinity purified with Ni-NTA column and analyzed by α-LptD and α-LptE immunoblot under reducing conditions.

3.2.5. LptE mediates the interaction between LptD and BamD

There are two essential Bam proteins that function to fold β-barrel proteins, BamA and BamD. Defective LptD substrate, LptD4213, could be accumulated on BamD with LptE present (Fig. 3.5, lane 2). However, when LptE is limiting, we did not observe wild type LptD crosslinked to BamD (Fig. 3.5, lane 3). This suggests that, unlike the interaction between LptD and BamA, LptD cannot interact with BamD without LptE. These experiments suggests that LptE is also present as part of a Bam complex that is required to fold wild type LptD. Specifically, these results imply that LptE modulates the binding of BamD and LptD.

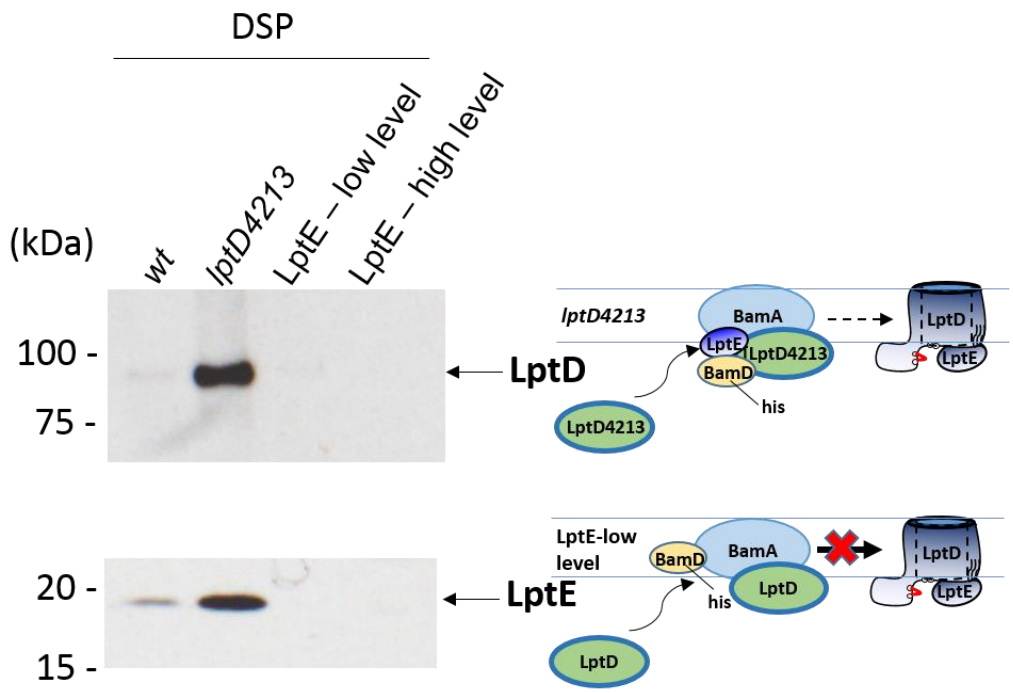

Figure. 3.5. LptE mediates the interaction between LptD and BamD. *wt*, *lptD4213* and LptE-limiting strains with different LptE levels expressing BamD-his were crosslinked with DSP, affinity purified with Ni-NTA column and analyzed by α-LptD and α-LptE immunoblot under reducing conditions.

3.2.6. LptE and BamA form a stable complex *in vitro*

As we mentioned before, LptE arrives at the OM through a separate Lol pathway, which sorts lipoproteins to their destinations by chaperoning their lipid anchor (*9*). Interestingly, the lipid anchor of LptE is not required for cell viability (*10*). These results seem to suggest that there may be an independent pathway for LptE to reach the Bam complex for LptD folding.

One implication of the preceding experiments is that LptE is present on the Bam complex only when LptD is there. We wonder if LptE also forms a complex with BamA without LptD.

To test this hypothesis, Dr. Joseph Wzorek performed Ni-NTA affinity purification with his-tagged BamCDE and LptE, and monitored how much FLAG-tagged BamA can be co-purified (Fig. 3.6). To our surprise, LptE pulled down BamA to a similar extent comparable to BamCDE (Fig. 3.6, compare lane 4 with 5), indicating that BamA can co-purify with LptE. Furthermore, when purified BamA and his-tagged LptE were mixed together *in vitro*, they form a stable complex that could be purified by Fast Protein Liquid Chromatography (FPLC), suggesting that this interaction is quite stable (Fig. 3.7).

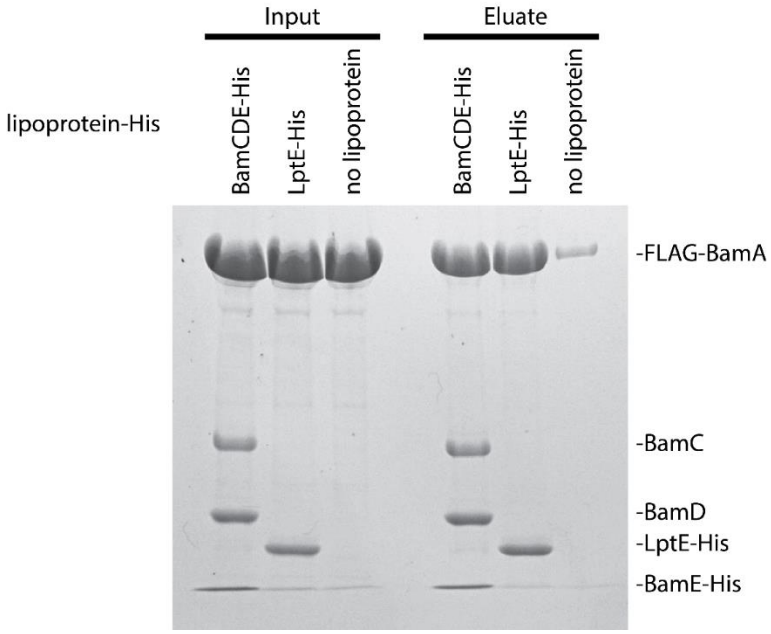

by Dr. Wzorek

Figure 3.6. BamA co-purifies with LptE *in vitro*. Ni-NTA affinity purification of BamCDE-his and LptE-his with FLAG-tagged BamA, visualized by SDS-PAGE followed by Coomassie Blue stain.

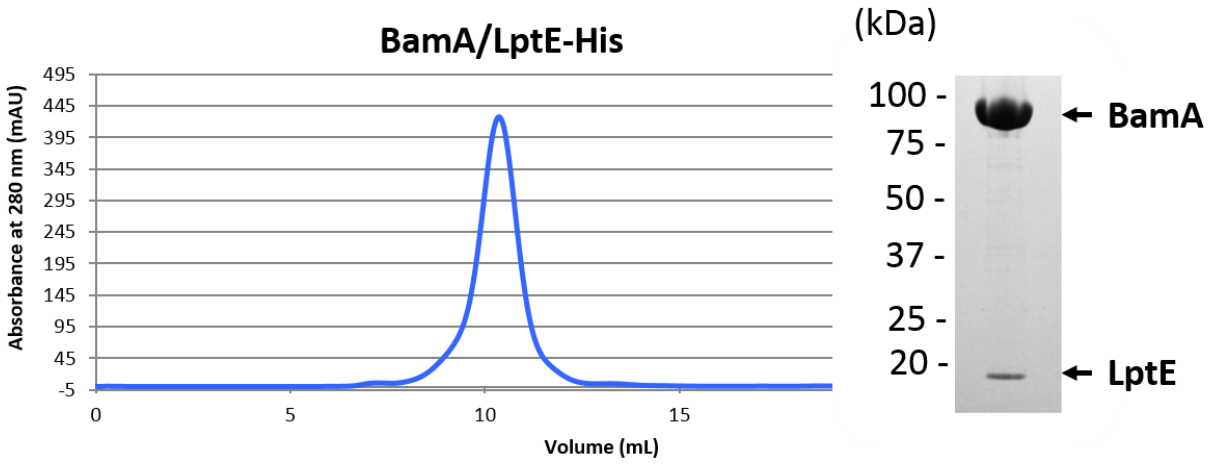

by Dr. Wzorek

Figure 3.7. BamA-LptE forms a stable complex *in vitro*. FPLC purification of BamA/LptE-his complex formed by mixing purified components, visualized by SDS-PAGE followed by Coomassie Blue stain.

3.2.7. LptE modulates the activity of BamA *in vitro*

We wondered if the BamA-LptE complex is capable of folding β-barrel substrates. To test the activity of the Bam-LptE complex *in vitro*, we took advantage of a proteoliposome-based β-barrel protein folding assay that we have developed (*11-13*). We made proteopliposomes that contained either BamA or a BamA-LptE complex, and monitored their activity in folding FLAG-tagged, urea denatured BamA substrate. Proteoliposomes containing BamA alone showed moderate activity in folding FLAG-BamA, judging by the appearance of some folded FLAG-BamA at 2 hours and that the amount of folded protein increased to 15% over a course of 4 hours (Fig. 3.8, left panel). However, the proteoliposomes that contained the BamA-LptE complex showed much higher activity on FLAG-BamA substrate compared to proteoliposomes that contained BamA alone (Fig. 3.8, right panel). 25% of FLAG-BamA is folded by BamA-LptE complex at the end of a 4-hour period, while only 15% is folded by BamA alone. Moreover,

significantly more FLAG-BamA (12% vs. 2%) is folded after 2 hours by BamA-LptE than BamA itself (Fig. 3.8, plotted chart), suggesting that BamA-LptE is better at initiating folding compared to BamA alone. This result implies that LptE is able to form an active Bam complex with BamA without LptD *in vitro*.

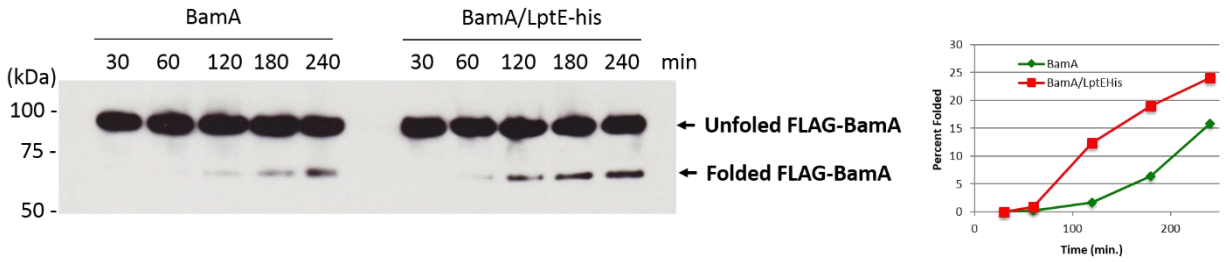

by Dr. Wzorek

Figure 3.8. LptE-BamA forms an active complex in vitro. Urea denatured FLAG-BamA was incubated with proteoliposomes containing BamA or BamA/LptE-his. Samples were processed using non-denaturing conditions and analyzed by seminative SDS-PAGE that preserve the β-barrel fold. α-FLAG immunoblot analyses of the samples at different time points during the folding reaction. Bands were quantified by densitometry and plotted against reaction time.

3.2.8. A model for LptD folding on Bam complex

Based on the preceding results, we propose a model for LptD folding by the Bam complex (Fig. 3.9). LptD is delivered to BamA by the periplasmic chaperone SurA (Fig. 3.10), which interacts with the P1 domain of BamA that resides in the periplasm (*14, 15*). LptD could be delivered to an LptD-compatible Bam complex that already contains LptE, or an LptD-non-compatible Bam complex that requires an LptE that arrives later to fold LptD. We are not sure which pathway is preferred in the wild-type cells. Once all four essential OM proteins are together, LptD transitions into a folding intermediate which further progresses to yield a folded LptD/E

complex with intermediary disulfide bonds. Disulfide rearrangement finally produces a functional LPS translocon.

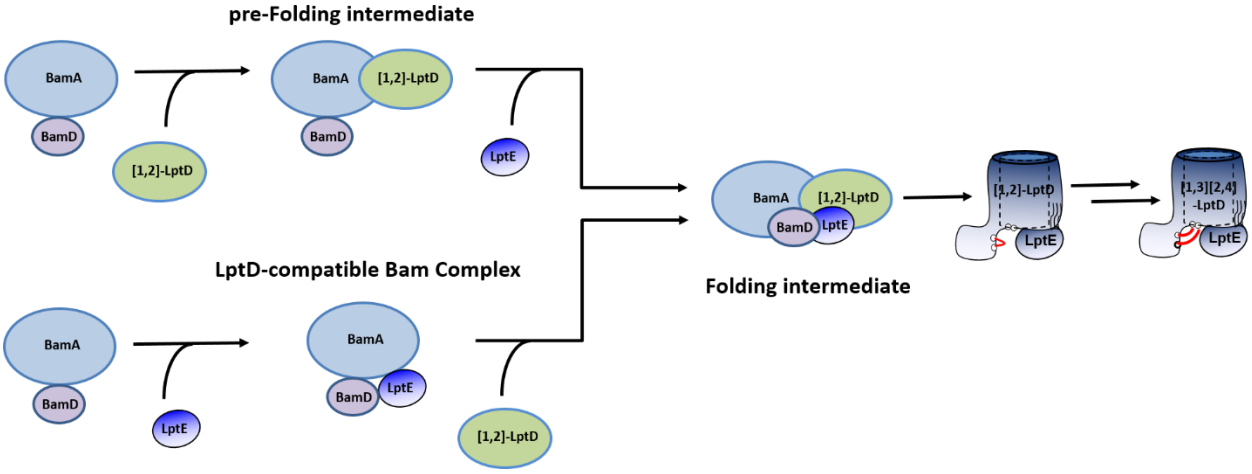

Figure 3.9. A model for LptD folding by Bam complex. Two independent pathways that lead to the formation of a folding intermediate are shown.

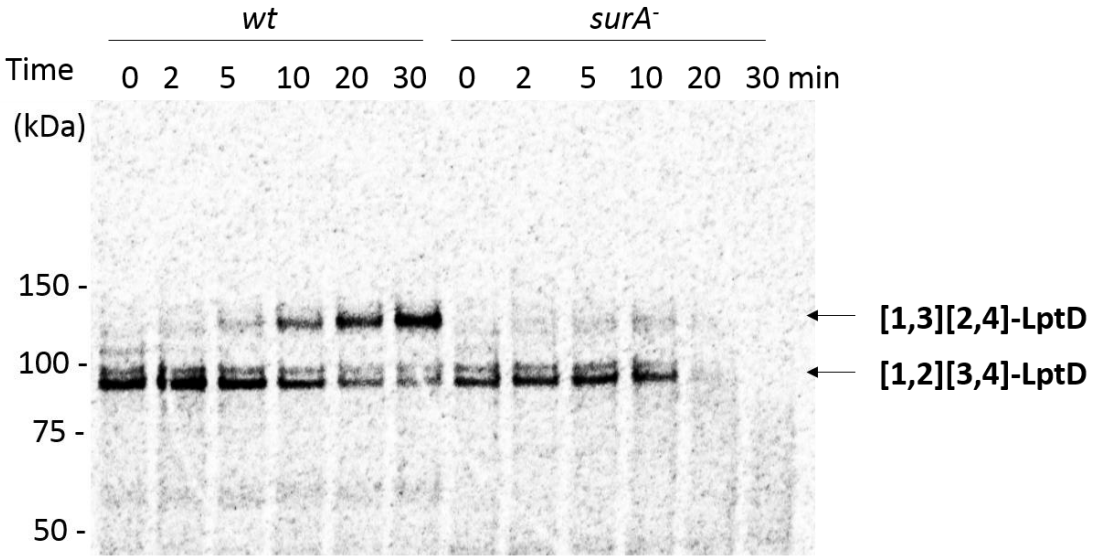

Figure 3.10. SurA is required to fold LptD. [^{35}S]-Met pulse-chase of newly-synthesized LptD-FLAG$_3$ in wild type (see Chapter Two) and a *ΔsurA* background.

3.3. Conclusion and Future Work

We and others have shown that LptE is required to form the functional, properly oxidized LPS translocon (*6*-*9*, 10). In this chapter, we characterize Bam assisted folding of LptD in the context of LptE. We have identified LptE as a part of a Bam complex that is required to fold LptD. A folding intermediate on the Bam complex containing all four essential OM proteins, LptD/E and BamA/D, is identified. LptD can be loaded to BamA independent of LptE, forming a folding competent pre-complex. However, LptD does not interact with BamD without LptE, suggesting that folding does not occur before an LptD-compatible Bam complex is ready. We have also shown that LptE and BamA form an active complex that is capable of folding β-barrels *in vitro*.

As mentioned in Chapter Two, Bam assisted folding of general β-barrels is rapid (*4*). In *E. coli*, there are millions of copies of β-barrel proteins in each cell and the Bam complex needs to fold all of them in a very limited time. A typical β-barrel protein takes very little time (<30s) (*4*) to fold, however, it takes ¼ of a cell cycle to fold the LPS translocon (*1*). This imposes a huge challenge for the Bam complex as one substrate that consists of less than 0.1% of the substrate pool is taking 25% of the cell's capacity to fold β-barrel proteins. Making a different kind of Bam complex that contains LptE be required to fold LptD may provide a capacity control mechanism at the OM.

We have demonstrated that LptE can complex with BamA in the absence of LptD *in vitro*. We are trying to see if this interaction is relevant in the cell as well. Also, we have no evidence that LptE is part of a Bam complex when folding β-barrel proteins other than LptD *in vivo*.

Our long term goal is to elucidate a mechanism of β-barrel folding on the Bam complex. Over the past few years, X-ray crystal structures of all the individual Bam components have been

solved (*16-18*), but how the Bam complex handles substrates is still unclear. Structural information of the Bam complex with or without LptE could be valuable in understanding how the multi-protein complex functions. Substrates with photo-activatable amino acids that crosslink to different components of the Bam complex could provide information on site-specific interfaces that are important in substrate-Bam interactions.

3.4. Materials and Methods

3.4.1. Bacterial strains and growth conditions

The wild-type strain used is MC4100 [*F*$^{-}$ *araD139 Δ(argF-lac) U169 rpsL150 relA1 flbB5301 ptsF25 deoC1 ptsF25 thi*]. The *lptD*$_{\Delta 330\text{-}352}$ (*lptD4213*) mutant strain used is NR698 (*20*). The *lptD*$_{\Delta 330\text{-}352,\ N274I}$ (*lptD61*) mutant strain used is NR731 (*20*). The LptE-depletion strain used that makes varying levels of LptE according to growth phase is MC4100 *ara*$^{+}$ *lptE*$^{-}$ λ_{att}(*P*$_{BAD}$-*lptE)*. It is constructed by removing the kanamycin resistance cassette on AM689 using methods previously described (*28*). The *surA*$^{-}$ strain used is NR1215. Luria-Bertani (LB) broth and M63/glucose minimal broth and agar were prepared as described previously (*27*). Arabinose (0.2% w/v) was added for the growth of MC4100 *ara*$^{+}$ *lptE*$^{-}$ λ_{att}(*P*$_{BAD}$-*lptE)*. Growth of strains was carried out at 37 ^{o}C unless explicitly indicated. When appropriate, kanamycin (50 μg/ml) and spectinomycin (50 μg/ml) were added. Amino acids were added at 50 μg/ml when indicated.

3.4.2. Plasmid construction

To construct pET9a*His-BamA*, a cassette containing the coding sequence of the His-BamA was inserted into pET9a. Briefly, pET23/42*His-BamA* template was amplified by PCR (using primers 5'- AAT TGG ATC CAT GGC GAT GAA AAA GTT GCT C -3' and 5'- ATA TGC TCA

GCT TAC CAG GTT TTA CCG ATG TTA AAC -3') and the resulting PCR product was digested with BamHI and BlpI for > 3 h at 37 ºC. The digested PCR product was ligated to a pET9a vector that had been digested with BamHI and BlpI for > 3 h at 37 ºC. NovaBlue (Novagen) cells were transformed with 1 µl of the ligation product and plated onto LB plates containing 50 µg/ml kanamycin. For each construct, plasmids from six colonies were isolated and sequenced.

To construct pET9a*BamD-His*, a cassette containing the coding sequence of the BamD-His was inserted into pET9a. Briefly, pET23/42*BamD-His* was digested with digested with XbaI and BlpI for > 3 h at 37 ºC. The digested product was gel purified and the coding sequence of the BamD-His was ligated to a pET9a vector that had been digested with XbaI and BlpI for > 3 h at 37 ºC. NovaBlue (Novagen) cells were transformed with 1 µl of the ligation product and plated onto LB plates containing 50 µg/ml kanamycin. For each construct, plasmids from six colonies were isolated and sequenced.

To construct pET9a*FLAG$_3$-BamA*, a cassette containing the coding sequence of the FLAG$_3$ tag was inserted into pET9a*His-BamA* to replace the original His$_6$ tag. Briefly, the entire pET9a*His-BamA* template was amplified by PCR (using primers 5'- A GAT CAT GAT ATC GAC TAT AAA GAC GAT GAT GAC AAA GAA GGG TTC GTA GTG AAA GAT-3' and 5'- TCG ATA TCA TGA TCT TTG TAG TCG CCG TCG TGA TCT TTA TAA TCA GCA CCG TAT ACG GTG-3') and the resulting PCR product mixture digested with DpnI for > 1 h at 37 ºC. NovaBlue (Novagen) cells were transformed with 1 µl of digested PCR product and plated onto LB plates containing 50 µg/ml kanamycin. For each construct, plasmids from six colonies were isolated and sequenced.

3.4.3. *In vivo* DSP crosslinking

Crosslinking experiments are based on techniques described by Thanabalu et al. (1998) with modifications. Stains MC4100, NR698, NR731, MC4100 *ara*$^{+}$ *lptE*$^{-}$ λ_{att}*(*P_{BAD}*-lptE)* containing either pET9a*His-BamA* or pET9a*BamD-His* were used in *in vivo* DSP crosslinking experiments. Cells were grown in 500 mL of LB to OD_{600} ~0.6 unless explicitly indicated. Cells were pelleted by centrifugation at 5000 x *g* for 15 min and the cell pellets were washed twice with 25 ml of 150 mM of NaCl and 10 mM of NaH_2PO_4, pH = 7.2, and resuspended in the same buffer. DSP dissolved in DMSO was added to the cell suspension at a final concentration of 200 μg/mL and the cells were incubated for 30 min at 37ºC. The crosslinking reaction was quenched by addition 1 M Tris.HCl (pH = 8.0) to a final concentration of 20 mM, and cells were harvested by centrifugation at 5000 x g for 10 min. Cell pellets were resuspended in 5 mL of 20 mM Tris.HCl (pH = 8.0), 150 mM NaCl, and 1% Anzergent 3-14 containing lysozyme (50 μg/mL), DNase I (50 μg/mL), and RNase I (50 μg/mL), and were lysed by sonication. In order to remove cell debris after lysis, the mixture was then centrifuged at 10,000 x g for 10 min. The cleared lysate was supplemented with 20 mM Imidazole (pH = 8.0), and incubated with 200 μL of pre-equilibrated Ni-NTA resin for 30 min at 4 ºC. The column was then washed 4 times with 10 mL of 20 mM Tris.HCl (pH = 8.0), 300 mM NaCl, 40 mM Imidazole, 0.1% Triton X-100, and 0.1% SDS. The column was eluted with 4 mL of 20 mM Tris.HCl (pH = 8.0), 300 mM NaCl, and 200 mM Imidazole. The eluate was concentrated via ultrafiltration at 5000 x g for 20 min. The concentrated sample was used for SDS-PAGE and Western blot analysis.

3.4.4. *In vivo* DSP crosslinking of [^{35}S]-pulse-labeled cells

Stains MC4100 containing *pET9aFLAG$_3$-BamA* and p*LptD/LptD4213/LptD61-Myc$_3$* were used in *in vivo* DSP crosslinking of [^{35}S]-pulse-labeled cells. A 25 mL culture was grown to OD_{600}

~0.6 in M63/glucose minimal media supplemented with eighteen amino acids (minus methionine and cysteine) at 37 ^{o}C. The culture was pulse-labeled with [^{35}S]-methionine (200 μCi/ml final concentration) (American Radiochemicals) for 2 min and then chased with cold methionine (5 mM) at 37 ^{o}C. At the indicated time points during the chase, a 5 mL culture aliquot was pelleted by centrifuging at 14,000 x g for 1 min. The cell pellet was resuspended in 300 μL of 150mM of NaCl and 10mM of NaH_2PO_4, pH = 7.2, pelleted again at 18,000 g for 30 seconds, and resuspended in 300 μL of the same buffer. 3 μL of DMSO containing 75 μg of DSP was added to the resuspended cells and incubate at 37 ^{o}C for 30 min. The crosslinking reaction was quenched by addition 1 M Tris.HCl (pH = 8.0) to a final concentration of 20 mM followed by addition of 50 μl of trichloroacetic acid (TCA, 70% in water) and incubated on ice for 20 min. Precipitated proteins were pelleted at 18,000 x *g* for 10 min at 4 ^{o}C, washed with 1 mL of ice-cold acetone, and then solubilized in 150 μl of 100 mM Tris.HCl, pH = 8.0 containing 1% SDS. The sample was sonicated for 30 s to aid solubilization. Following that, 1.4 mL of ice-cold IP buffer (50 mM Tris.HCl, pH = 8.0 containing 150 mM NaCl, 2% Triton X-100, 1 mM EDTA) was added and the sample was centrifuged at 18,000 x *g* for 10 min at 4 ^{o}C. 1.4 mL of the supernatant was transferred to another 1.5-ml tube containing 25 μl of anti-FLAG® M2 magnetic beads (Sigma). The beads were washed and pre-equilibrated with 3 x 1 ml IP buffer before use. The mixture was incubated on a rotary shaker for 3~4 h at 4 ^{o}C, and the beads were washed with 4 x 1 mL of ice-cold high salt buffer (50 mM Tris.HCl, pH = 8.0 containing 1 M NaCl, 1% Triton X-100, 1 mM EDTA) and 1 x 1mL ice-cold 10 mM Tris.HCl, pH = 8.0 using a magnetic separation rack (New Englands Biolabs). 160 μl 100 mM Tris.HCl, pH = 8.0 containing 1% SDS was then added to the beads and the mixture heated for 10 min at 100 ^{o}C to elute the bound proteins. 10 μl of the eluate was mixed with 2X SDS reducing sample buffer. 1.4 mL of ice-cold IP buffer (50 mM Tris.HCl, pH 8.0

containing 150 mM NaCl, 2% Triton X-100, 1 mM EDTA) was added to the remaining 150 µl of the eluate and the sample was centrifuged at 18,000 x *g* for 10 min at 4 ^{o}C. 1.4 mL of the supernatant was transferred to another 1.5-ml tube containing 120 µl of anti-Myc agarose beads (Sigma). The beads were washed and pre-equilibrated with 3 x 1 ml IP buffer before use. The mixture was incubated on a rotary shaker for 3~4 h at 4 ^{o}C, and the beads were washed with 4 x 1 mL of ice-cold high salt buffer (50 mM Tris.HCl, pH = 8.0 containing 1 M NaCl, 1% Triton X-100, 1 mM EDTA) and 1 x 1mL ice-cold 10 mM Tris.HCl, pH = 8.0. 80 µl 2X SDS non-reducing sample buffer was then added to the beads and the mixture heated for 10 min at 100 ^{o}C to elute the bound proteins. 15 µl of eluted sample was applied to SDS-PAGE directly. 4-20% Tris.HCl polyacrylamide gels were used (running conditions: 150 V for 90 min). The gel was then dried and exposed to phosphor storage screens for autoradiography.

3.4.5. *In vivo* EGS crosslinking

Stains MC4100, NR698 containing pET9a*His-BamA* were used in *in vivo* EGS crosslinking experiments. The protocol is largely similar to that of *in vivo* DSP crosslinking with modifications. Cells were grown in 500mL of LB to OD_{600} ~0.6, pelleted by centrifugation at 5000 x *g* for 15 min. The cell pellets were washed twice with 25 ml of 150 mM of NaCl and 10 mM of NaH_2PO_4, pH = 7.2 and resuspended in the same buffer. EGS dissolved in DMSO was added to the cell suspension at a final concentration of 200 µg/mL, and the cells were incubated for 30 min at 37^{o}C. The crosslinking reaction was quenched by addition 1 M Tris.HCl (pH = 7.4) to a final concentration of 20 mM, and cells were harvested by centrifugation at 5000 x g for 10 min. Cell pellets were resuspended in 5 mL of 20 mM Tris-HCl (pH = 8.0), 150 mM NaCl, and 1% Anzergent 3-14 containing lysozyme (50 µg/mL), DNase I (50 µg/mL), and RNase I (50

μg/mL), and were lysed by sonication. In order to remove cell debris after lysis, the mixture was then centrifuged at 10,000 x g for 10 min. The cleared lysate was supplemented with 20 mM Imidazole (pH 8.0), and incubated with 200μL of pre-equilibrated Ni-NTA resin for 30 min at 4 ^{o}C. The column was then washed 4 times with 10 mL of 20 mM Tris buffer (pH = 8.0), with 300 mM NaCl, 40 mM Imidazole, 0.1% Triton X-100, and 0.1% SDS. The column was eluted with 4 mL of 20 mM Tris.HCl (pH = 8.0), 300 mM NaCl, and 200 mM Imidazole. The eluate was concentrated via ultrafiltration at 5000 x g for 20 min (~30 μl) and added to 470 μl of freshly made 1 M hydroxylamine.HCl, pH = 8.5, 0.02% Anzergent 3-14 and incubate at 37 ^{o}C for 4 hours, followed by dialysis against 1 L of 20mM Tris.HCl, pH = 8.0, 150 mM NaCl, 0.02% Anzergent 3-14 overnight. The resulting solution was concentrated via ultrafiltration at 18,000 x g for 20 min. The concentrated sample was used for SDS-PAGE and Western blot analysis.

3.4.6. Isolation of OM for analysis of LptD oxidation states

OM analysis is performed as previously described (*1*).

3.4.7. Growth of MC4100 *ara*$^{+}$ *lptE*$^{-}$ λ_{att}(*P*$_{BAD}$-*lptE*) for OM analysis and DSP crosslinking

10-ml cultures were grown overnight at 37 ^{o}C in LB broth containing 0.2% arabinose. Cultures were pelleted and washed twice in equal volume of LB broth. Fresh LB cultures (1.5-l) either containing 0.2% arabinose were inoculated with the washed cells to an initial OD_{600} of ~0.01 and were grown at 37 ^{o}C until OD_{600} reaches ~0.21 and ~0.63. The amount of cells equivalent to that in a 500-ml culture of OD_{600} ~0.5 was pelleted by centrifugation at 5000 x *g* for 20 min and subjected to OM analysis or DSP crosslinking (see above).

3.4.8. Expression and Isolation of Denatured BamA or FLAG-BamA

BamA and FLAG-BamA were expressed as inclusion bodies in a BL21(DE3) strain harboring pCH103 or pCH128, respectively. A 15 mL overnight culture was diluted 1:100 with LB containing 50 μg/mL carbenicillin. The cultures were shaken at 37 °C until an OD_{600} of 0.6 was reached. Protein expression was induced via addition of 150 μL of 1 M IPTG (100 μM final concentration) and the cultures were shaken for an additional four hours. The cells were harvested via centrifugation at 5250 x g for 12 minutes, resuspended in 25 mL TBS (pH 8), and lysed via cell disrupter. The lysate was centrifuged at 5000 x g for 10 minutes and the resulting supernatant was discarded. The pellet was resuspended in 25 mL TBS (pH 8) and centrifuged once more at 5000 x g. The resulting white pellet was treated with 4 mL of 8 M urea and rocked at room temperature for one hour. The resulting mixture was transferred to an epi-tube and spun at 16000 x g for 10 minutes. The supernatant containing urea denatured BamA or FLAG-BamA was transferred to a new epi-tube for storage.

3.4.9. Expression and Purification of LptE-His

LptE-His was expressed in a BL21(DE3) strain harboring pLptE-His. Overnight cultures (8 x 15 mL) were diluted 1:100 with LB containing 50 μg/mL streptomycin. The cultures were shaken at 37 °C until an OD_{600} of 0.1 was reached. At this time, the temperature of the shaker was reduced to 30 °C and the cultures were shaken until an OD_{6oo} of 0.6 was reached. Protein expression was induced via addition of 150 μL of 1 M IPTG (100 μM final concentration) and the cultures were shaken for an additional fourteen hours at 30 °C. The cells were harvested via centrifugation at 5250 x g for 12 minutes, resuspended in 4 x 25 mL TBS (pH 8), and lysed via two passes through

the cell disrupter. The lysate was centrifuged at 5000 x g for 10 minutes and the resulting supernatant was spun at 100,000 x g for 30 minutes. The pellet was resuspended in 30 mL TBS (pH 8), 2% TX-100 and 300 μL of 10 mg/mL lysozyme was added. The suspension was rocked at 4 °C for 1.5 hours, upon which time the mixture was centrifuged once more at 100,000 x g. The resulting supernatant was applied to a Ni-NTA column (2 x 4 mL slurry) and rocked for 30 minutes at 4 °C. The resin was washed 2 x 20 mL of 20 mM imidazole, TBS (pH 8), 0.05% DDM and the protein was eluted with 16 mL of 200 mM imidazole, TBS (pH 8), 0.05% DDM. The eluate was concentrated with a 30 kDa concentrator and further purified via size exclusion chromatography (0.03% DDM, TBS (pH 8), 1 mM TCEP).

3.4.10. Expression and Purification of BamCDE-His

BamC, BamD, and BamE-His_8 were co-expressed in a BL21(DE3) strain harboring both pSK46 and pBamE-His. Overnight cultures (4 x 15 mL) were diluted 1:100 with LB containing 50 μg/mL streptomycin and 50 μg/mL carbenicillin. The cultures were shaken at 37 °C until an OD_{600} of 0.6 was reached. Protein expression was induced via addition of 150 μL of 1 M IPTG (100 μM final concentration) and the cultures were shaken for an additional four hours at 37 °C. The cells were harvested via centrifugation at 5250 x g for 12 minutes, resuspended in 4 x 25 mL TBS (pH 8), and lysed via two passes through the cell disrupter. The lysate was centrifuged at 5000 x g for 10 minutes and the resulting supernatant was spun at 100,000 x g for 30 minutes. The pellet was resuspended in 30 mL TBS (pH 8), 2% TX-100 and 300 μL of 10 mg/mL lysozyme was added. The suspension was rocked at 4 °C for 1.5 hours, upon which time the mixture was centrifuged once more at 100,000 x g. The resulting supernatant was applied to a Ni-NTA column (2 x 4 mL slurry) and rocked for 30 minutes at 4 °C. The resin was washed 2 x 20 mL of 20 mM imidazole,

TBS (pH 8), 0.05% DDM and the protein was eluted with 16 mL of 200 mM imidazole, TBS (pH 8), 0.05% DDM. The eluate was concentrated with a 50 kDa concentrator and further purified via size exclusion chromatography (0.03% DDM, TBS (pH 8), 1 mM TCEP).

3.4.11. Folding and Purification of BamA

Urea denatured BamA prepared at a concentration of 1.0 mM in 8 M urea (see above) was diluted 10-fold into 20 mM Tris (pH 8), 0.25% DDM. This solution was rocked at room temperature for 24 hours, upon which time the solution was concentrated in a 50 kDa cutoff concentrator. The resulting solution was purified via size exclusion chromatography using TBS (pH 8), 0.03% DDM, 1 mM TCEP as buffer. Individual fractions containing primarily folded BamA were combined and re-subjected to size exclusion chromatography with the same buffer as above in order to remove any residual unfolded BamA.

3.4.12. Folded FLAG-BamA Affinity Purifications

FLAG-BamA was prepared at a concentration of 1.0 mM in 8 M urea (see above) and diluted 10-fold into 20 mM Tris (pH 8), 0.25% DDM. This solution was rocked at room temperature for 24 hours, upon which time the solution was concentrated in a 50 kDa cutoff concentrator. Next, 100 μL of a 50 μM solution containing both folded FLAG-BamA substrate and 50 μM either BamCDE-His or 50 μM LptE-His was prepared (both BamCDE-His and LptE-His were independently purified via size exclusion chromatography as described above). The protein mixtures were incubated at room temperature for 15 minutes, upon which time 10 μL was removed for an "input" sample and 85 μL was added to a Ni-NTA column (prepared by pre-equilibrating 200 μL Ni-NTA

slurry with 0.05% DDM, TBS (pH 8), 20 mM imidazole). The resin was washed with 2 x 1 mL 0.05% DDM, TBS (pH 8), 20 mM imidazole and the residual protein complex was eluted with 600 μL 0.05% DDM, TBS (pH 8), 200 mM imidazole. The protein present in the eluate was TCA precipitated and analyzed via SDS-PAGE on a 4-20% gradient gel at 200 V for 40 minutes. The proteins were then detected by staining with Coomassie blue.

3.4.13. Size-Exclusion Chromatography with BamA and LptE-His

A 1 mL solution of 20 μM BamA and 40 μM LptE-His (both expressed and purified as described above) was prepared in 0.03% DDM, TBS (pH 8), 1 mM TCEP and concentrated to 250 μL in a 50 kDa concentrator. This material was immediately purified via size exclusion chromatography in the same buffer, and the fractions were analyzed via SDS-PAGE. The fractions containing both BamA and LptE-His were combined and concentrated in a 50 kDa concentrator to 250 μL. This procedure was repeated twice more to yield the purified BamA/LptE-His complex used for the proteoliposome activity assay.

3.4.14. Preparation of Proteliposomes Containing BamA or BamA/LptE-His

A 200 uL solution of 10 μM BamA or BamA/LptE-His in 0.03% DDM, TBS (pH 8), 1 mM TCEP was prepared in a 1.5 mL epi-tube and treated with 40 μL of freshly dissolved 20 mg/mL *E. coli* phospholipids. This mixture was incubated on ice for 5 minutes, upon which time the solutions were diluted with 8 mL TBS (pH 8) and incubated on ice for 30 additional minutes. The solutions were spun at 300,000 x g for 2 hours and the resulting supernatant was removed. The pellets were resuspended in 200 μL TBS and used directly in the folding assay.

3.4.15. Folding of FLAG-BamA into Proteoliposomes

Folding reactions were performed in 0.2 mL PCR tubes containing 13 µL TBS, 5 µL proteoliposome suspension, and 2 µL of 5 µM FLAG-BamA (denatured in 8 M urea). Reactions were performed in a reverse time course manner. Following incubation for the designated time period at room temperature, reactions were quenched with 2x SDS sample buffer (125 mM Tris (pH 6.8), 4% SDS, 30% glycerol, 0.005% bromophenol blue, and 5% β-mercaptoethanol) and immediately subjected to SDS-PAGE on a 4-20% gradient gel at 150 V for 80 minutes at 4 °C. The proteins were transferred from the gel to a PVDF membrane by semi-dry transfer at 25 V for 10 minutes. The products of the reaction were detected by immunoblotting with FLAG-HRP antibodies (used at a dilution of 1:100,000).

3.4.16. Pulse-chase analysis

Strains MC4100, NR1215 containing pET23/42*lptD-FLAG*$_3$ were used in pulse-chase experiments. Pulse-chase experiments were essentially carried out according to published protocols (*21*). Briefly, a 5-ml culture was grown to OD_{600} ~0.5 in M63/glucose minimal media supplemented with eighteen amino acids (minus methionine and cysteine) at 37 ºC. The culture was pulse-labeled with [^{35}S]-methionine (100 µCi/ml final concentration) (American Radiochemicals) for 2 min and then chased with cold methionine (5 mM) at 37 ºC. At the indicated time point during the chase, a 800 µl culture aliquot was transferred to a 1.5-ml tube containing 80 µl of trichloroacetic acid (TCA, 70% in water), incubated on ice for 20 min. Precipitated proteins were pelleted at 18,000 x *g* for 10 min at 4 ºC, washed with 700 µl ice-cold acetone, and then solubilized in 80 µl 100 mM Tris.HCl, pH 8.0 containing 1% SDS and 20 mM *N*-ethylmaleimide (NEM, Sigma). The sample was sonicated for 30 s to aid solubilization. Following that, 800 µl

of ice-cold IP buffer (50 mM Tris.HCl, pH 8.0 containing 150 mM NaCl, 2% Triton X-100, 1 mM EDTA) was added and the sample was centrifuged at 18,000 x *g* for 10 min at 4 ºC. 700 µl of the supernatant was transferred to another 1.5-ml tube containing 2.5 µl of anti-FLAG® M2 magnetic beads (Sigma). The beads were washed and pre-equilibrated with 3 x 1 ml IP buffer before use. The mixture was incubated on a rotary shaker for 1 h at 4 ºC, and the beads were washed with 3 x 800 µl of ice-cold high salt buffer (50 mM Tris.HCl, pH 8.0 containing 1 M NaCl, 1% Triton X-100, 1 mM EDTA) and 1 x 800 µl ice-cold 10 mM Tris.HCl, pH 8.0 using a magnetic separation rack (New Englands Biolabs). 60 µl 2X SDS non-reducing sample buffer was then added to the beads and the mixture heated for 10 min at 100 ºC to elute the bound proteins. 15 µl of eluted sample was applied to SDS-PAGE directly. For reduction of disulfide bonds, 0.5 µl β-mercaptoethanol (β-ME, Sigma) was added to 20 µl eluted sample and heated for 5 min at 100 ºC before loading. 4-20% Tris.HCl polyacrylamide gels were used (running conditions: 150 V for 120 min). The gel was then dried and exposed to phosphor storage screens for autoradiography.

3.4.17. Antibodies

Monoclonal α-His conjugated to horseradish peroxidase was purchased from Qiagen. Monoclonal α-FLAG conjugated to horseradish peroxidase was purchased from Sigma. α-LptD (*21*) and α-LptE (*6*) antiserum were already described. LptD antibody used in DSP and EGS crosslinking experiments is courtesy of Dr. Shin-ichiro Narita.

3.5. References

1. Chng SS, Xue M, Garner RA, Kadokura H, Boyd D, Beckwith J, Kahne D (2012) Disulfide rearrangement triggered by translocon assembly controls lipopolysaccharide export. *Science* 337:1665-1668.

2. Wiedemann N, Kozjak V, Chacinska A, Schönfisch B, Rospert S, Ryan MT, Pfanner N, Meisinger C (2003) Machinery for protein sorting and assembly in the mitochondrial outer membrane. *Nature* 424:565-571.

3. Noinaj N, Fairman JW, Buchanan SK (2011) The crystal structure of BamB suggests interactions with BamA and its role within the BAM complex. *J Mol Biol* 407:248–260.

4. Ureta AR, Endres RG, Wingreen NS, Silhavy TJ (2007) Kinetic analysis of the assembly of the outer membrane protein LamB in *Escherichia coli* mutants each lacking a secretion or targeting factor in a different cellular compartment. *J Bacteriol* 189:446-454.

5. Hagan CL, Silhavy TJ, Kahne D (2011) β-Barrel membrane protein assembly by the Bam complex. *Annu Rev Biochem* 80:189-210.

6. Chng SS, Ruiz N, Chimalakonda G, Silhavy TJ, Kahne D (2010) Characterization of the two-protein complex in Escherichia coli responsible for lipopolysaccharide assembly at the outer membrane. *Proc Natl Acad Sci* USA 107:5363-5368.

7. Freinkman E, Chng SS, Kahne D (2011) The complex that inserts lipopolysaccharide into the bacterial outer membrane forms a two-protein plug-and-barrel. *Proc Natl Acad Sci* USA 108:2486-2491.

8. Chimalakonda G, Ruiz N, Chng SS, Garner RA, Kahne D, Silhavy TJ (2011) Lipoprotein LptE is required for the assembly of LptD by the beta-barrel assembly machine in the outer membrane of *Escherichia coli*. *Proc Natl Acad Sci* USA 108:2492-2497.

9. Tokuda H (2009) Biogenesis of outer membranes in Gram-negative bacteria. *Biosci Biotechnol Biochem* 73:465-473.

10. Ruiz N, Chng SS, Hiniker A, Kahne D, Silhavy TJ (2010) Nonconsecutive disulfide bond formation in an essential integral outer membrane protein. *Proc Natl Acad Sci* USA 107:12245-12250.

11. Hagan CL, Kim S, Kahne D (2010) Reconstitution of outer membrane protein assembly from purified components. *Science* 328: 890-2.

12. Hagan CL, Kahne D (2011) The reconstituted Escherichia coli Bam complex catalyzes multiple rounds of β-barrel assembly. *Biochemistry* 50(35):7444-6.

13. Hagan CL, Westwood DB, Kahne D (2013) Bam Lipoproteins Assemble BamA in Vitro. *Biochemistry*.52(35):6108-13.

14. Sklar JG, Wu T, Kahne D, Silhavy TJ (2007) Defining the roles of the periplasmic chaperones SurA, Skp and DegP in *Escherichia coli*. *Genes Dev* 21:2473-2484.

15. Workman P, Heide K, Giuliano N, Lee N, Mar J, Vuong P, Bennion D, Misra R (2012) Genetic, biochemical, and molecular characterization of the polypeptide transport-associated domain of *Escherichia coli* BamA. *J Bacteriol* 194(13):3512-21.

16. Noinaj N, Kuszak AJ, Gumbart JC, Lukacik P, Chang H, Easley NC, Lithgow T, Buchanan SK (2013) Structural insight into the biogenesis of β-barrel membrane proteins. *Nature.* 501(7467):385-90.

17. Kim S, Malinverni JC, Sliz P, Silhavy TJ, Harrison SC, Kahne D (2007) Structure and function of an essential component of the outer membrane protein assembly machine. *Science* 317:961-964.

18. Kim KH, Aulakh S, Paetzel M (2011) Crystal structure of β-barrel assembly machinery BamCD protein complex. *J Biol Chem* 286:39116–39121.

19. Wu T, Malinverni J, Ruiz N, Kim S, Silhavy TJ, Kahne D (2005) Identification of a multicomponent complex required for outer membrane biogenesis in *Escherichia coli*. *Cell* 121 :235-245.

20. Kadokura H, Beckwith J (2009) Detecting folding intermediates of a protein as it passes through the bacterial translocation channel. *Cell* 138:1164-1173.

21. Braun M, Silhavy TJ (2002) Imp/OstA is required for cell envelope biogenesis in *Escherichia coli*. *Mol Microbiol* 45:1289-1302.

22. Malinverni JC, Werner J, Kim S, Sklar JG, Kahne D, Misra R, Silhavy TJ (2006) YfiO stabilizes the YaeT complex and is essential for outer membrane protein assembly in Escherichia coli. *Mol Microbiol* 61:151-164.

23. Sklar JG, Wu T, Gronenberg LS, Malinverni JC, Kahne D, Silhavy TJ (2007) Lipoprotein SmpA is a component of the YaeT complex that assembles outer membrane proteins in *Escherichia coli*. *Proc Natl Acad Sci* USA 104:6400-6405.

24. Silhavy TJ, Berman ML, Enquist LW (1984) *Experiments with gene fusions* (Cold Spring Harbor Laboratory Press, Plainview, NY)